N-1846

NCEL

Technical Note

September 1992

By E.E. Cooper and
C. Dahl

Sponsored By Naval Facilities
Engineering Command

AN EXPERIMENTAL EXAMINATION OF THE THERMAL AND ACOUSTIC ENVIRONMENTS ON RUNWAY JOINT SEALS

ABSTRACT A test series was conducted at Edwards Air Force Base to determine noise and temperature environments that joint seal materials experience on an operational runway. Impingement of exhaust flow from jet engines creates an "aerothermal environment" for joint seal materials that contributes to, and accelerates, the deterioration and failure of joint seals. The aerothermal environment consists of noise (considered in this report as acoustically-induced as well as flow-induced fluctuations) and temperature. Current specifications for runway joint seal materials do not consider the effects of noise. The test data in this report show noise levels of 164 db at the joint seal surface. The conclusion is that the potential for energy transfer from exhaust flow noise is almost as high as the potential for energy transfer from exhaust flow temperature.

NAVAL CIVIL ENGINEERING LABORATORY PORT HUENEME CALIFORNIA 93043-5003

METRIC CONVERSION FACTORS

Approximate Conversions to Metric Measures

Symbol	When You Know	Multiply by	To Find	Symbol
		LENGTH		
in	inches	*2.5	centimeters	cm
ft	feet	30	centimeters	cm
yd	yards	0.9	meters	m
mi	miles	1.6	kilometers	km
		AREA		
in^2	square inches	6.5	square centimeters	cm^2
ft^2	square feet	0.09	square meters	m^2
yd^2	square yards	0.8	square meters	m^2
mi^2	square miles	2.6	square kilometers	km^2
	acres	0.4	hectares	ha
		MASS (weight)		
oz	ounces	28	grams	g
lb	pounds	0.45	kilograms	kg
	short tons (2,000 lb)	0.9	tonnes	t
		VOLUME		
tsp	teaspoons	5	milliliters	ml
Tbsp	tablespoons	15	milliliters	ml
fl oz	fluid ounces	30	milliliters	ml
c	cups	0.24	liters	l
pt	pints	0.47	liters	l
qt	quarts	0.95	liters	l
gal	gallons	3.8	liters	l
ft^3	cubic feet	0.03	cubic meters	m^3
yd^3	cubic yards	0.76	cubic meters	m^3
		TEMPERATURE (exact)		
°F	Fahrenheit temperature	5/9 (after subtracting 32)	Celsius temperature	°C

*1 in = 2.54 (exactly). For other exact conversions and more detailed tables, see NBS Misc. Publ. 286, Units of Weights and Measures, Price $2.25, SD Catalog No. C13.10:286.

Approximate Conversions from Metric Measures

Symbol	When You Know	Multiply by	To Find	Symbol
		LENGTH		
mm	millimeters	0.04	inches	in
cm	centimeters	0.4	inches	in
m	meters	3.3	feet	ft
m	meters	1.1	yards	yd
km	kilometers	0.6	miles	mi
		AREA		
cm^2	square centimeters	0.16	square inches	in^2
m^2	square meters	1.2	square yards	yd^2
km^2	square kilometers	0.4	square miles	mi^2
ha	hectares (10,000 m^2)	2.5	acres	
		MASS (weight)		
g	grams	0.035	ounces	oz
kg	kilograms	2.2	pounds	lb
t	tonnes (1,000 kg)	1.1	short tons	
		VOLUME		
ml	milliliters	0.03	fluid ounces	fl oz
l	liters	2.1	pints	pt
l	liters	1.06	quarts	qt
l	liters	0.26	gallons	gal
m^3	cubic meters	35	cubic feet	ft^3
m^3	cubic meters	1.3	cubic yards	yd^3
		TEMPERATURE (exact)		
°C	Celsius temperature	9/5 (then add 32)	Fahrenheit temperature	°F

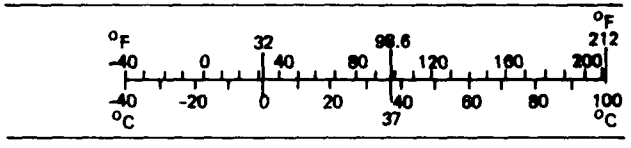

REPORT DOCUMENTATION PAGE

Form Approved
OMB No. 0704-018

1. AGENCY USE ONLY *(Leave blank)*	2. REPORT DATE	3. REPORT TYPE AND DATES COVERED
	September 1992	Final: Jun 1988 through Sep 1989

4. TITLE AND SUBTITLE
AN EXPERIMENTAL EXAMINATION OF THE THERMAL AND ACOUSTIC ENVIRONMENTS ON RUNWAY JOINT SEALS

5. FUNDING NUMBERS
PR - Y1316-001-04-040
WU - DN668078

6. AUTHOR(S)
E.E. Cooper and C. Dahl

7. PERFORMING ORGANIZATION NAME(S) AND ADDRESSE(S)
Naval Civil Engineering Laboratory
Port Hueneme, CA 93043-5003

8. PERFORMING ORGANIZATION REPORT NUMBER
TN - 1846

9. SPONSORING/MONITORING AGENCY NAME(S) AND ADDRESSE(S)
Naval Facilities Engineering Command
Alexandria, VA 22332-2300

10. SPONSORING/MONITORING AGENCY REPORT NUMBER

11. SUPPLEMENTARY NOTES

12a. DISTRIBUTION/AVAILABILITY STATEMENT
Approved for public release; distribution unlimited.

12b. DISTRIBUTION CODE

13. ABSTRACT *(Maximum 200 words)*

A test series was conducted at Edwards Air Force Base to determine noise and temperature environments that joint seal materials experience on an operational runway. Impingement of exhaust flow from jet engines creates an "aerothermal environment" for joint seal materials that contributes to, and accelerates, the deterioration and failure of joint seals. The aerothermal environment consists of noise (considered in this report as acoustically-induced as well as flow-induced fluctuations) and temperature. Current specifications for runway joint seal materials do not consider the effects of noise. The test data in this report show noise levels of 164 db at the joint seal surface. The conclusion is that the potential for energy transfer from exhaust flow noise is almost as high as the potential for energy transfer from exhaust flow temperature.

14. SUBJECT TERMS
Jet engine exhaust flow, turbulent jet noise, runway materials, joint seal materials

15. NUMBER OF PAGES
103

16. PRICE CODE

17. SECURITY CLASSIFICATION OF REPORT	18. SECURITY CLASSIFICATION OF THIS PAGE	19. SECURITY CLASSIFICATION OF ABSTRACT	20. LIMITATION OF ABSTRACT
Unclassified	Unclassified	Unclassified	UL

CONTENTS

1.0 INTRODUCTION

1.1 Objective

The objective of this test series was to determine noise and temperature environments that joint seal materials experience on an operational runway. This test series was part of the Joint Seals Project sponsored by the Naval Facilities Engineering Command (NAVFACENGCOM) Materials RDT&E Program. The overall objective of the Joint Seals Project is to determine the characteristics of joint seal material, equipment, and procedures for sealing and resealing joints in Portland cement concrete airfield pavements.

1.2 Background

Impingement of exhaust flow from jet engines creates an "aerothermal environment" for joint seal materials that contributes to, and accelerates, the deterioration and failure of joint seals. The term "aerothermal environment" was coined during preparation of this report to mean the properties of jet engine exhaust flow with potential to transfer energy from the flow to joint seal materials. The aerothermal environment possibly causes deleterious changes in the sealants. Specifically, two aerothermal properties of the flow were investigated in this test series. They were:

1. Flow temperature.

2. Noise-induced and flow-induced pressure fluctuations (the combined effects are called "noise" throughout this report due to the inability to separate or distinguish between them).

Reference 1 discusses other factors contributing to the deterioration and failure of joint seals, and gives examples of problems. In addition to the aerothermal environment, joint seal deterioration and failure may result from attack of chemicals spilled or dripped from aircraft, from natural aging and weathering of the joint seal materials, from improper installation of the joint seal, from deficient materials, or from other factors. This report is concerned only with the noise and temperature contributions to the aerothermal environment for joint seal materials.

The potentially damaging effects of noise- and flow-induced pressure fluctuations as contributors to the deterioration of joint seal materials were apparently not considered significant during development of the current procurement specifications for joint seal materials (Ref 2, 3, and 4). Thermal requirements are stated in Section 3 and testing procedures for quality assurance are stated in Section 4 of each of the above-referenced Military Specifications. There are no requirements or

testing procedures for withstanding the noise environment. Sealant materials are tested and shown to meet the thermal specifications; however, the materials often fail within 3 months after application on operational runways. The conclusion is that the specifications may not accurately represent conditions that the joint sealants will experience after installation on an operational runway. The question is: "What are the conditions that are not represented?" One possibility is that the effects of noise and/or flow pressure are contributors to the failures of joint sealants. This test program was conducted to determine the relative magnitudes of energy input to the joint seal materials from the thermal environment and from the noise environment.

2.0 DESCRIPTION OF TEST PROGRAM

The tests were conducted on Runway 04/22 at Edwards Air Force Base (Edwards AFB). Figure 2-1 gives an overview of the main flightline area. Runway 04/22 is the main runway at Edwards AFB. It is a concrete runway, 15,000 feet long and 300 feet wide, capable of handling all aircraft in the military inventory. The designation 04/22 indicates the orientation of the runway with respect to magnetic north. Planes taking off from the southern end of the runway show a heading of approximately 40 degrees clockwise from due north, while planes taking off from the northern end of the runway show a heading of 220 degrees clockwise from due north. The ends of the runway are designated as "Runway 04" (southern end) and "Runway 22" (northern end). Because of the prevailing winds, most of the takeoff and landing operations take place on "Runway 22," typically in the first 3,000 to 4,000 feet.

Data were taken at two different time periods during the summer of 1988. The first set of data was taken 15-16 June 1988, and the second set was taken 4 August 1988. Instrumentation was installed 10-14 June 1988 for the first test series, and was left in place after acquisition of the first set of data. Immediately prior to the second test series, however, some of the instrumentation was removed and the placement of other instrumentation was changed. Instrumentation for each of the test series is described below.

2.1 Instrumentation for the Test Series of 15-16 June 1988

Instrumentation was placed in three transverse joints and in the centerline joint of Runway 22. The instrumentation consisted of:

1. Twenty-one thermocouples (only 15 were connected to data recorders).

2. Three pressure transducers.

3. Three microphones.

Figure 2-2 shows that instrumentation was placed at Runway Stations 102+50, 104+00, and 105+50. During aircraft takeoff and landing operations, personnel conducting the tests had to remain more than 300 feet from the edge of the runway (i.e., outside the "clear zone" of the runway). Therefore, the recorders were placed 300 feet from the runway, and wiring was laid out to bring the signals from the instrumentation to the recorders. Figure 2-3 is a photograph showing the test site (Runway 22 is in the background, 300 feet on the other side of the van). Recorders were set up in the van. Since the nearest 110-volt power source was more than 3,000 feet from the test site, power was provided by a 2-kW portable generator brought from NCEL and a 15-kW mobile generator on loan from the Edwards AFB Public Works Department. Electronic noise from the generators resulted in some problems during data acquisition, which will be discussed later in the report.

Figure 2-4 shows the placement of the instrumentation relative to the centerline at each of the runway stations. Most of the thermocouples were at the joint seal surface, but three were detached in order to measure air temperatures and two were embedded 1/8 inch beneath the surface in order to measure subsurface temperatures. Placement of instrumentation for the first series of tests was:

Station	Instrumentation and Location Relative to Centerline of Runway 22 (+ is to right, - is to left)
102+50:	Air temperature: +3 feet Joint seal surface temperatures: 0, -3, -6, -12, -15 feet Joint seal subsurface temperatures: -3, -6 feet Microphone: 0 feet Pressure transducer: 0 feet
104+00:	Air temperature: +3 feet Joint seal surface temperatures: 0, -3, -6, -12, -15, -40 feet Joint seal subsurface temperatures: none Microphone: 0 feet Pressure transducer: 0 feet
105+50:	Air temperature: +3 feet Joint seal surface temperatures: 0, -3, -6, -12, -15 feet Joint seal subsurface temperatures: none (The temperatures at Station 105+50 were not recorded. See the discussion in Appendix A.) Microphone: 0 feet Pressure transducer: 0 feet

Figure 2-5 illustrates typical installations of the thermocouples to measure air temperatures, joint seal surface temperatures, and joint seal subsurface temperatures. Figure 2-6 illustrates typical installations of the microphones and the pressure transducers. Figure 2-7 is a photograph of one of the thermocouples and one of the extensions from a pressure transducer installed at the centerline of the runway. Figure 2-8 is a photograph showing the case for the reference temperature junction adjacent to the runway at Station 104+00, with instrumentation leads to it from each station. Figure 2-9 is a photograph showing continuation of the instrumentation leads from the reference temperature junction to the recorders in the van outside the "clear zone."

Procedures for calibrating the instrumentation and for reducing and displaying the data are described in Appendix A.

2.2 Instrumentation for the Test Series of 4 August 1988

The second test series was run to measure temperatures of the flow just above the joint seal as the aircraft engine exhaust heats the surface. Prior to this test series, the pressure transducers and microphones were removed from the runway centerline joint. Thermocouples previously measuring joint seal surface temperatures at Stations 102+50

and 104+00 were detached from the joint seal surfaces so they would measure air temperatures. Placement of instrumentation for the second series of tests was:

Station	Instrumentation and Location Relative to Centerline of Runway 22 (+ is to right, - is to left)
102+50:	Air temperatures: +3, 0, -3, -6, -12, -15 feet Joint seal surface temperatures: none Joint seal subsurface temperatures: none (previous instrumentation went bad) (The temperatures at Station 102+50 were not recorded. See the discussion in Appendix A.) Microphone: none Pressure transducer: none
104+00:	Air temperatures: +3, 0, -3, -6, -12, -15, -40 feet Joint seal surface temperatures: none Joint seal subsurface temperatures: none Microphone: none Pressure transducer: none
105+50:	Air temperature: +3 Joint seal surface temperatures: 0,-3, -6, -12, -15 feet Joint seal subsurface temperatures: none (The temperatures at Station 105+50 were not recorded. See the discussion in Appendix A.) Microphone: none Pressure transducer: none

During the second test series, battery-powered Campbell dataloggers were used to record the temperature data. Procedures for calibrating the instrumentation and for reducing the data are described in Appendix A.

2.3 Test Sequence

Table 2-1 lists the takeoff and landing operations during which data were acquired on 15-16 June 1988. After the instrumentation had been installed, the test team waited for opportunities to take data (i.e., they waited until aircraft arrived at Runway 22 for takeoff or landing). For each takeoff data acquisition, notation was made of: (1) the time and date of the takeoff, (2) the type(s) of aircraft (many of the takeoffs involved two aircraft, one to the left of centerline of the runway and one to the right of centerline), and (3) the approximate location of the engine exhaust plane of each aircraft at the time it increased power and started to roll. For each landing data acquisition, notation was made of: (1) the time and date of the landing, (2) the type of aircraft, and (3) the approximate height of the aircraft as it passed Station 102+50.

Observations of the takeoffs and landings were made from approximately 500 feet perpendicular to the centerline of the runway. It was not possible to see if the aircraft were aligned with the centerline, or to see how far off the centerline they were. This information would have been very helpful in interpreting the data; specifically, in determining whether the aircraft were aligned so that the engine exhaust flows were impinging directly on the instrumentation and creating the highest noise levels and temperatures experienced by the joint seals.

During the tests in June, the test team members did not realize that arrangements could be made through the control tower to have each aircraft stop at a marked station of the runway before increasing power and starting its takeoff roll. In the first test series, there was wide variation in the starting points for takeoffs. In some cases the instrumentation of Station 102+50 was of no value because the aircraft started its takeoff after it was well past that station. During the tests in August, however, the control tower requested that each pilot align the cockpit with a marker at Runway Station 102+50, and begin his takeoff roll from that point.

Table 2-2 lists the takeoff operations during which data were acquired on 4 August 1988. No data were taken during landing operations because early assessment of the data from the first tests showed that temperatures and noise levels were very low during landing operations compared to those during takeoffs. The obvious conclusion is that the environment of the joint seals created during takeoffs, not landings, is responsible for deterioration and loss of the joint seal material.

TIME	AIRCRAFT	STARTING LOCATION	DATA	
			TEMPS	NOISE
	Takeoffs, 15 Jun 88			
1131	T-2	102+50-20		X
1221	T-2	102+50-75	X	X
1511	F-4	102+50+33	X	X
1517	F-15	102+50-20	X	X
1528	T-38	102+50+27	X	X
1607	F-16	102+50-100	X	X
	F-4	102+50-150	X	X
1610	KC-135			X
1617	KC-135	105+50	X	X

TIME	AIRCRAFT	HEIGHT AT 102+50	DATA	
			TEMPS	NOISE
	Landings, 15 Jun 88			
1140	F-4	5-10 ft	X	X
	A-7	0 ft	X	X
	T-38	10 ft	X	X
	T-38	10 ft	X	X
1206	F-16	10-15 ft	X	X
1209	F-16	10-15 ft	X	X
1424	B-1	20 ft	X	X
1429	B-1	20 ft	X	X
1437	F-111	2 ft	X	X
1446	F-15	1 ft		X
1450	F-15	5-10 ft	X	X
1500	F-4	30 FT	X	X

TIME	AIRCRAFT	STARTING LOCATION	DATA	
			TEMPS	NOISE
	Takeoffs, 16 Jun 88			
0754	A-7	102+50-30	X	
	F-4	102+50-60		X
0804	F-15	102+50-15	X	X
0807	KC=135	102+50	X	X
0854	KC-135	102+50-150	X	X
0858	F-4	102+50-100	X	
	F-16	102+50-60		X
0916	747	102+50+05	X	X
0927	F-4	102+50-40	X	X
	F-18	102+50-60	X	X
0930	T-38	102+50-05		X
0946	F-16	102+50-75	X	X
	T-38	102+50-75	X	X
0952	T-38	102+50+150	X	
	F-4	102+50+70	X	
	F-15	102+50+50	X	
1103	T-38	102+50-200	X	
1109	T-38	102+50-40	X	
1126	A-7	102+50-30	X	X
	A-7	102+50-40	X	X
1134	F-16	102+50+20	X	X

TABLE 2.1. TAKEOFF AND LANDING OPERATIONS DURING DATA ACQUISITION, 15-16 JUNE 1988

TIME	AIRCRAFT	STARTING LOCATION	DATA	
			TEMPS	NOISE
Takeoffs, 4 Aug 88				
0931	C-130	102+50-25	X	
0946	T-38	102+50-25	X	
	F-15	102+50-25	X	
0947	B-52	102+50-25	X	
0951	F-16	102+50-25	X	
0954	KC-135	102+50-25	X	
0957	F-104	102+50-25	X	
	F-14	102+50-25	X	
1009	F-16	102+50-25	X	
	T-38	102+50-25	X	
1013	T-38	102+50-25	X	
	F-14	102+50-25	X	
1015	F-4	102+50-25	X	
	F-4	102+50-25	X	
1020	T-38	102+50-25	X	
1027	F-16	102+50-25	X	
1054	F-4	102+50-25	X	
1056	T-38	102+50-25	X	
	T-38	102+50-25	X	
1057	F-14	102+50-25	X	
1110	F-4	102+50-25	X	

TIME	AIRCRAFT	STARTING LOCATION	DATA	
			TEMPS	NOISE
1113	F-16	102+50-25	X	
1117	T-38	102+50-25	X	
	T-38	102+50-25	X	
1124	T-38	102+50-25	X	
1137	C-130	102+50-25	X	
1138	F-104	102+50-25	X	
	F-18	102+50-25	X	
1337	F-4	102+50-25	X	
1338	F-15	102+50-25	X	
1342	KC-135	102+50-25	X	
1425	F-18	102+50-25	X	
1430	F-16	102+50-25	X	

TABLE 2.2. TAKEOFF OPERATIONS DURING DATA ACQUISITION, 4 AUGUST 1988

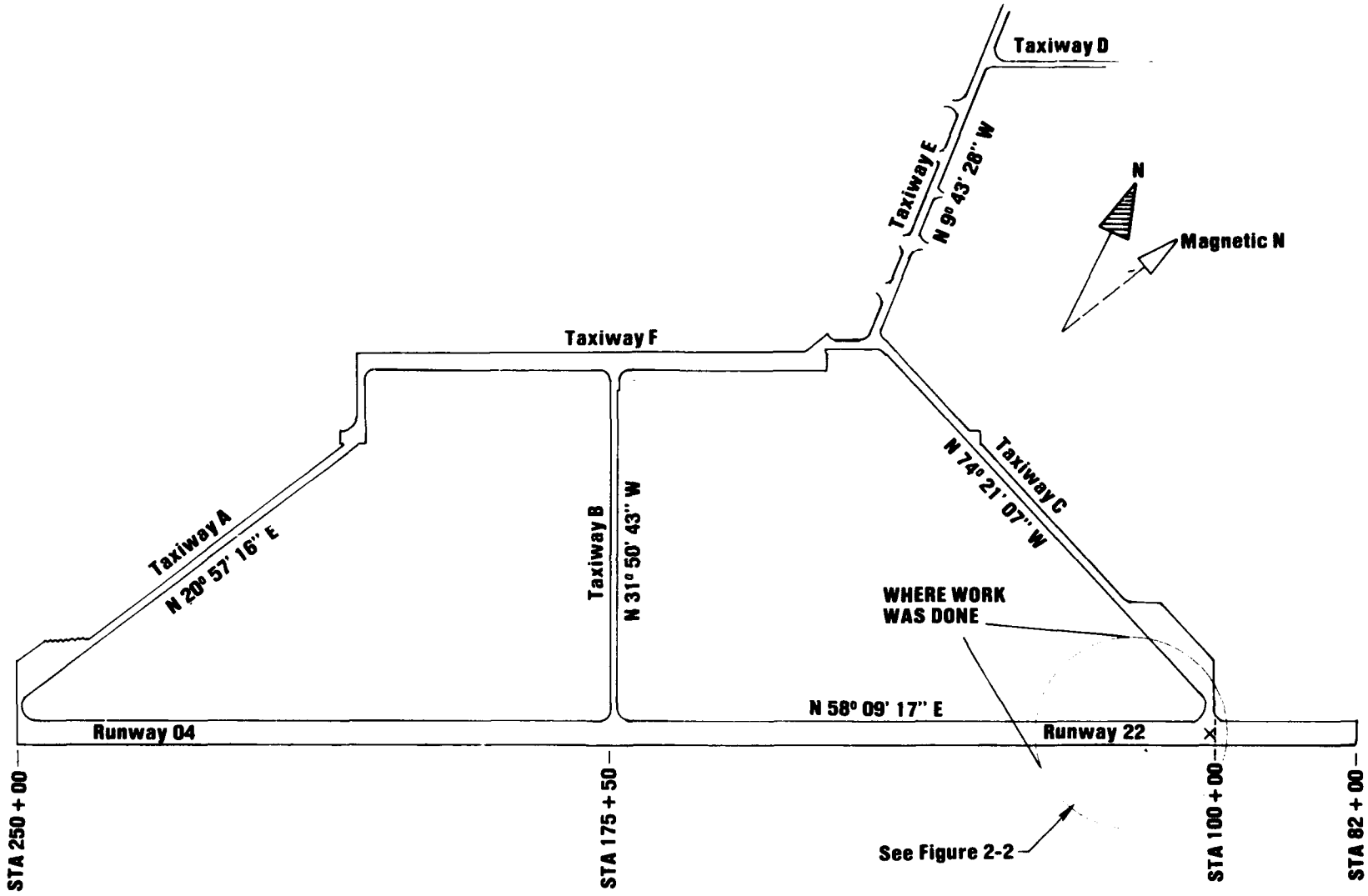

Figure 2-1. Main flightline at Edwards Air Force Base, California.

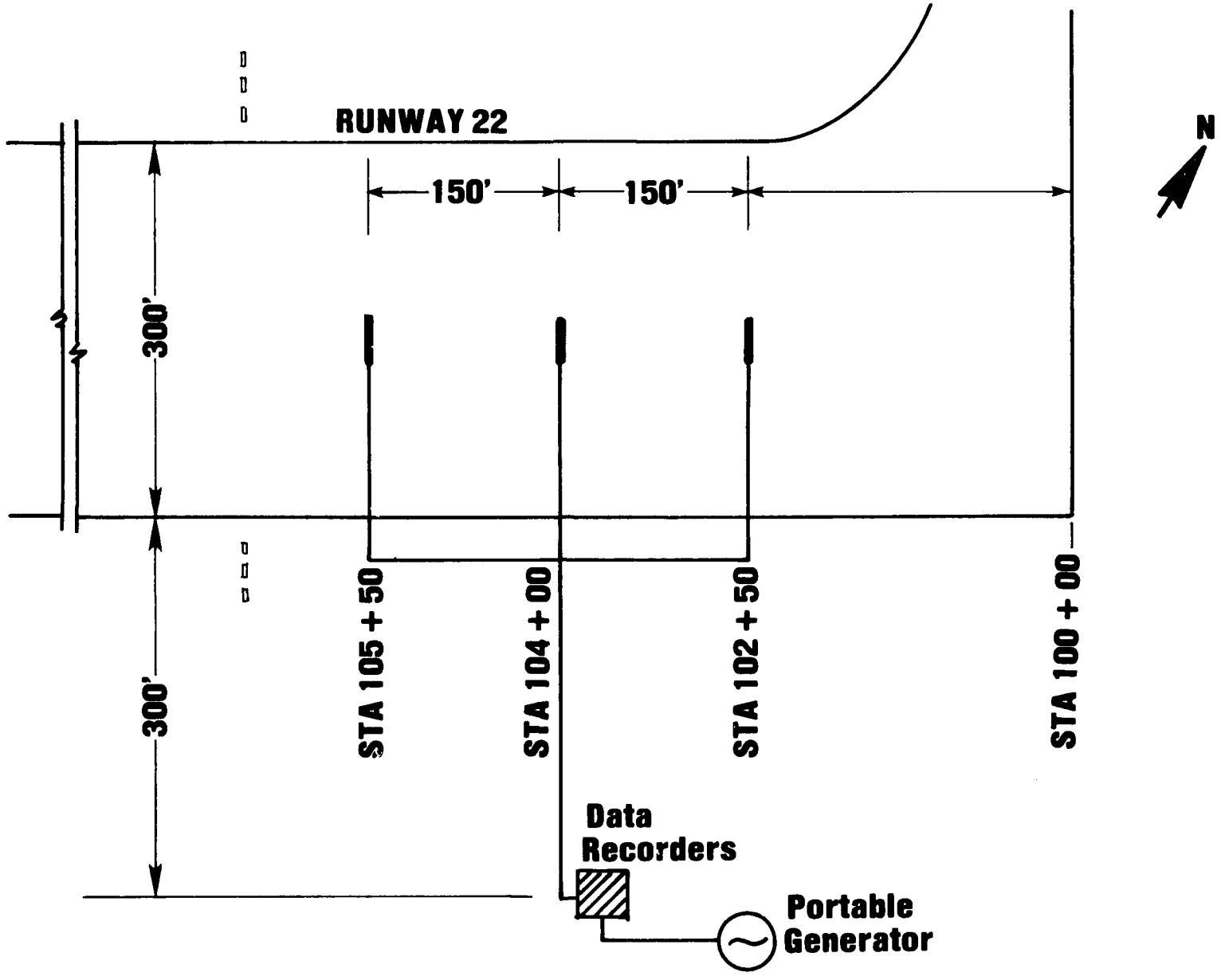

Figure 2-2. Locations of instrumentation and recorders for joint seal environment tests.

Figure 2-3. Instrumentation van and mobile generator 300 feet to side of Edwards Air Force Base, Runway 22.

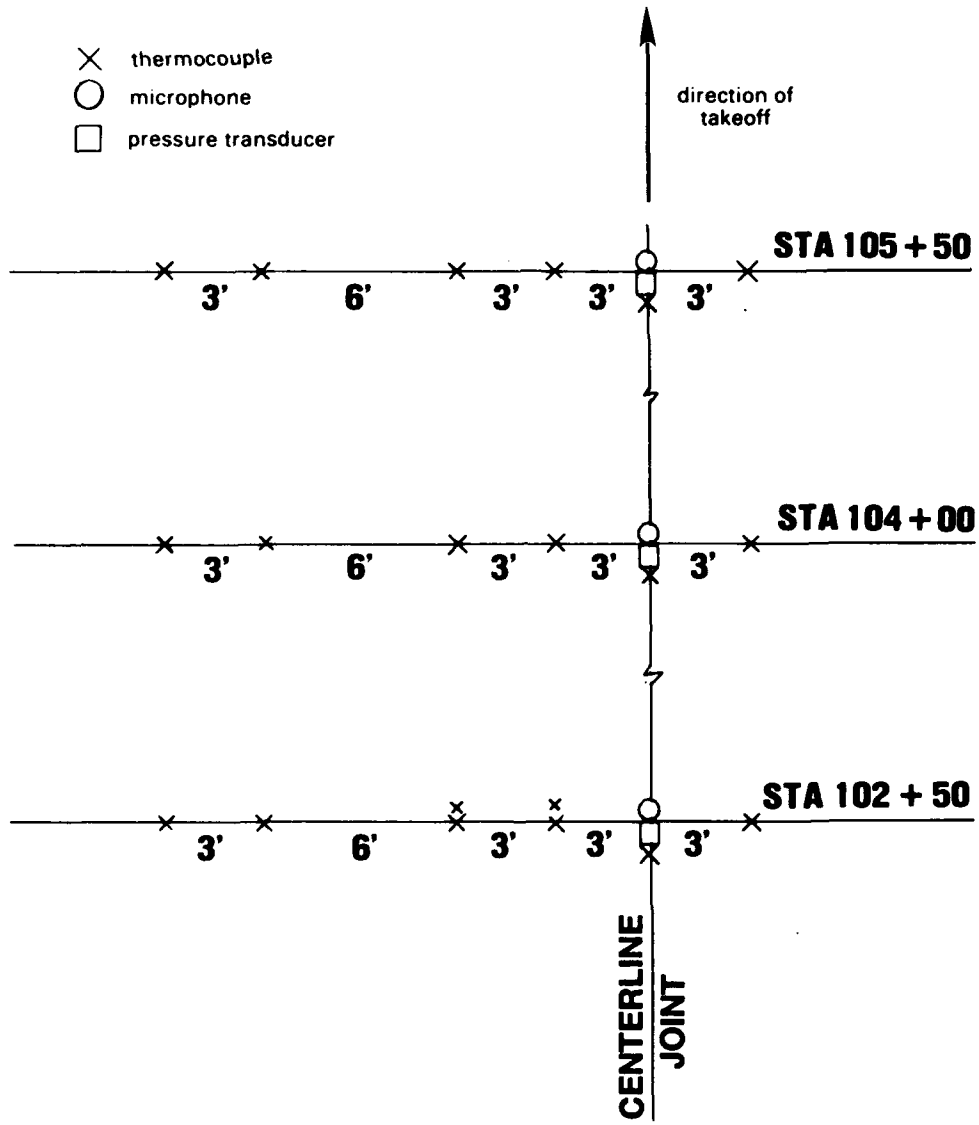

Figure 2-4. Locations of instrumentation for tests of aerothermal environment at Edwards Air Force Base, Runway 22.

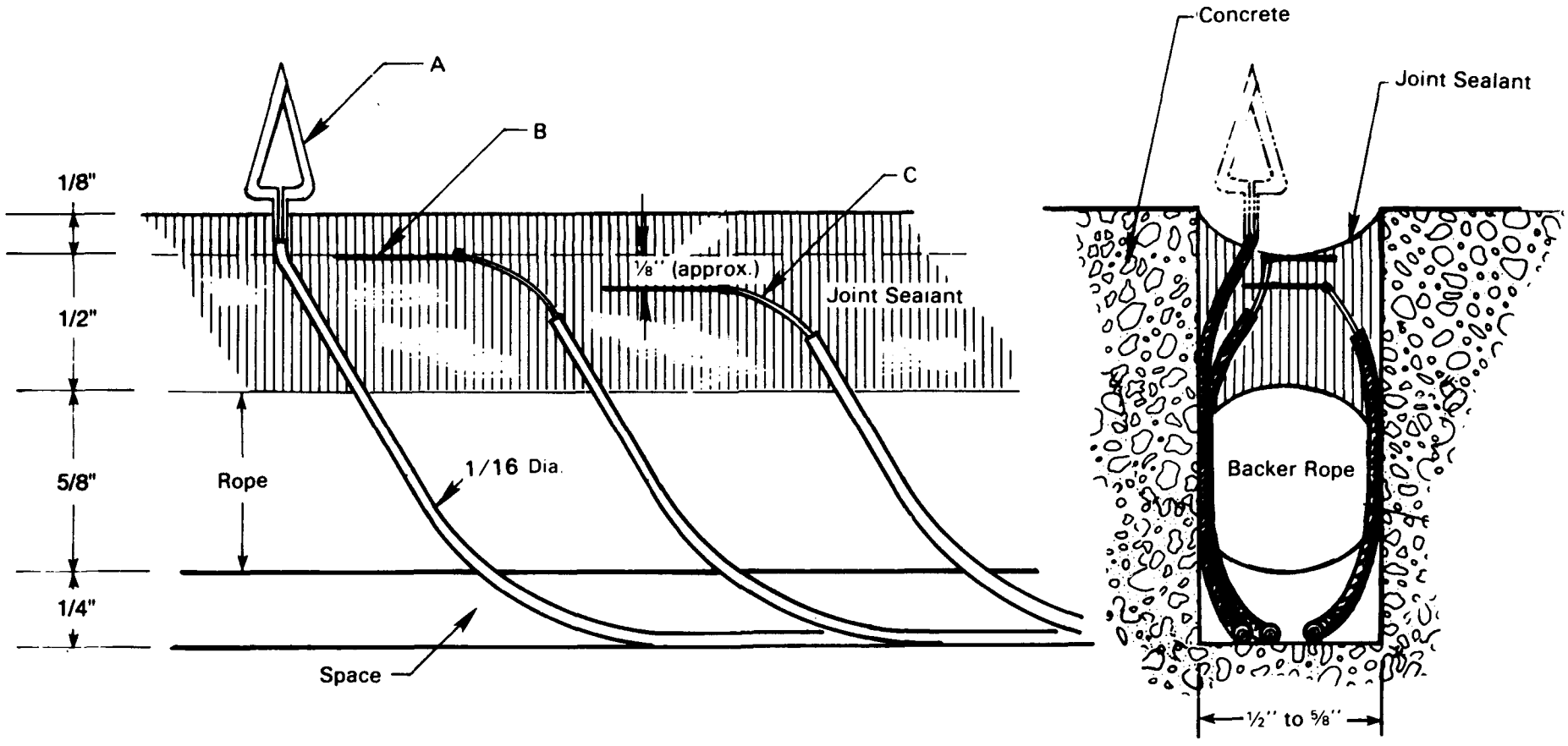

Figure 2-5. Typical installation of thermocouples to ensure flow temperature (A), joint seal surface temperature (B), and joint seal subsurface temperature (C).

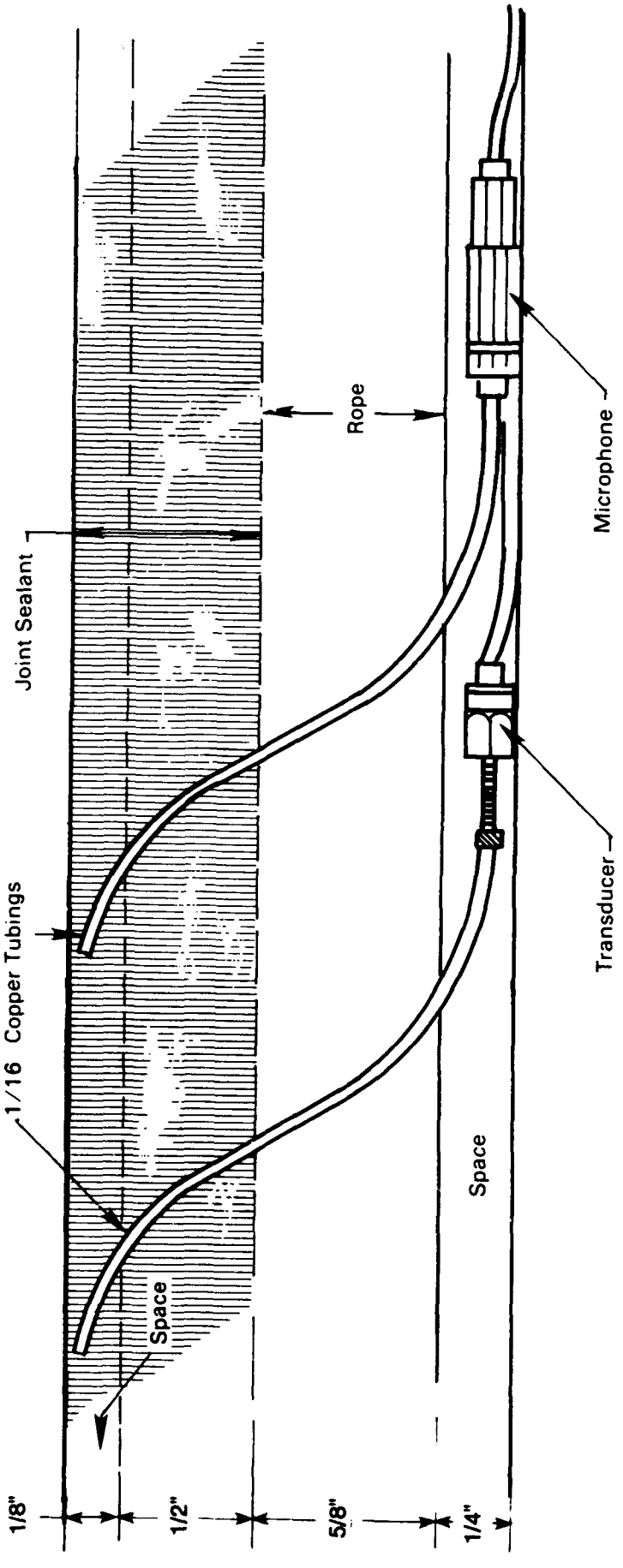

Figure 2-6. Typical installation of pressure transducers and microphones to measure noise at Edwards Air Force Base, Runway 22, centerline joint.

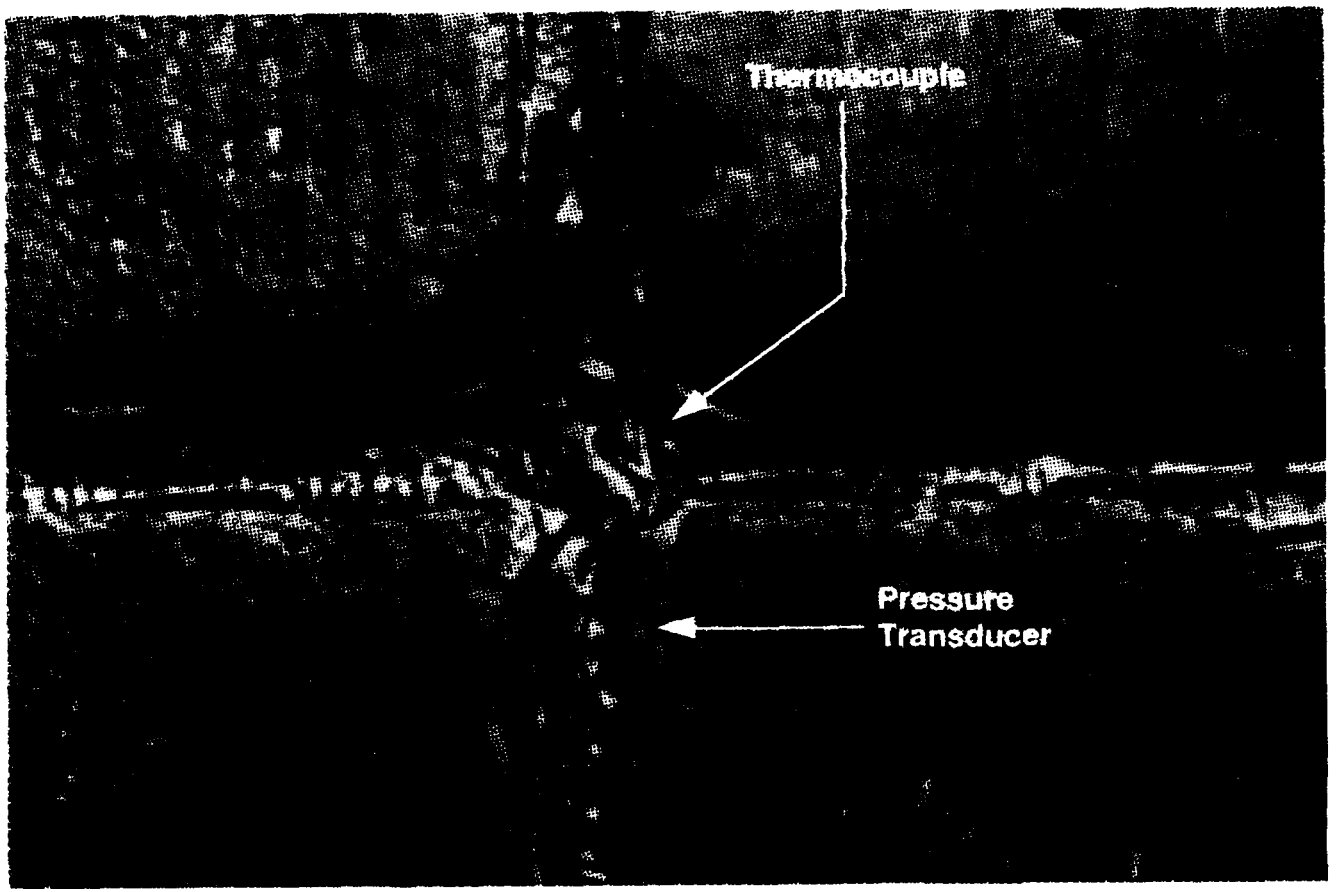

Figure 2-7. Surface thermocouple and pressure transducer at Edwards Air Force Base, Runway 22, centerline joint.

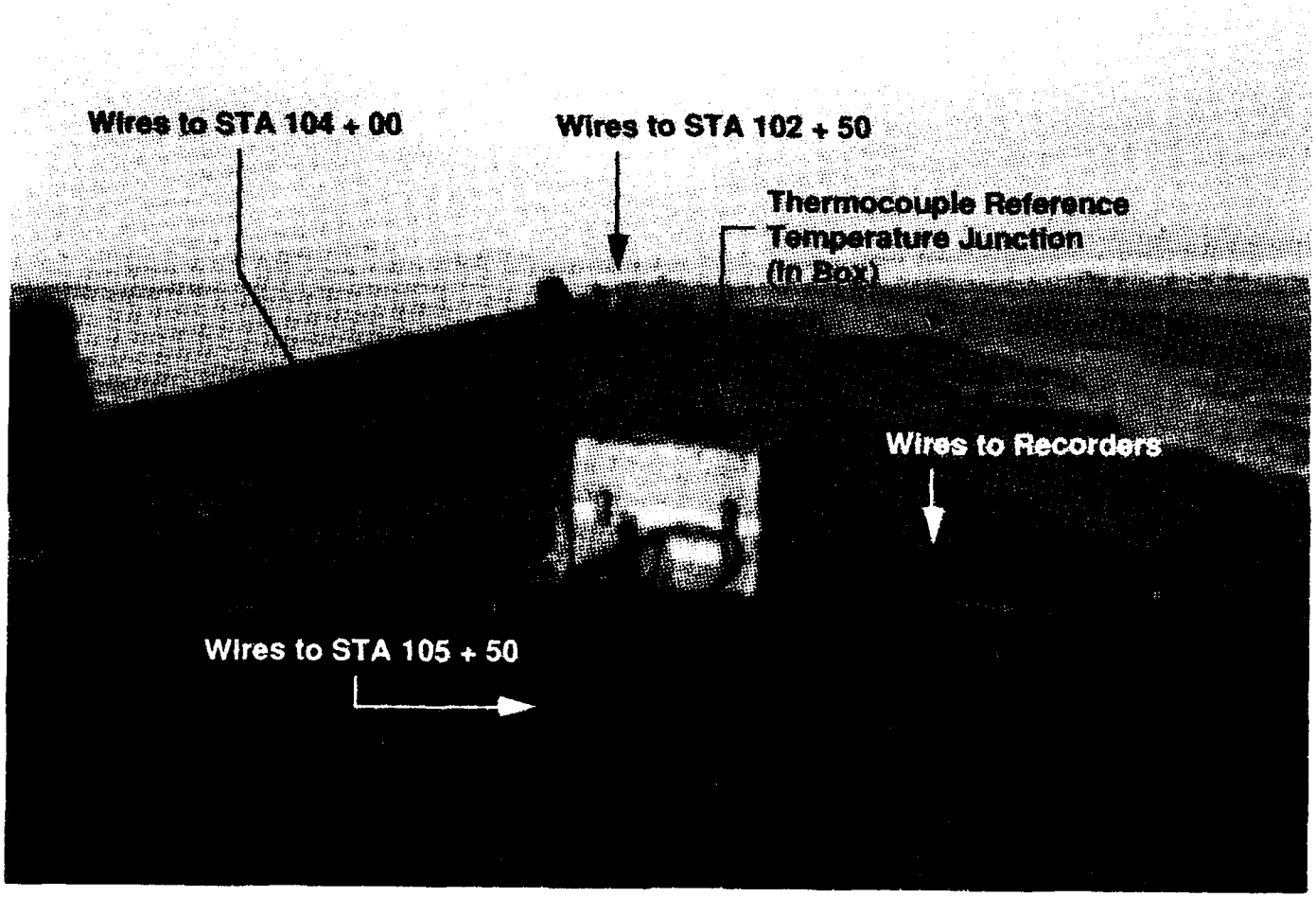

Figure 2-8. Reference temperature junction (in case) and instrumentation leads from each instrumented joint seal.

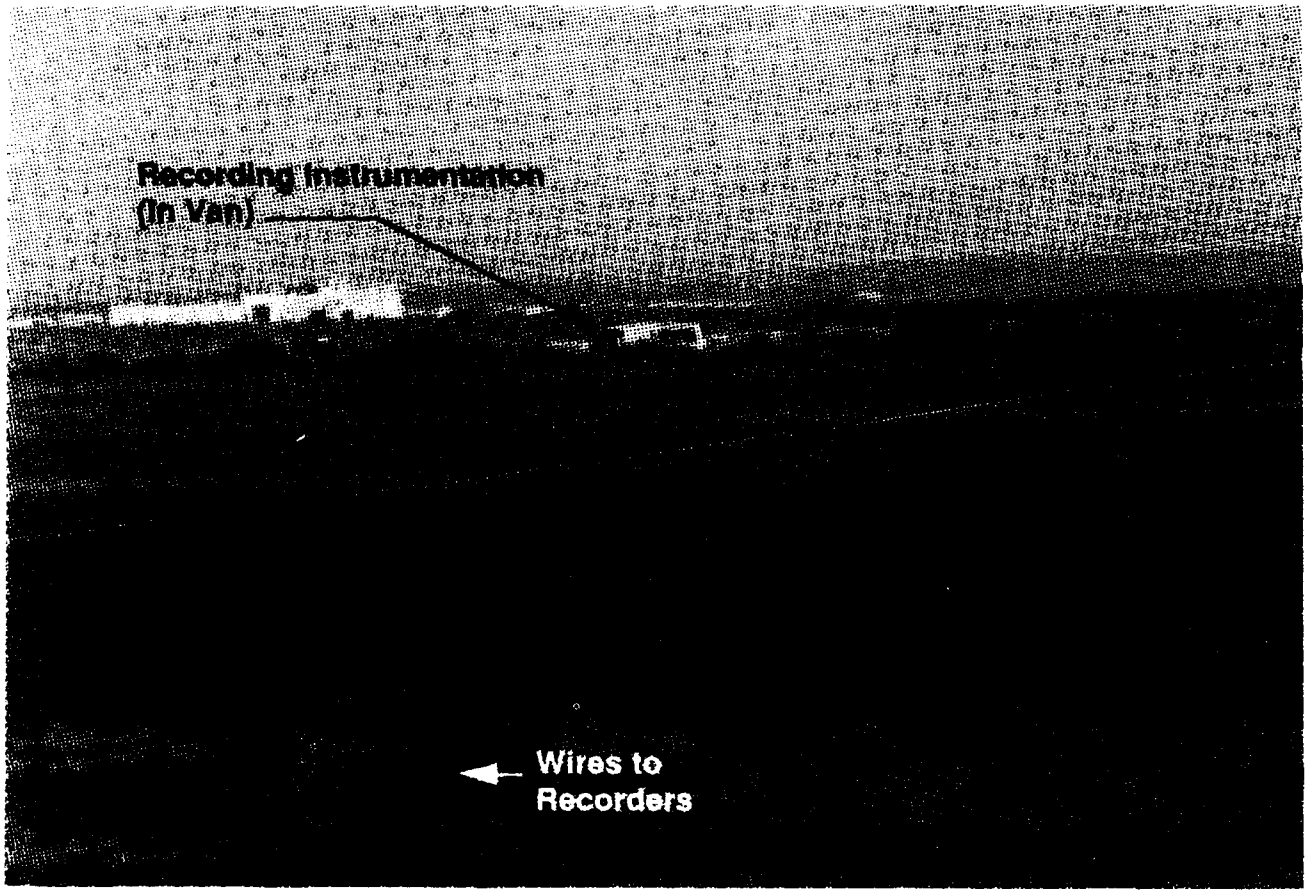

Figure 2-9. Continuation of instrumentation wiring from reference temperature junction to recorders in van.

3.0 RESULTS

Data are presented only from selected tests. Presentation of all data would have been too voluminous. Furthermore, during landing operations and many of the takeoff operations, there were insignificant changes in temperatures and the noise levels remained relatively low. During takeoff operations in which two aircraft were on the runway at the same time, it was usually the case that one plane was too far to the right of the instrumentation and the other was too far to the left of the instrumentation for exhaust flow to cause response of the thermocouples. The engines were audible to the microphones and pressure transducers, but the sound power levels were very low compared to sound power levels during tests in which the engines passed directly over the instrumentation. During landing operations, the planes passed rapidly over the instrumentation with their engines at low power. Often the planes had not "touched down" as they passed over the instrumentation. Under these conditions, temperature changes were barely measurable and noise levels were relatively low. Data from these operations offered little or no information for presentation.

3.1 Temperatures of the Exhaust Flow Just Above the Surface

Figures 3-1 through 3-10 are plots of temperatures of the exhaust flow approximately 1/2 inch above the joint sealant surface as various aircraft perform takeoff operations. Data for these plots were taken 4 August 1988. The instrumentation is described in Section 2.2 of this report and in Appendix A.

Data are presented for seven aircraft: an F-4 (Figures 3-1 and 3-2); an F-16 (Figure 3-3); an F-15 (Figure 3-4); an F-14 (Figure 3-5); a T-38 (Figure 3-6); a KC-135 (Figure 3-7); and a B-52 (Figure 3-8). The order of presentation is generally in decreasing order of temperature of the exhaust flow just above the surface of the runway. Figures 3-9 and 3-10 are crossplots of selected data from Figures 3-1 through 3-8. Specifically, they show the maximum temperature reading of each thermocouple plotted versus distance from the runway centerline.

The data for Figures 3-1 through 3-8 were all taken at the transverse joint at Station 104+00. Although the aircraft were usually rolling fast when they reached Station 104+00, the response rate of the thermocouples was fast enough to follow the changes in temperature of the hot exhaust gases.

Some observations and explanations of the flow temperature data are given below:

1. The F-4 aircraft created the highest temperatures in the flow just above the runway surface. Data from two different takeoff operations are presented in Figures 3-1 and 3-2. In one case, the flow temperature exceeded 600 °F, and in the other case, the flow temperature exceeded 500 °F. The F-4 creates the most severe temperature environment because the exhausts of its J-79 engines are directed toward the runway surface at an angle of 5°15' from the horizontal, which is a more direct impingment than engine exhausts of any other aircraft monitored during this test. The F-4 engines are underneath the fuselage, placing

the centers of the exhausts only 66 inches above the runway, which are closer to the runway than exhausts of other aircraft. Very little mixing of ambient air and the engine exhaust gases can take place before the engine exhaust gases impinge on the runway. Furthermore, with thrust of 17,000 lbf at afterburner power, the J-79 engines are relatively powerful and the exhaust temperatures and flow velocities are relatively high.

2. The F-14, F-15, F-16, and T-38 aircraft all created flow temperatures of 275 to 325 °F just above the runway surface. Engines of these aircraft are higher above the runway surface than the engines of the F-4, and the exhaust flows are more horizontal as they leave the engine. Therefore, more mixing between the engine exhaust gases and ambient air takes place before impingement, thereby cooling the gases to a lower temperature at impingement.

3. Neither the KC-135 or the B-52 aircraft caused significant temperature rise of the exhaust flow just above the runway surface. The engines of these aircraft do not have afterburners, so the temperatures of the exhaust flows leaving the engines are much lower than the flows leaving the engines of the fighter-type aircraft. Also, the engines are so far out on the wings that the exhaust flows might have by-passed the instrumentation.

4. The crossplots of maximum temperature versus thermocouple position (Figures 3-9 and 3-10) show that some of the aircraft were not aligned with the runway centerline during takeoff. Whenever the maximum temperature did not occur on the centerline, the aircraft was not aligned with the centerline. Operationally this is no problem since the runway is wide enough to handle at least two fighter-type aircraft taking off together. However, from the standpoint of evaluating the test data, it indicates an uncontrolled condition from one takeoff to another. In the case of the F-15 (Figures 3-4 and 3-9), the aircraft was so far toward the left side of the runway that only the outboard thermocouple at 40 feet from the centerline showed any temperature response. From the data of Figures 3-4 and 3-9, it is not possible to determine where the centerline of the F-15 was, so it is not possible to determine if the maximum exhaust flow temperature was measured.

3.2 Temperatures of the Joint Seal Material

Figures 3-11 through 3-22 are plots of temperatures of the joint seal material as four different types of aircraft performed takeoff operations. Data for these plots were taken 15-16 June 1988. The instrumentation is described in Section 2.1 of this report and in Appendix A.

Data are presented for: an F-4 aircraft (Figures 3-11 through 3-13); an F-16 aircraft (Figures 3-14 through 3-16); an F-15 aircraft (Figures 3-17 through 3-19); and a T-38 aircraft (Figures 3-20 through 3-22). For each aircraft, the first figure of the set compares five surface temperatures and one flow temperature measured at Station 102+50; the second figure compares surface and subsurface temperatures

at 3 feet and 6 feet from the centerline at Station 102+50; and the third figure compares six surface and one flow temperature measured at Station 104+00.

Some observations and explanations of the joint seal temperature data are given below:

1. The F-4 aircraft caused the highest joint seal temperatures. Figures 3-11 and 3-13 show joint seal surface temperatures of 285 °F and 310 °F at Stations 102+50 and 104+00, respectively. The peak surface temperatures were 135 to 150 °F above the equilibrium temperature of the joint seal surface, where the equilibrium temperature is the temperature of the surface immediately prior to, or long after, impingement of the exhaust flow. The slightly lower temperatures at Station 102+50 are explained by referring to Table 2-1, and noting that takeoff of the F-4 started with the aircraft engine exhaust plane already 33 feet past Station 102+50 (i.e., 33 feet past the instrumentation). The aircraft then passed directly over Station 104+00, placing the engine exhaust plane closer to the instrumentation and exposing the instrumentation to the portion of the exhaust plume with higher temperatures and velocities.

2. The F-15, F-16, and T-38 aircraft all caused increases of 40 to 80 °F in the joint seal surface temperatures. The increases are less than those during F-4 takeoff, and follow the pattern of temperatures of the flow just above the surface of the joint seal material. As explained in Section 3.1, the F-15, F-16, and T-38 aircraft engines direct their exhaust flows more horizontally and are higher above the runway surface than those of the F-4, permitting more ambient air to mix with and cool the engine exhaust gases before they impinge on the runway surface.

3. Joint seal surface temperatures did not increase perceptibly during takeoff operations of KC-135, B-52, 747 and other multiengine cargo and bomber aircraft. This was expected since the instrumentation above the joint seal surface did not detect changes in the air temperature (see Figures 3-7 and 3-8), and increases in the air temperature are necessary for heat input to cause temperature increases of the joint seal material. Because all the surface temperature-time plots for these aircraft showed only flat traces, and included no information for analysis, none of the plots are included in this report.

4. Figures 3-12, 3-15, 3-18, and 3-21 include temperature-time curves from the two thermocouples placed approximately 1/8 inch below the surface of the joint seal material, at 3 feet and 6 feet to the left side of the runway centerline, at Station 102+50. None of the curves shows perceptible change of temperature due to energy input from the engine exhaust flow. On the other hand, temperature-time curves for the corresponding thermocouples at the surface do show temperature increases as the engine exhaust impinges on the joint seal. Transient temperature response of the joint seal to the energy input from the engine exhaust flows is confined near the joint seal surface. Factors contributing to this are the short duration of exposure to the engine exhaust, the low thermal conductivity of the joint seal material, and its thermal capacity (density times specific heat).

5. The joint seal surface temperature data are "noisy." Plots of the temperature readings fluctuate randomly as much as 5 to 10 °F. The noise is possibly due to the poor quality of power from the portable generators (i.e., deviation from a sinusoidal power signal), and the difficulty of establishing a common ground potential between the generators, instrumentation, and recorders. Another possibility is that the noise is introduced during digitizing of the data or other operations of the ASYST program (see the discussion in Appendix A). There was insufficient time during the test schedule to isolate the cause of the noise, and also insufficient time to eliminate it. However, it was determined that the magnitudes and durations of noise-induced fluctuations were small compared to temperature changes caused by flow impingement. For interpretation and analysis of the data, the effects of electronic noise were eliminated or minimized by simply drawing smooth curves through the temperature-time traces.

A second problem with the surface temperature data is that the temperatures differ by as much as 35 °F under ambient conditions (i.e., just before or long after exposure to exhaust flow). Figure 3-14, for example, shows thermocouples on the centerline and 12 feet to the left of the centerline to have an equilibrium temperature of 145 °F, while the thermocouple 3 feet to the left of the centerline has an equilibrium temperature of 110 °F. Four possible causes have been considered: (1) the shift could be related to the difficulty in establishing common ground potential for all the equipment; (2) natural convection from the runway surface could vary from one location to another, possibly due to localized breezes or currents, and could temporarily cool portions of the joint seal surface; (3) placement of the thermocouples at the joint seal surface was not done exactly the same at each location (e.g., some thermocouples were partially covered with joint seal material, and some were not exactly horizontal), or (4) some sensors were shaded by the aircraft awaiting takeoff. No firm conclusion was reached to explain the cause(s) of the temperature shifts at ambient conditions. In Section 4.1 of this report, thermal analysis of the joint seal material at ambient conditions shows that slight decreases in solar irradiation or slight increases in natural convection heat loss can change surface temperature at least 35 °F. Lacking a firm conclusion as to the causes(s) of the temperature shifts, the temperatures shown in Figures 3-11 through 3-22 were accepted as correct indications of what was sensed at the time by the thermocouples. Differences were assumed to be due to slight differences in installation. During analysis of the data, the recorded temperatures presented in Figures 3-11 through 3-22 were used.

3.3 Acoustic Measurements at the Joint Seal Surface

Figures 3-23 through 3-44 are plots of acoustic data taken at the surface of the joint seal material during takeoff operations of three different types of aircraft. Data for these plots were taken 15-16 June 1988. The instrumentation is described in Section 2.1 of this report and in Appendix A.

Data are presented for: an F-4 aircraft (Figures 3-23 through 3-30); a T-38 aircraft (Figures 3-31 through 3-38); and an F-15 aircraft (Figures 3-39 through 3-44). For the F-4 and the T-38 aircraft, the

eight plots of acoustic data include two plots for the microphone at Station 102+50, two plots for the pressure transducer at Station 102+50, two plots for the microphone at Station 104+00, and two plots for the pressure transducer at Station 104+00. This also applies for the F-15 aircraft, except that no data are presented for the microphone at Station 104+00. The two plots for each combination of instrument and aircraft are both of sound pressure level, expressed in decibels, versus frequency. One plot presents the narrow band spectrum versus a linear frequency scale, while the second plot presents the third octave band spectrum versus a logarithmic frequency scale. The plots were printed from the spectrum analyzer screen, and include notations to show the settings of the spectrum analyzer. Appendix B describes the spectrum analyzer notations.

Data from the microphone and pressure transducer located at Station 105+50 are not presented because: (1) aircraft were moving fast at Station 105+50, and duration of the high intensity portion of the noise signal was too short to obtain multiple samples for averaging and transforming from the time domain to the frequency domain; and (2) temperatures from Station 105+50 were not recorded, so comparison of thermal and acoustic energy levels at Station 105+50 could not be made.

Some observations and explanations of the acoustic data are given below:

1. The F-4 aircraft caused the highest noise levels at the joint seal surface. Figures 3-27 and 3-29 show a noise level of approximately 164 decibels as the F-4 passed over Station 104+00. Figure 3-27 is from the microphone at that station, and Figure 3-29 is from the pressure transducer. Noise levels measured at Station 102+50 are shown in Figures 3-23 and 3-25. They were "only" approximately 152 decibels; however, Table 2-1 shows that the F-4 engine exhaust was 33 feet past Station 102+50 when afterburner power was applied. Instrumentation at Station 104+00 was much closer to the engine exhaust plane when the F-4 passed that location. By examining the temperature-time traces for the various thermocouples, it appears that the F-4 aircraft was aligned along the runway centerline, so 164 decibels is probably the maximum for the joint seal materials.

2. Noise levels measured during takeoff operations of F-15 and T-38 aircraft were approximately 155 decibels and 148 decibels, respectively. Drawing an analogy from the temperature data, one would expect lower noise levels with these aircraft than with the F-4 because the engines are higher and direct their exhaust flows more horizontally, and the T-38 engines have less thrust. From examination of the temperature-time traces from the takeoff of these aircraft, it appears that the F-15 was slightly to the left side of the runway centerline, but that exhaust flow from the right engine was passing over the runway centerline. The T-38 appeared to be displaced approximately 9 feet to the left side, and there was minimal engine exhaust flow directly over the instrumentation installed at the runway centerline. Possibly a noise level higher than 148 decibels would be measured during takeoff of a T-38 aircraft aligned along the centerline of the runway.

3. Noise levels measured with side-by-side microphones and pressure transducers were consistently almost the same. For example, the noise levels for the F-4 at Station 104+00 presented in Figures 3-27 and 3-29 differ by only 0.7 decibels (164.6 to 163.9). The noise levels for the F-15 at Station 102+50 presented in Figures 3-39 and 3-40 differ by only 0.5 decibels (154.9 to 154.4). And the noise levels for the T-38 at Station 104+00 presented in Figures 3-35 and 3-37 differ by only 0.1 decibels (145.7 to 145.8). Almost the same consistency was obtained between instrumentation at Stations 102+50 and 104+00. For example, noise levels for the F-15 were 154.9 or 154.4 decibels at Station 102+50 compared to 152.8 decibels at Station 104+00. Agreement was also close during T-38 takeoff. During F-4 takeoff, the aircraft started 33 feet past Station 102+50, so noise levels are not available with the engine directly over that station.

4. The noise of each aircraft had broad spectral distribution (i.e., it had significant energy at all frequencies up to at least 10,000 Hz). The peak energy was between 250 Hz and 400 Hz for all the aircraft. There were only slight differences in the spectral distribution measured by the microphones and the pressure transducers, including slight differences in the frequency at which peak energy occurs.

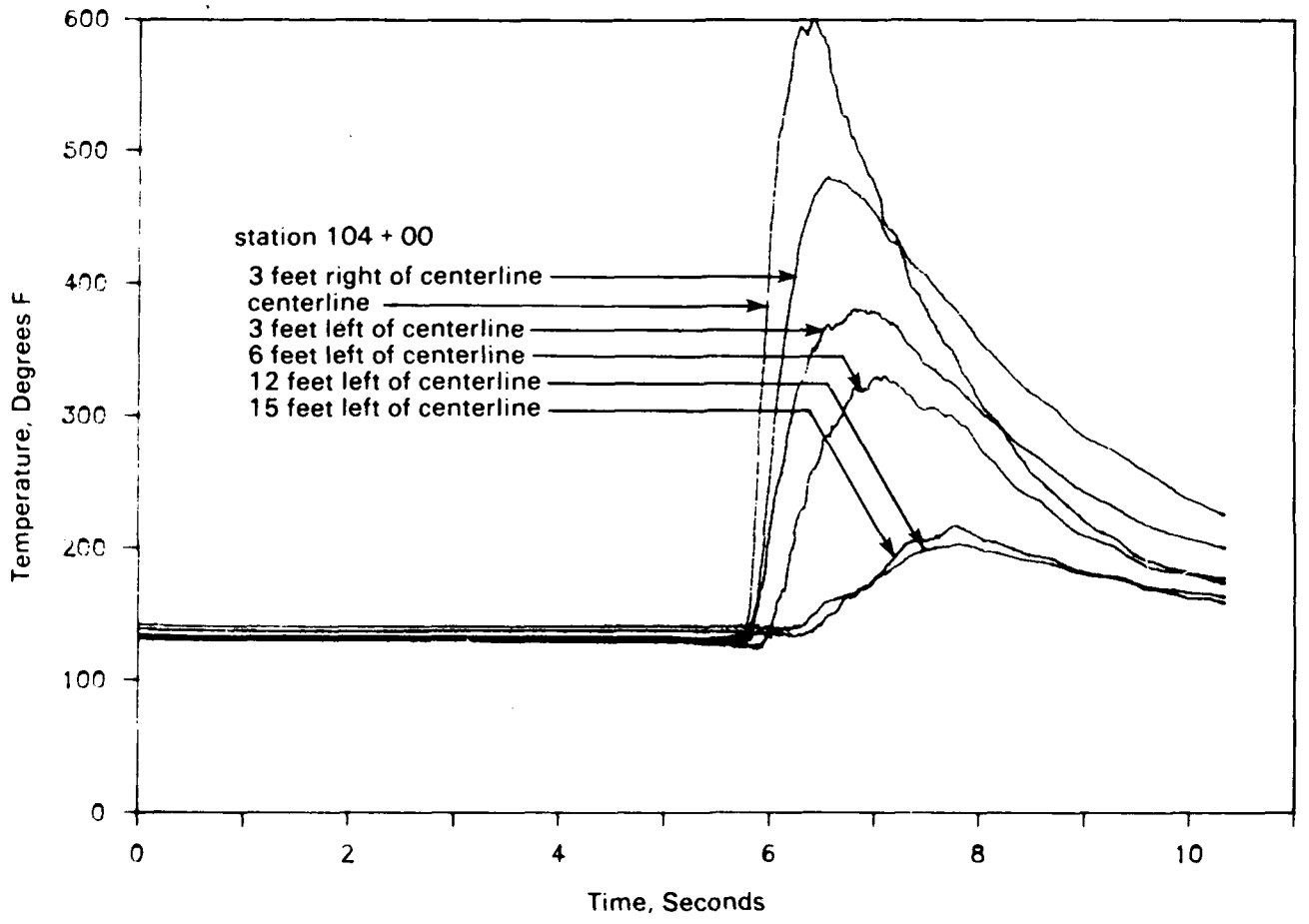

Figure 3-1. Temperatures of flow approximately 1/2 inch above surface of joint seal during F-4 takeoff (takeoff at 1054, 8/4/88).

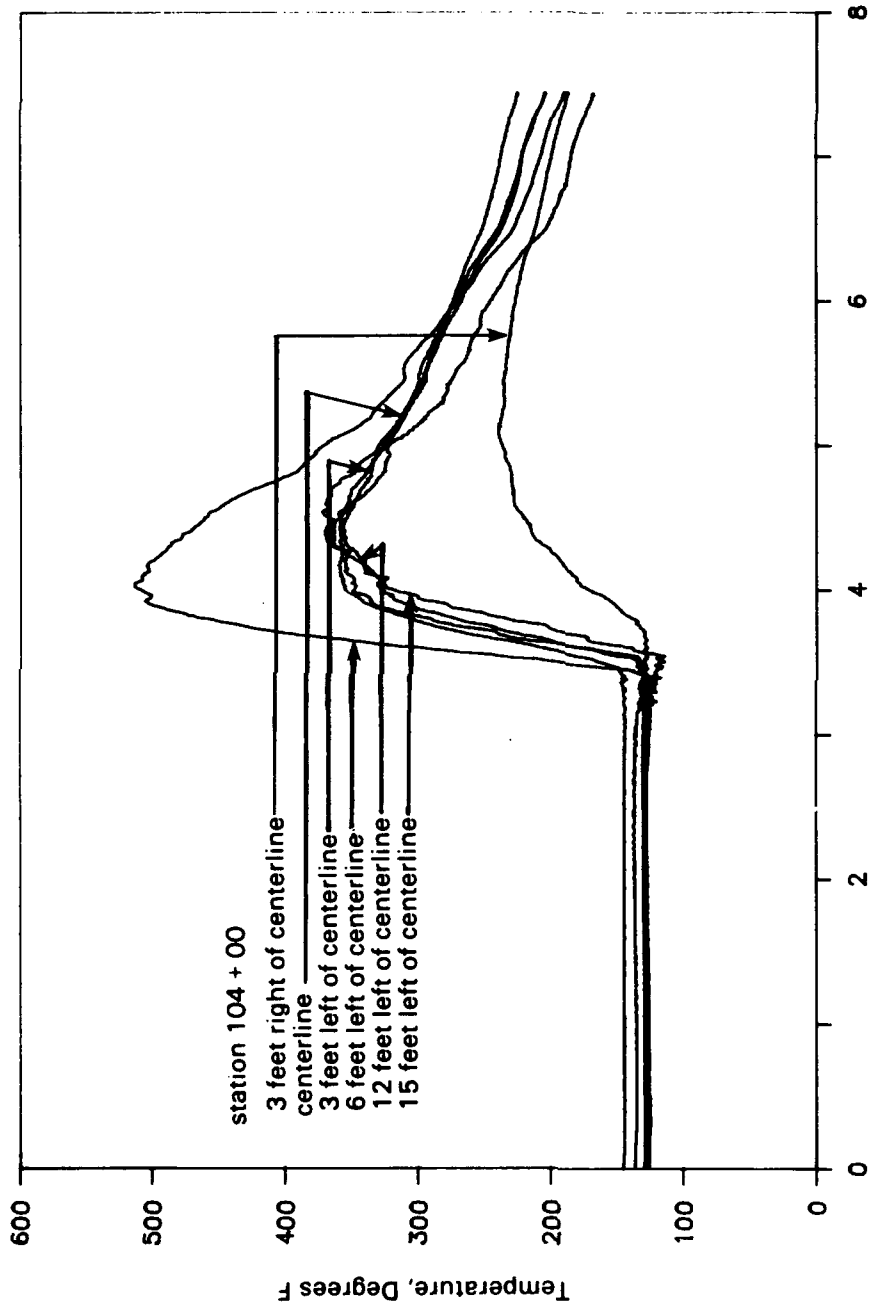

Figure 3-2. Temperatures of flow approximately 1/2 inch above surface of joint seal during F-4 takeoff (takeoff at 1110, 8/4/88).

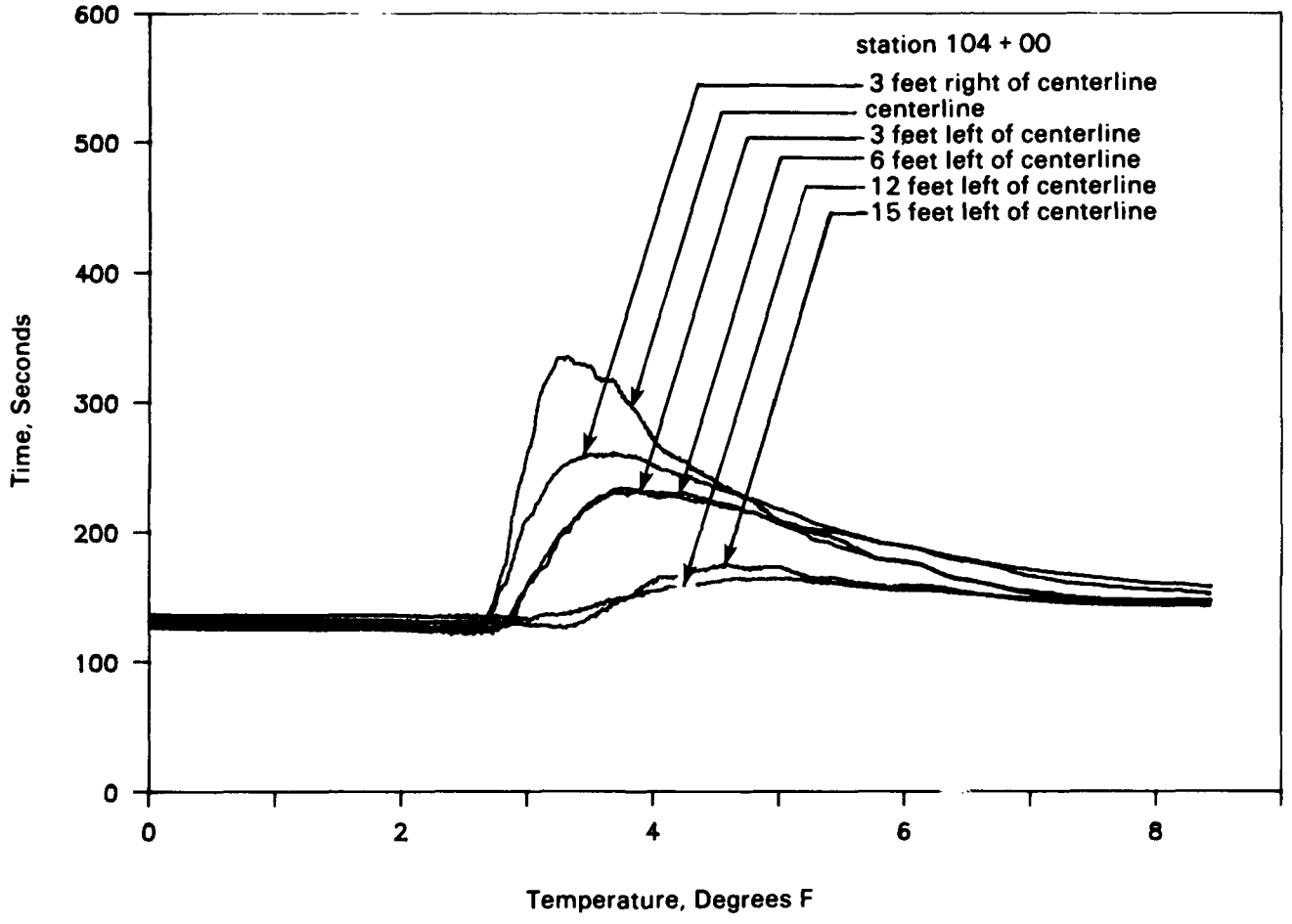

Figure 3-3. Temperatures of flow approximately 1/2 inch above surface of joint seal during F-16 takeoff (takeoff at 1027, 8/4/88).

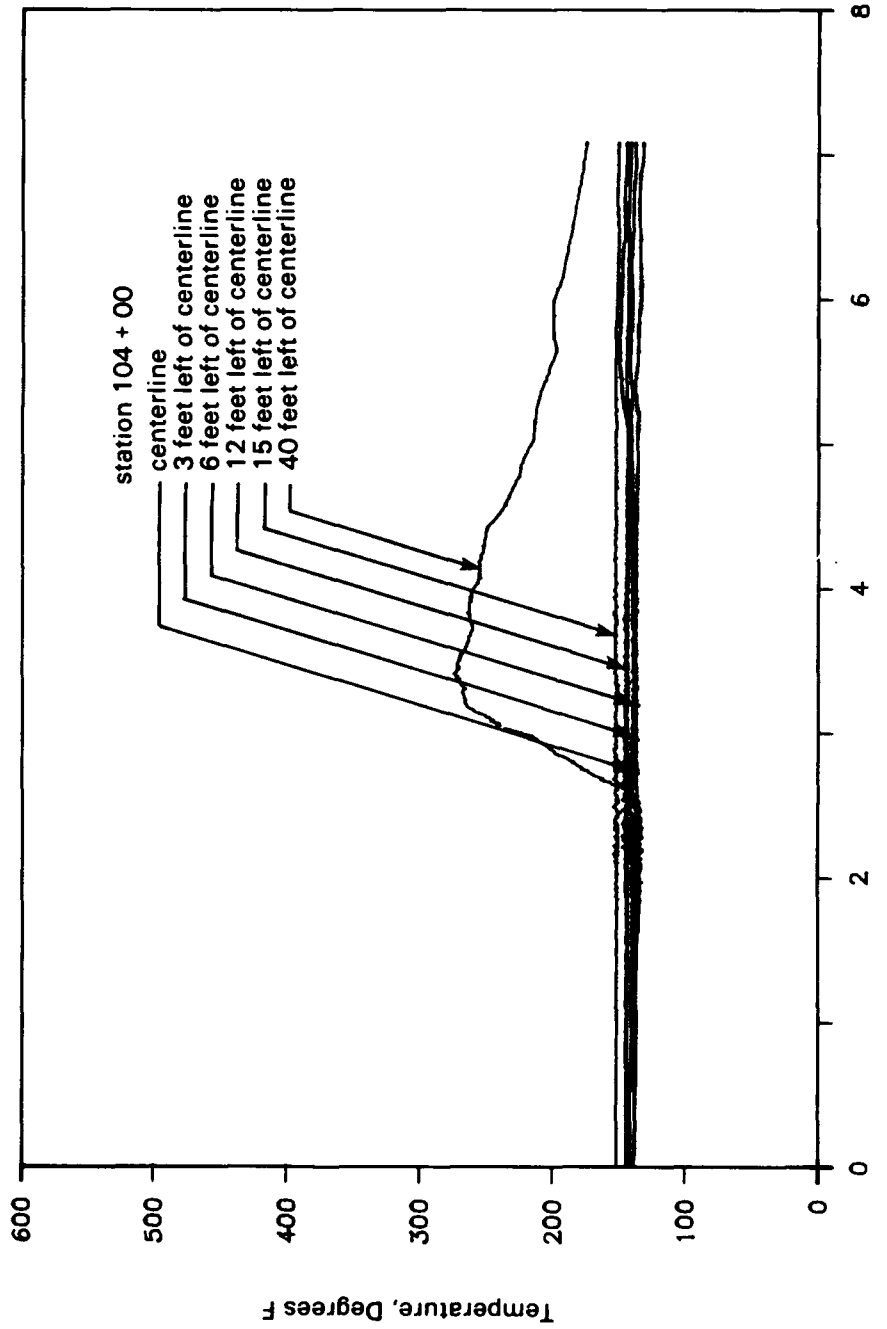

Figure 3-4. Temperatures of flow approximately 1/2 inch above surface of joint seal during F-15 takeoff (takeoff at 1338, 8/4/88).

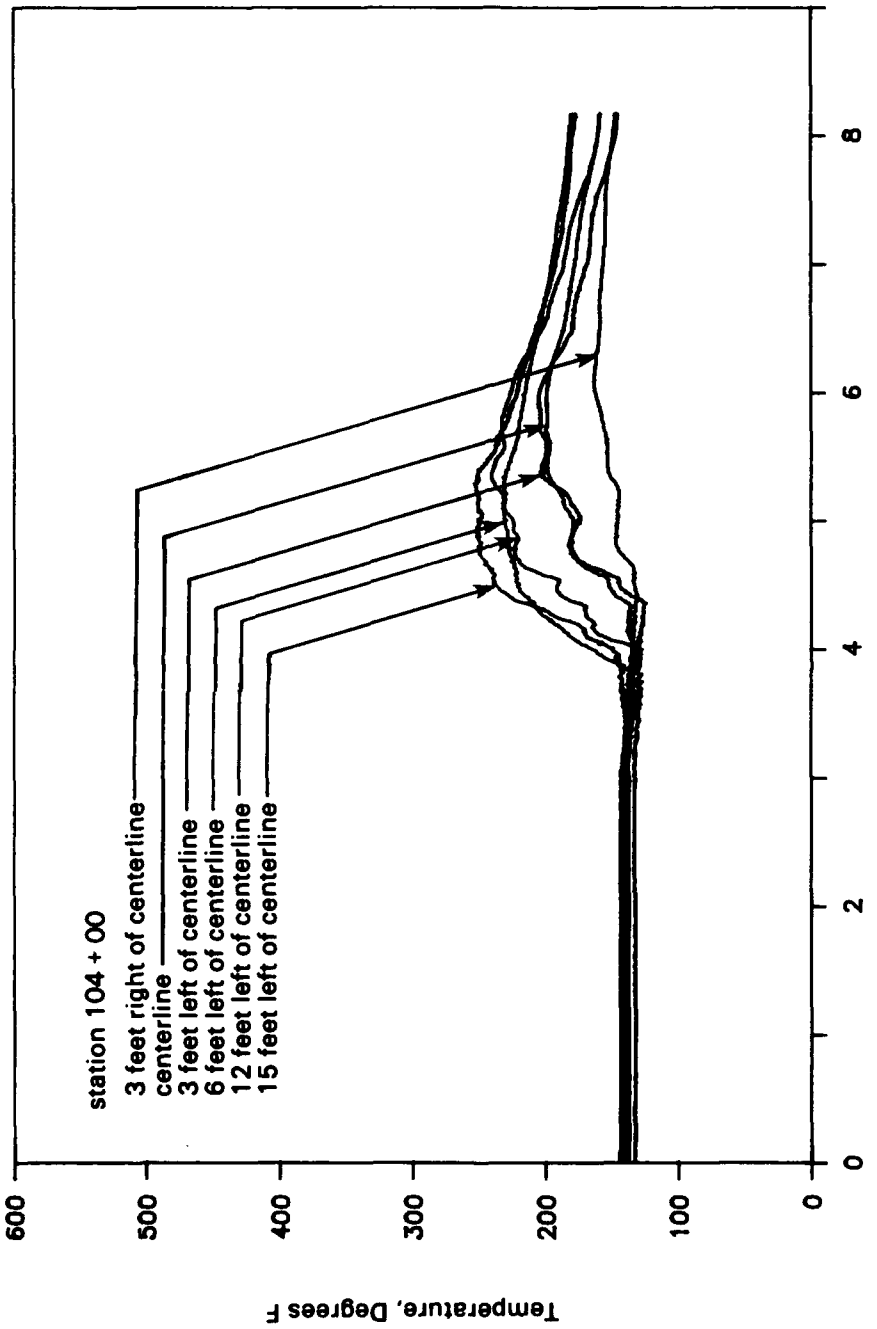

Figure 3-5. Temperatures of flow approximately 1/2 inch above surface of joint seal during F-14 takeoff (takeoff at 1057, 8/4/88).

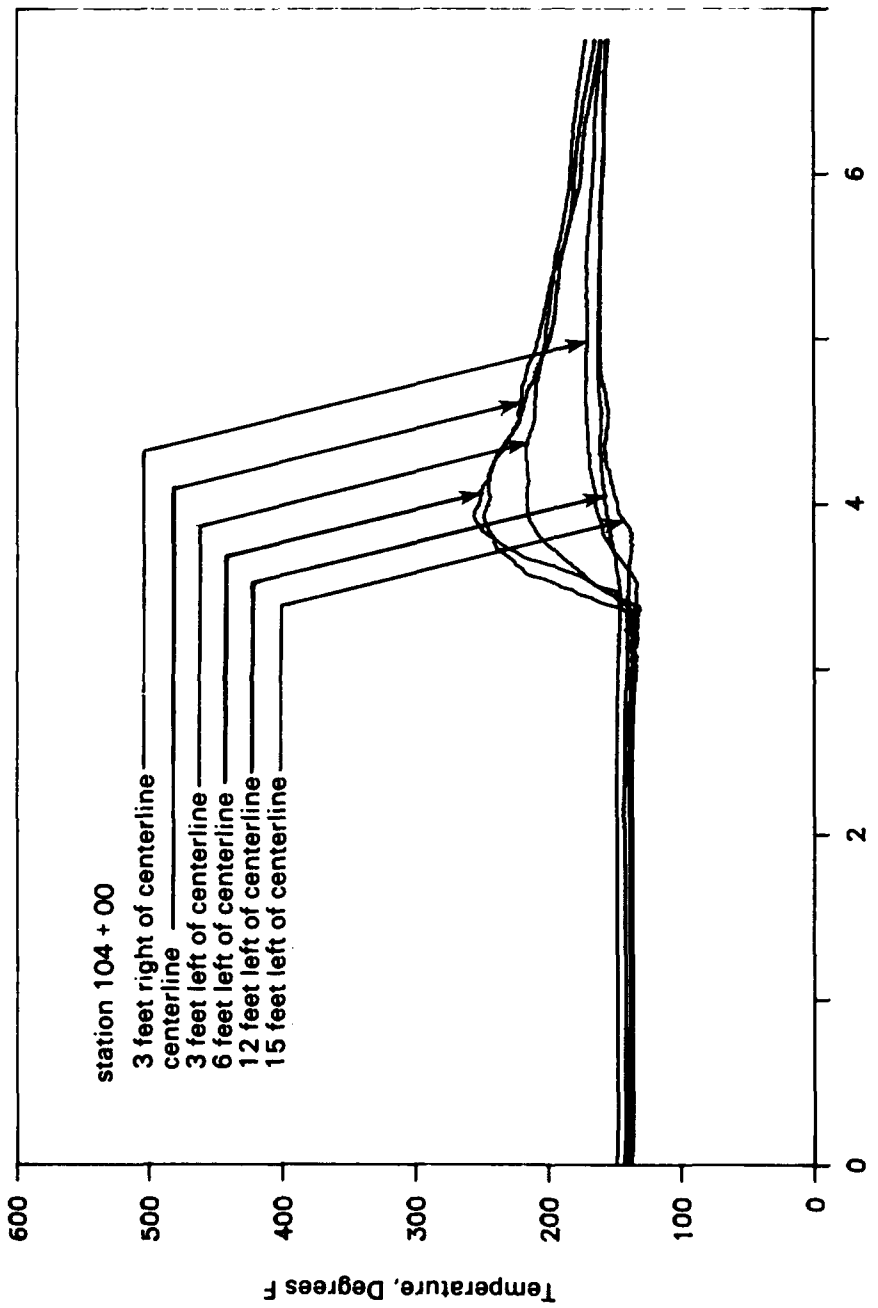

Figure 3-6. Temperatures of flow approximately 1/2 inch above surface of joint seal during T-38 takeoff (takeoff at 1124, 8/4/88).

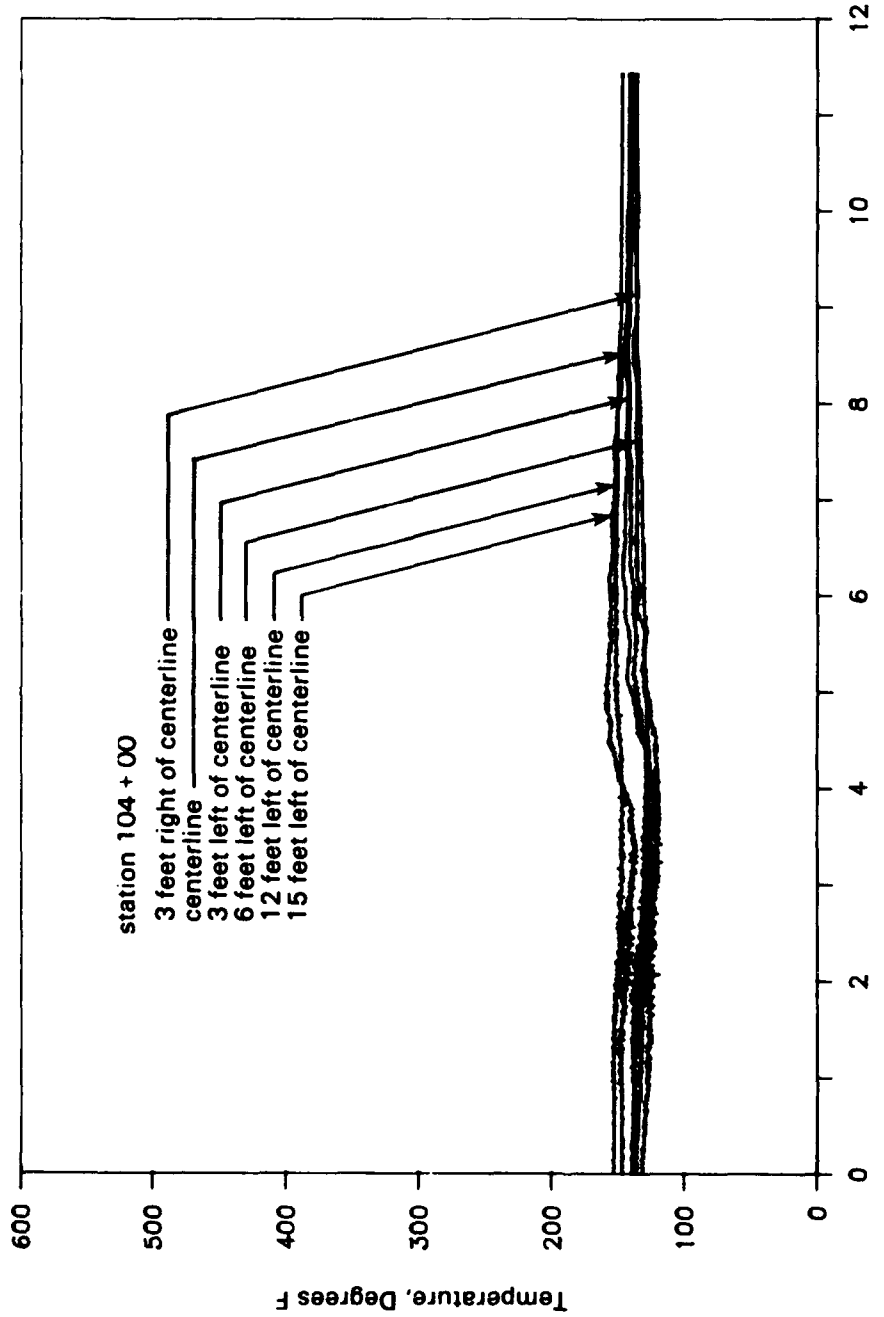

Figure 3-7. Temperatures of flow approximately 1/2 inch above surface of joint seal during KC-135 takeoff (takeoff at 1342, 8/4/88).

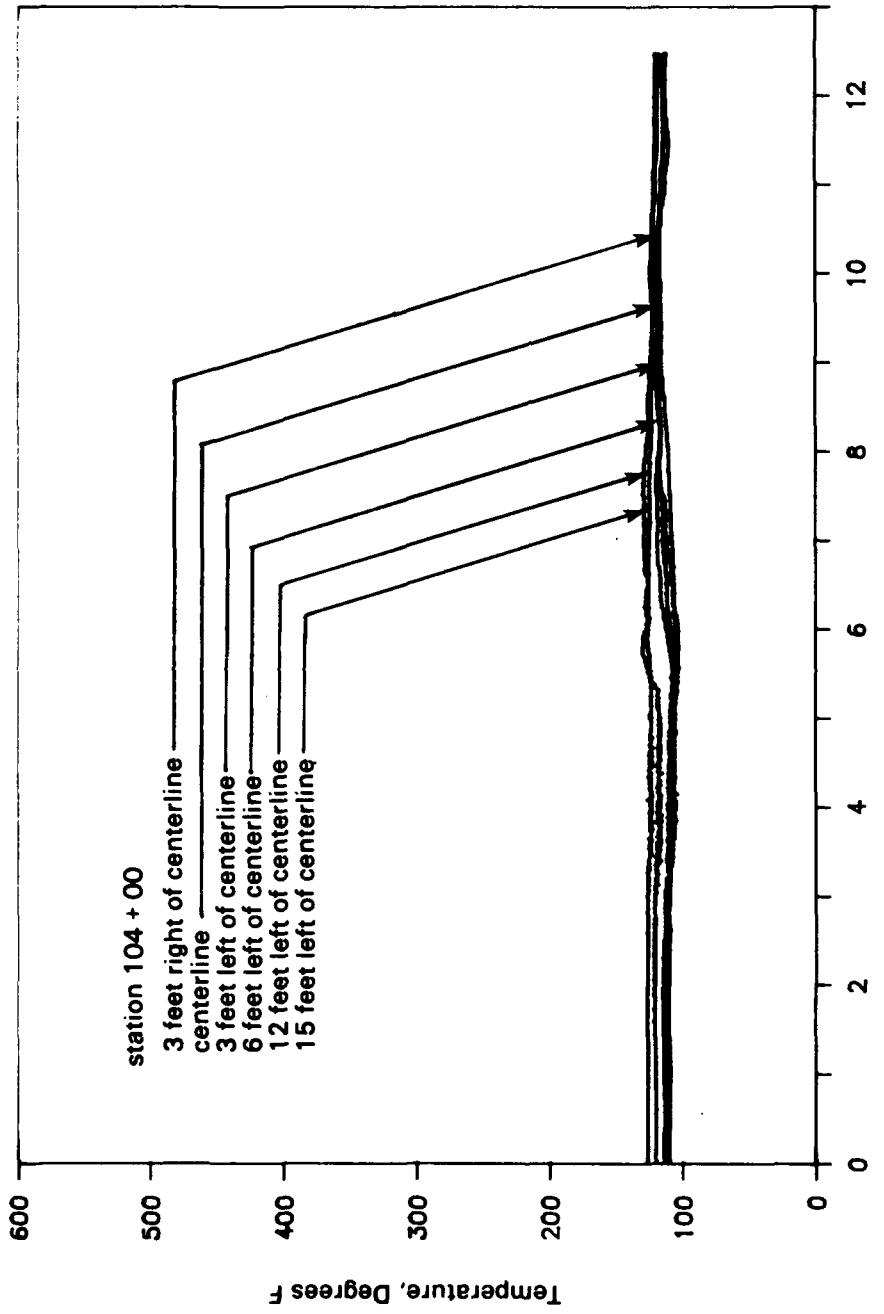

Figure 3-8. Temperatures of flow approximately 1/2 inch above surface of joint seal during B-52 takeoff (takeoff at 0947, 8/4/88).

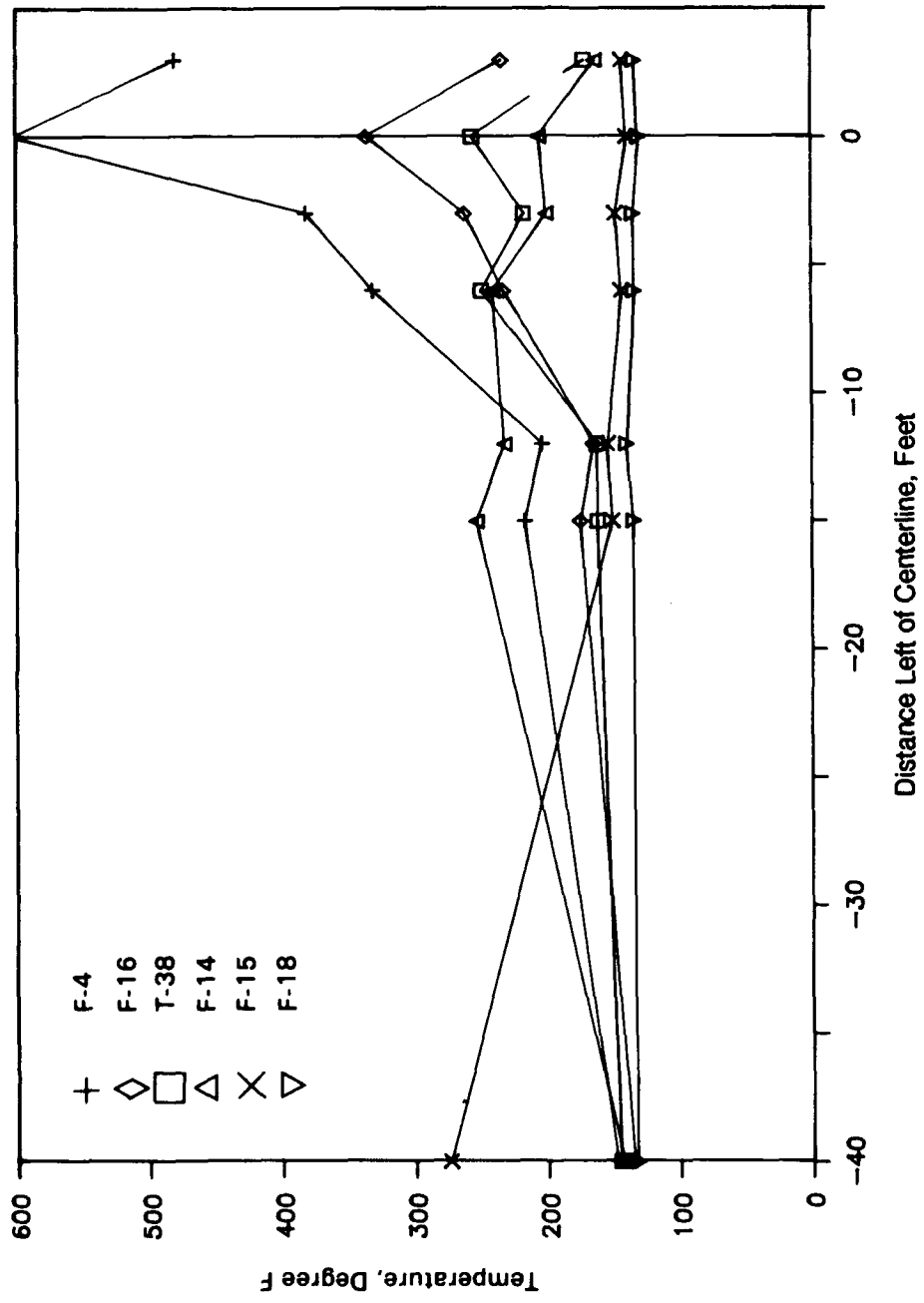

Figure 3-9. Distribution of maximum temperatures reached during takeoffs of various aircraft with afterburner engines.

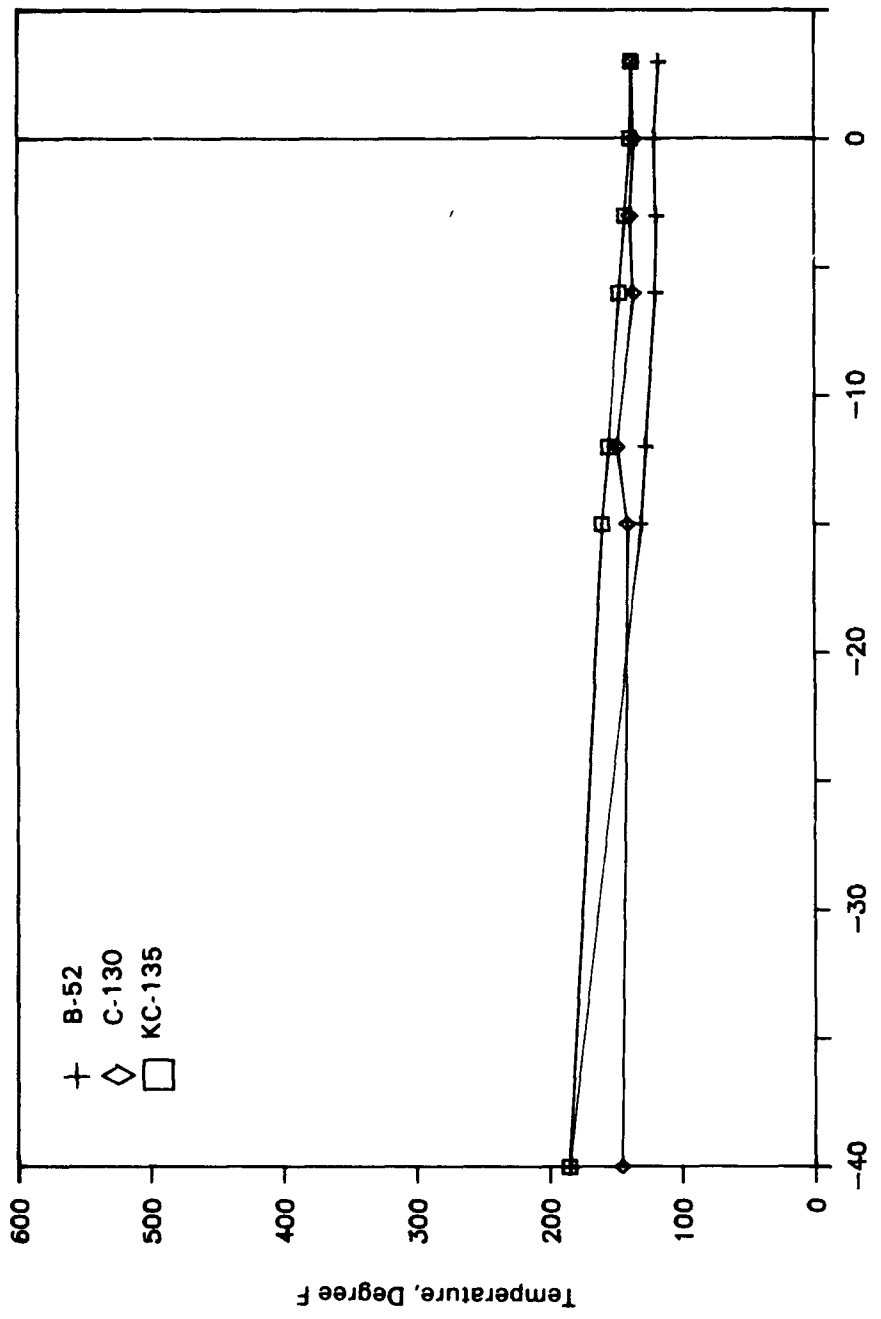

Figure 3-10. Distribution of maximum temperatures reached during takeoffs of various multi-engine cargo and bomber aircraft.

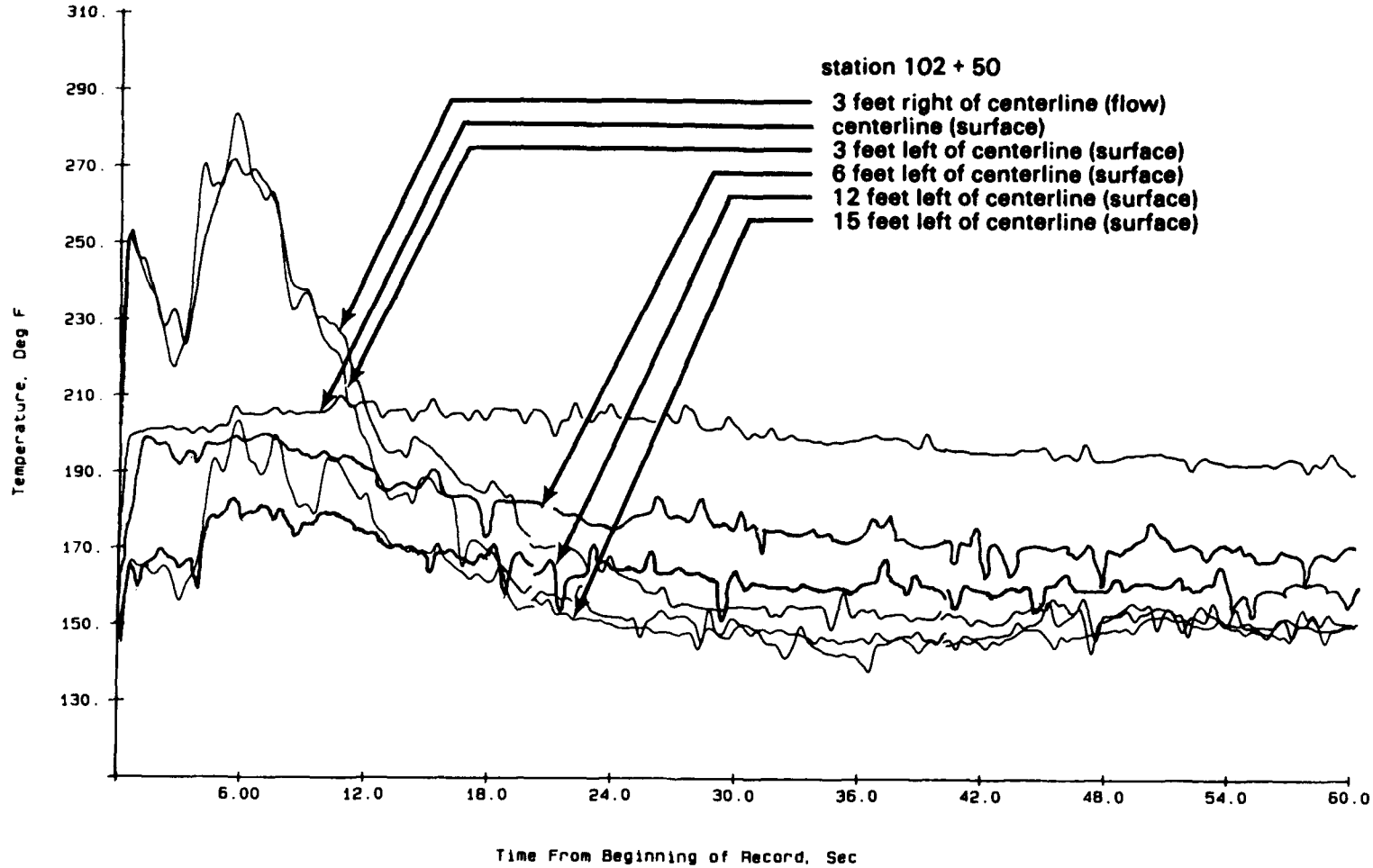

Figure 3-11. Temperatures at joint seal surface, and in flow 1/2 inch above surface of joint seal, during F-4 takeoff (takeoff at 1511, 6/15/88).

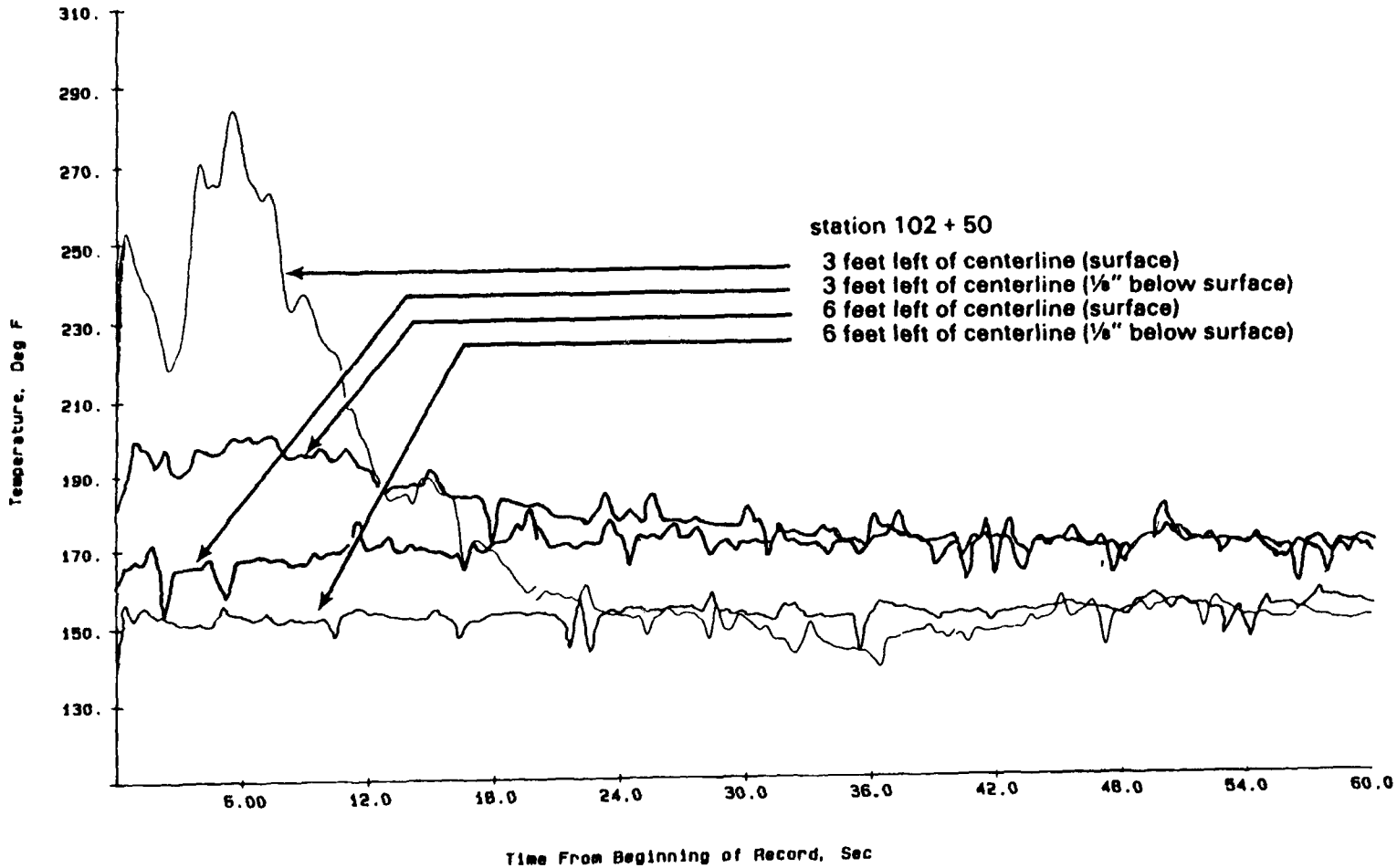

Figure 3-12. Temperatures at joint seal surface, and below surface during F-4 takeoff (takeoff at 1511, 6/15/88).

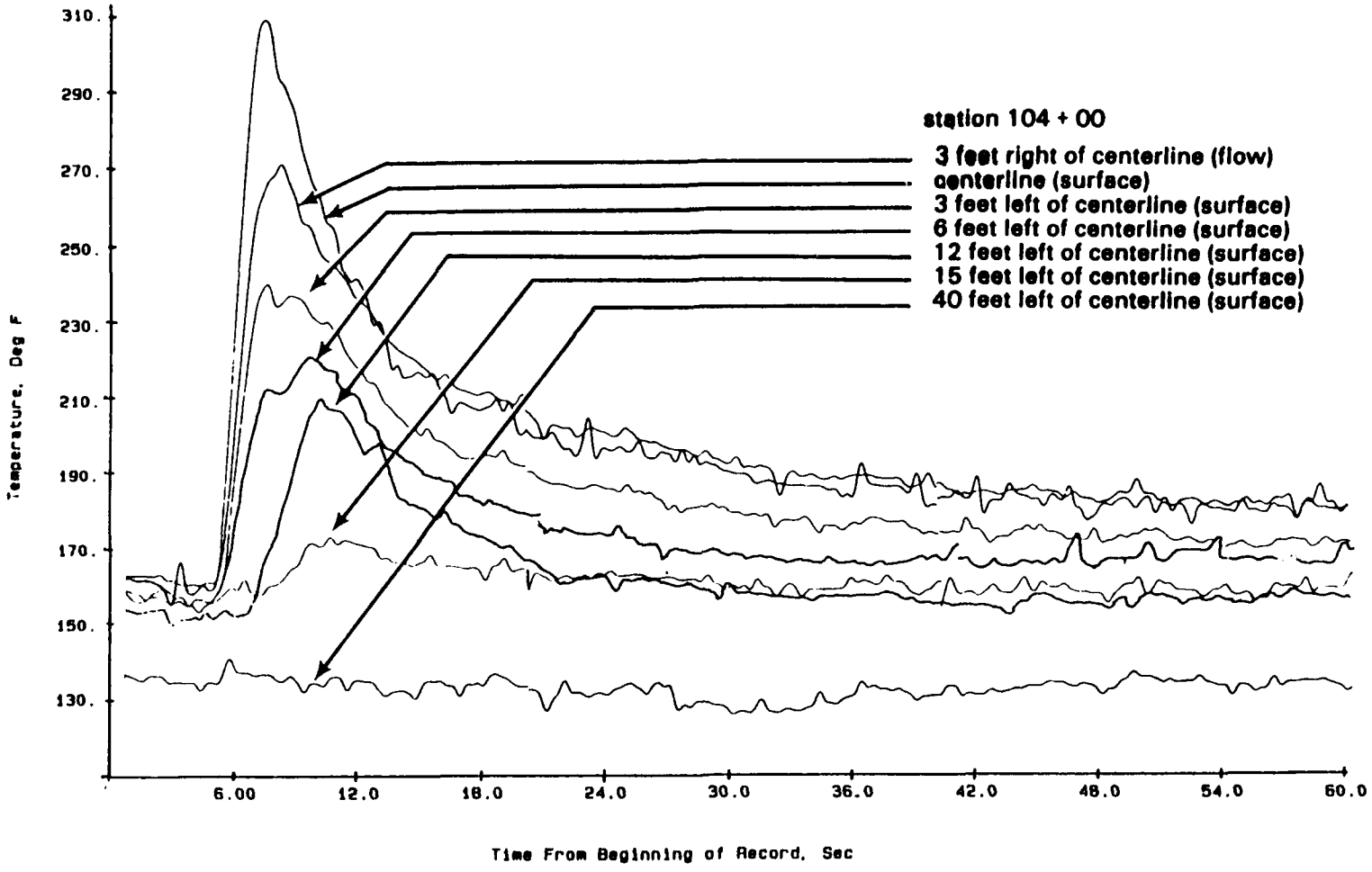

Figure 3-13. Temperatures at joint seal surface, and in flow 1/2 inch above surface of joint seal, during F-4 takeoff (takeoff at 1511, 6/15/88).

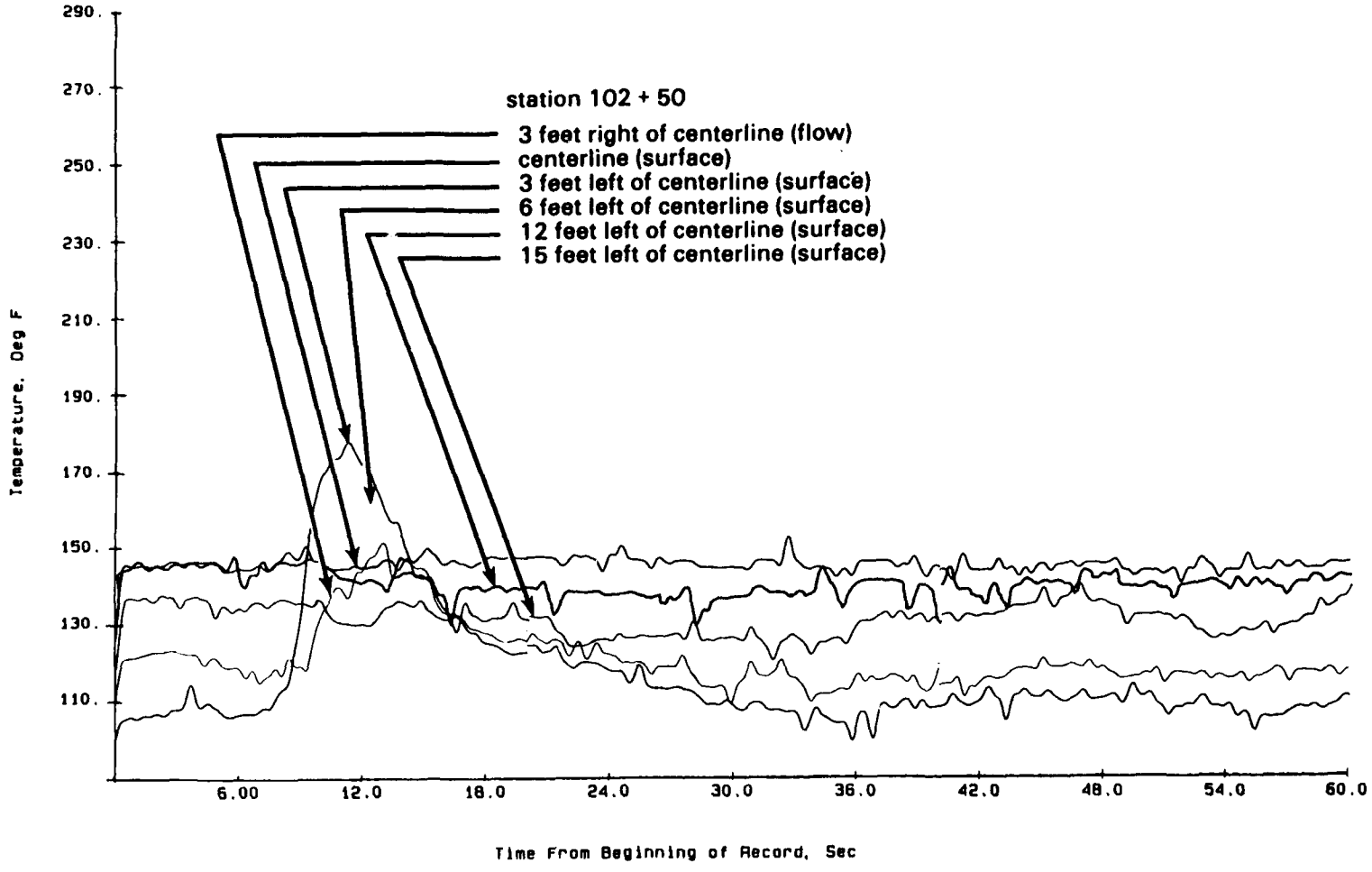

Figure 3-14. Temperatures at joint seal surface, and in flow 1/2 inch above surface of joint seal, during F-16 takeoff (takeoff at 1134, 6/16/88).

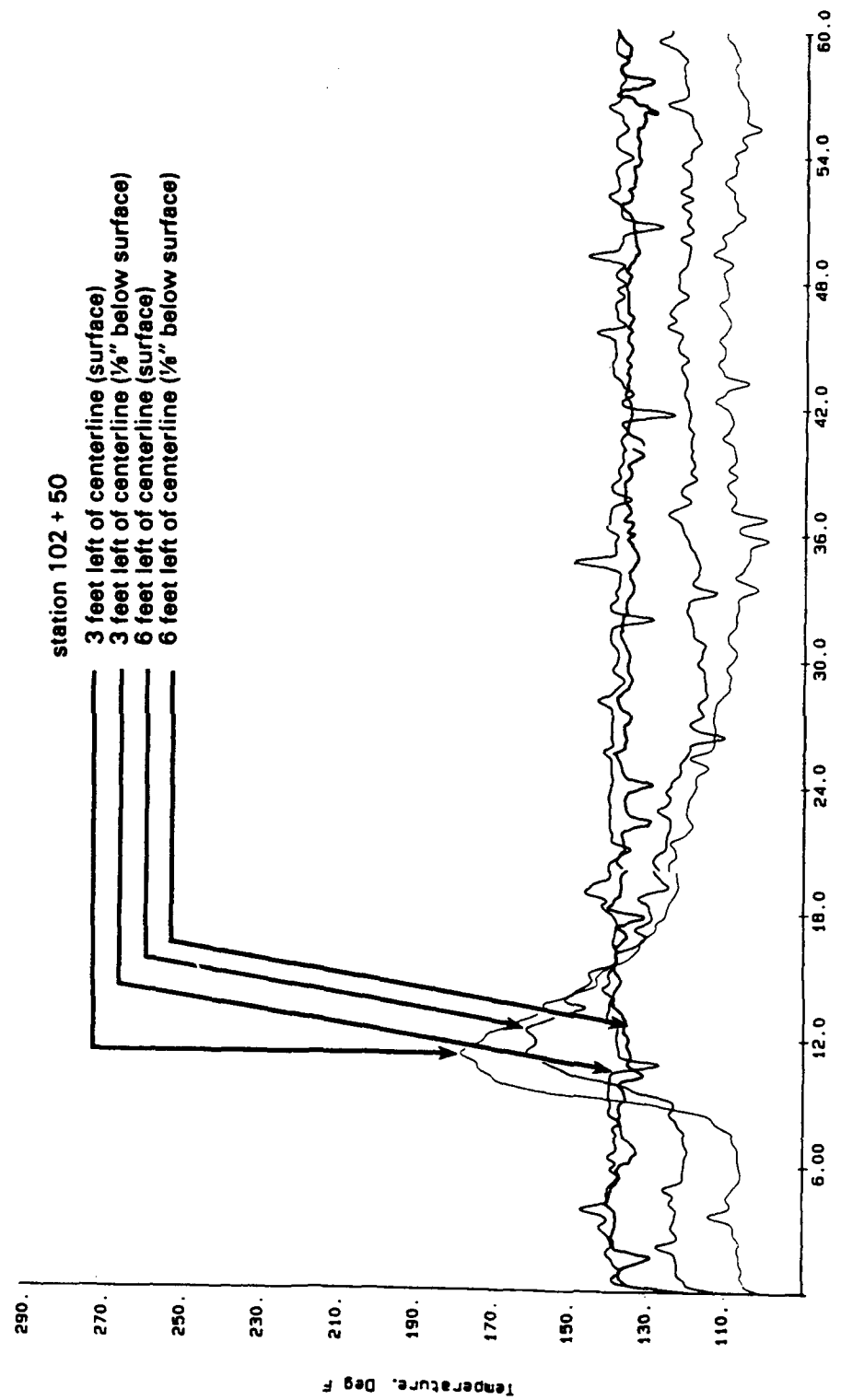

Figure 3-15. Temperatures at joint seal surface, and below surface during F-16 takeoff (takeoff at 1134, 6/16/88).

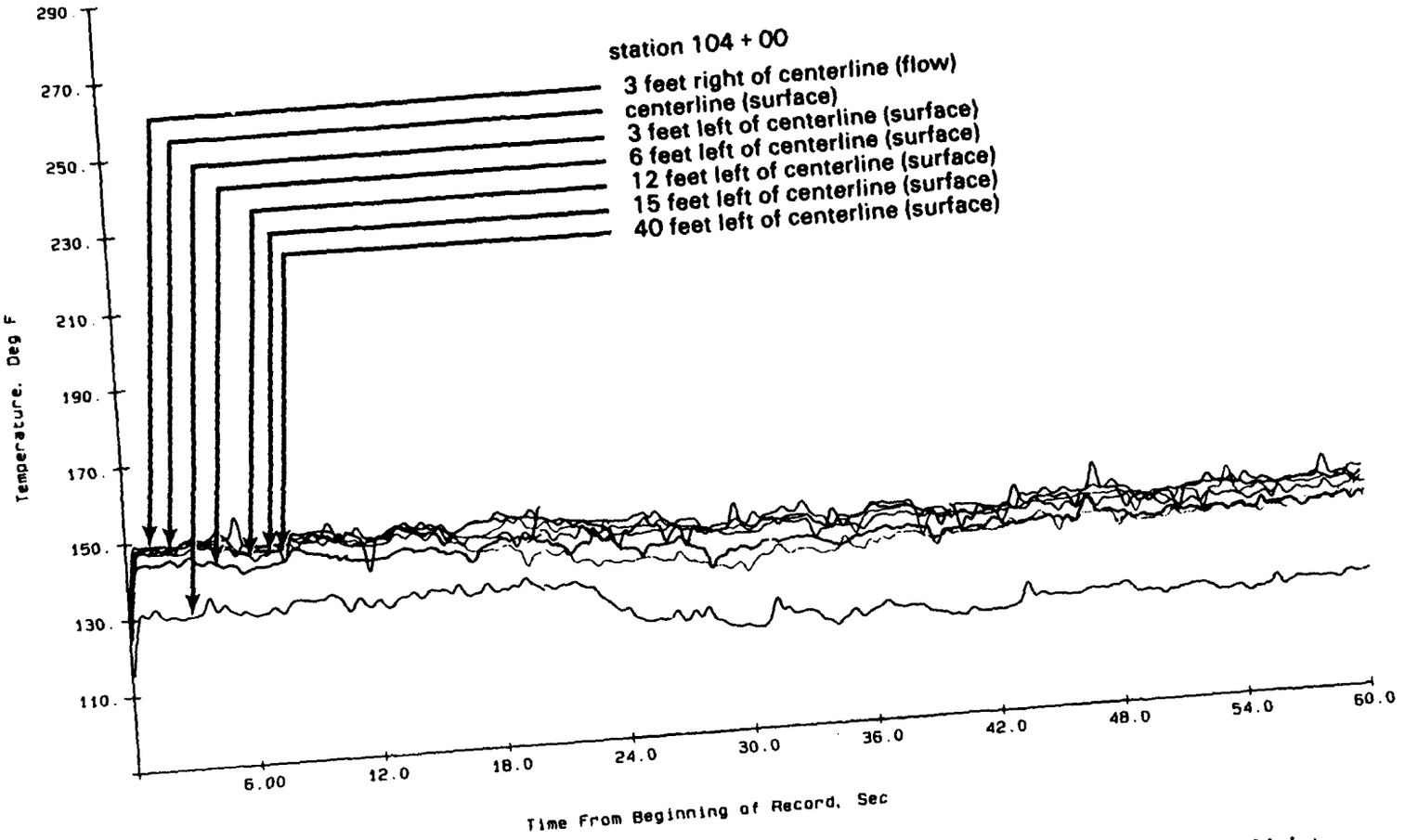

Figure 3-16. Temperatures at joint seal surface, and in flow 1/2 inch above surface of joint seal, during F-16 takeoff (takeoff at 1134, 6/16/88).

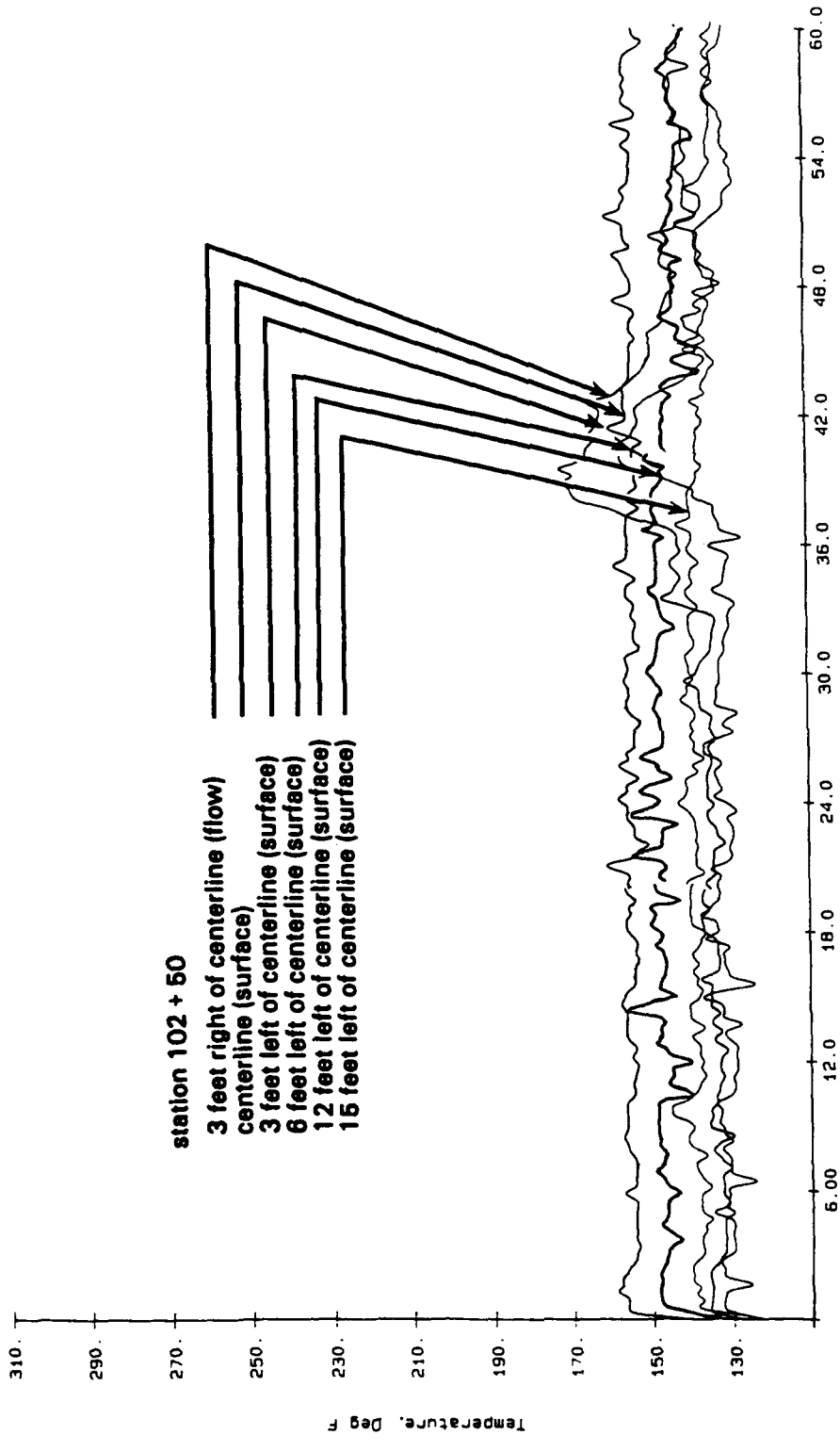

Figure 3-17. Temperatures at joint seal surface, and in flow 1/2 inch above surface of joint seal, during F-15 takeoff (takeoff at 1517, 6/15/88).

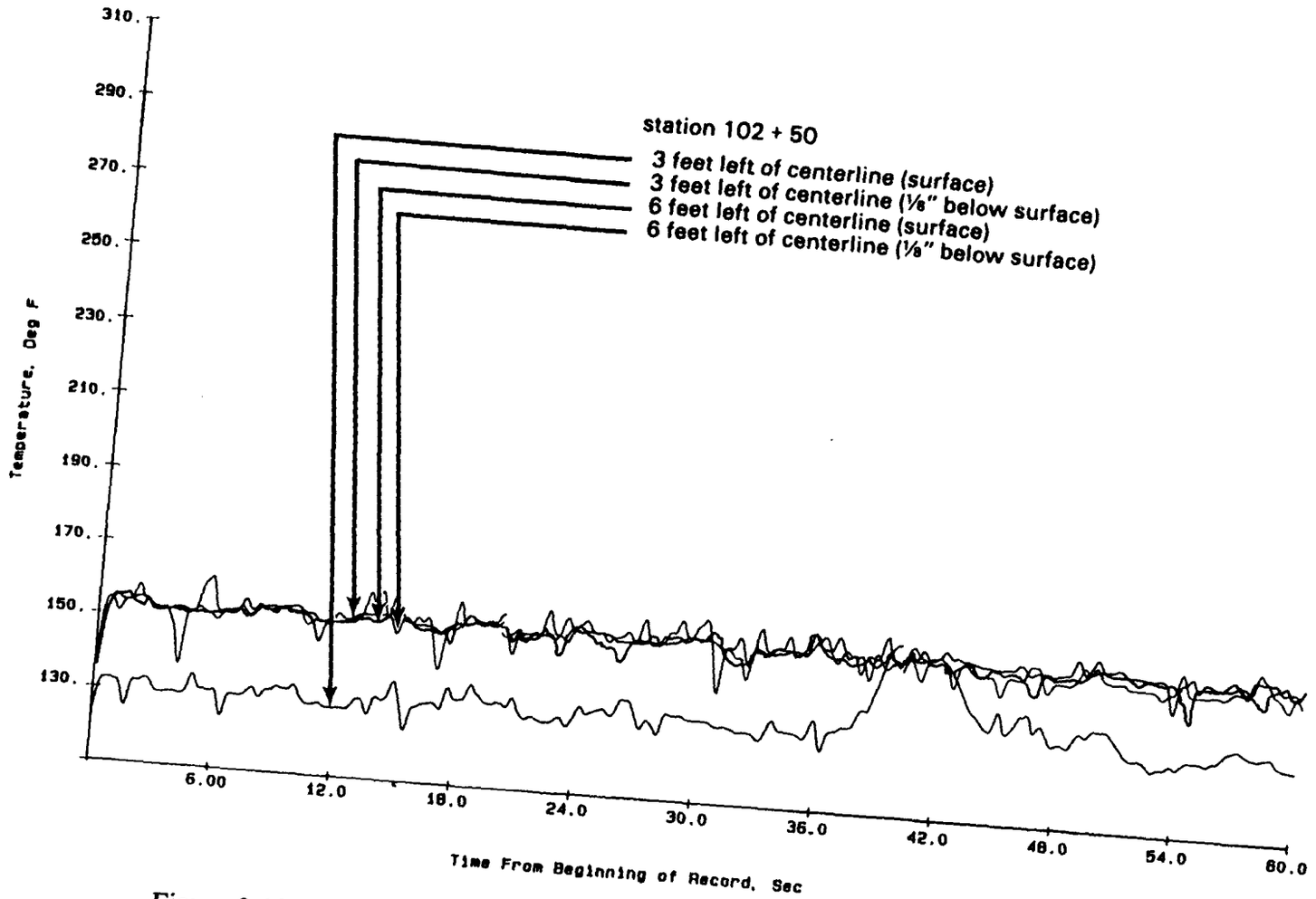

Figure 3-18. Temperatures at joint seal surface, and below surface during F-15 takeoff (takeoff at 1517, 6/15/88).

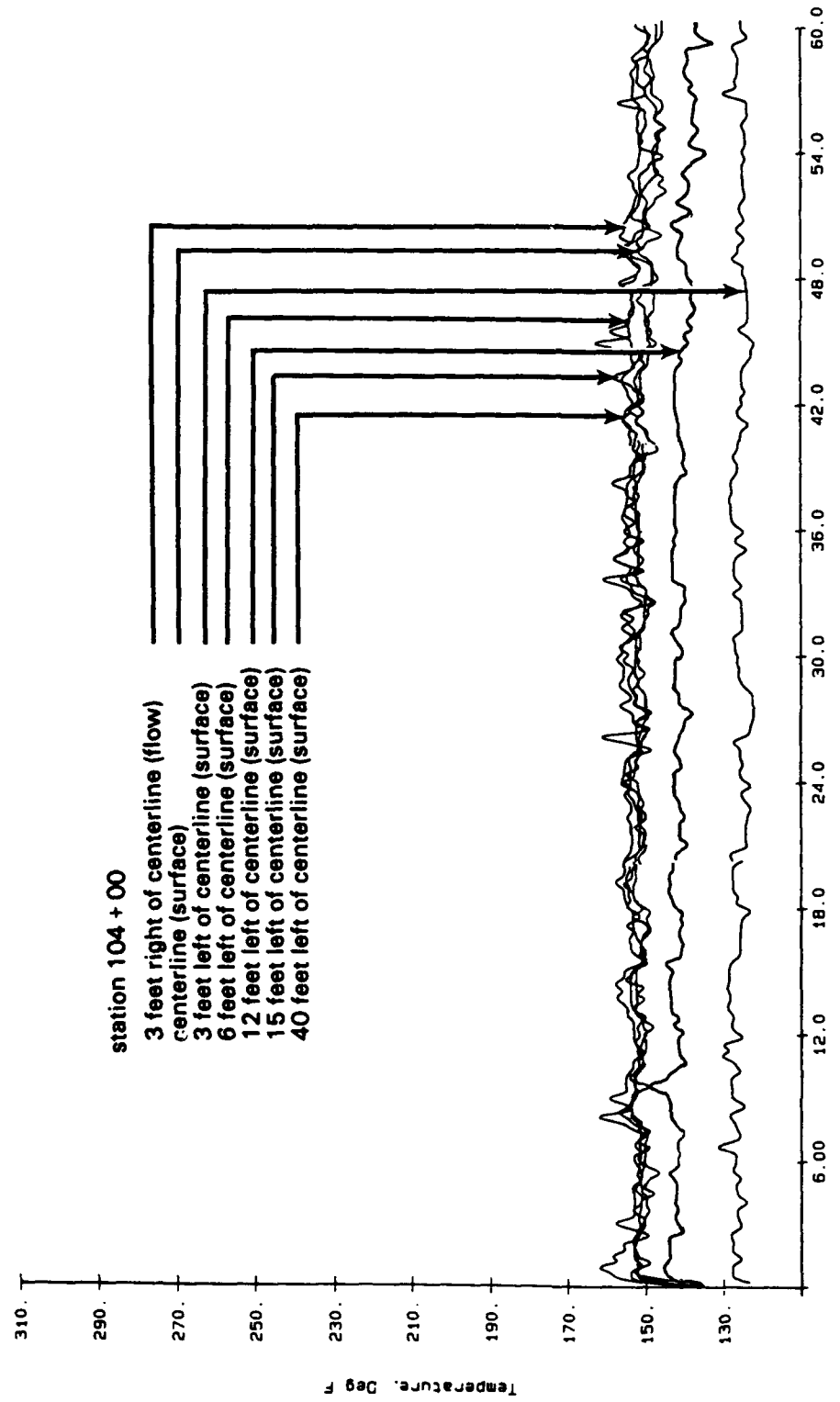

Figure 3-19. Temperatures at joint seal surface, and in flow 1/2 inch above surface of joint seal, during F-15 takeoff (takeoff at 1517, 6/15/88).

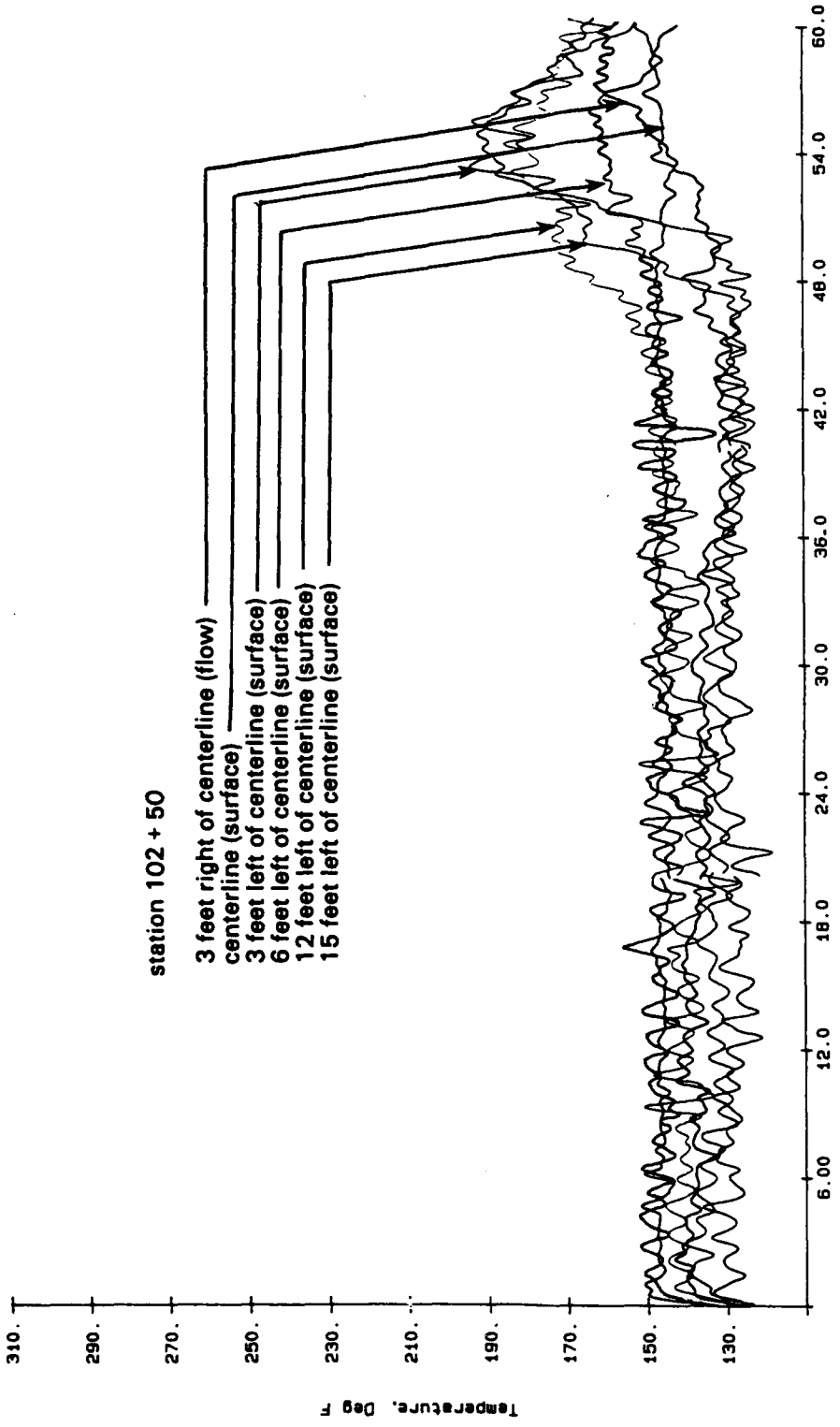

Figure 3-20. Temperatures at joint seal surface, and in flow 1/2 inch above surface of joint seal, during T-38 takeoff (takeoff at 1103, 6/16/88).

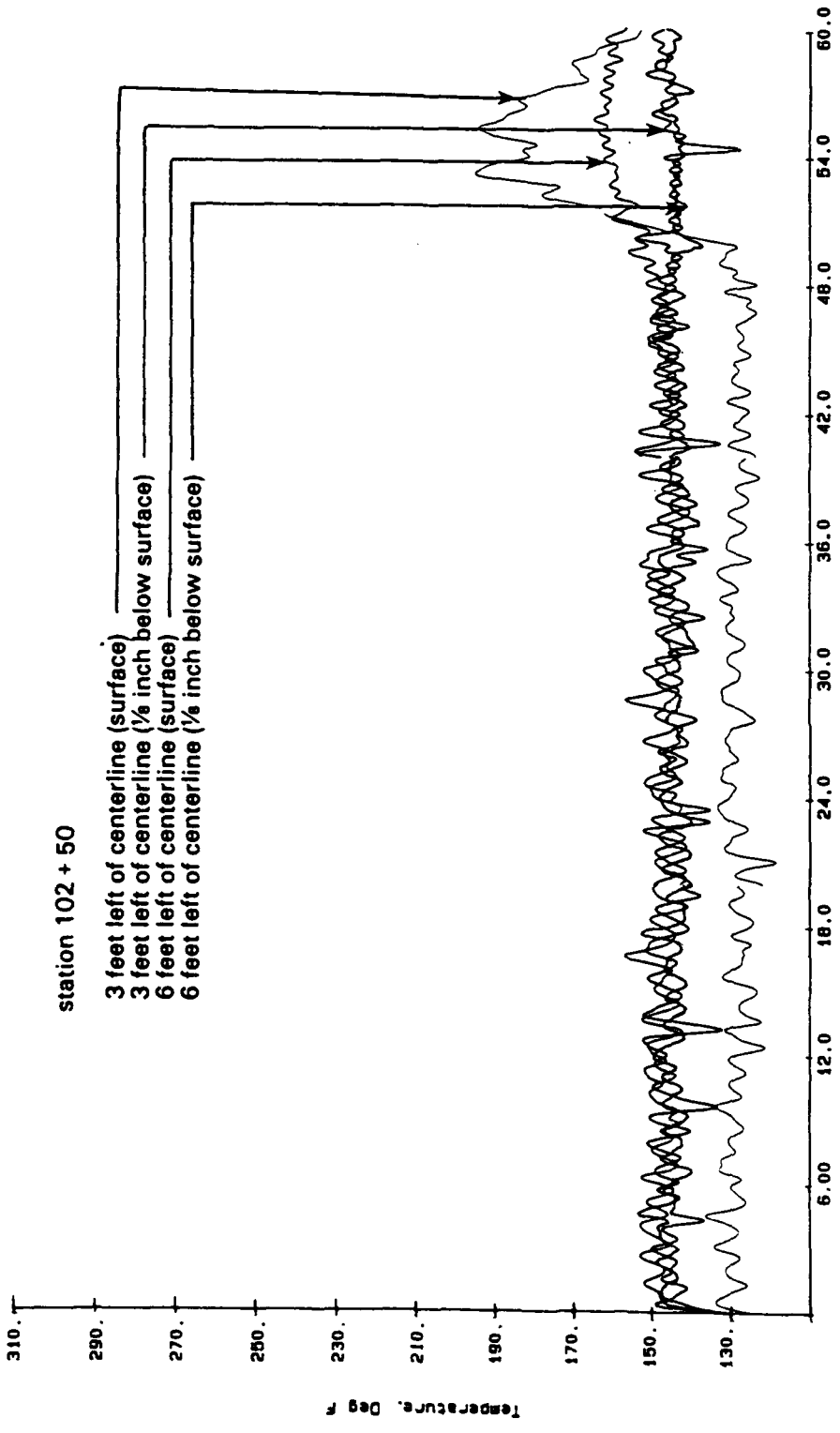

Figure 3-21. Temperatures at joint seal surface, and below surface during T-38 takeoff (takeoff at 1103, 6/16/88).

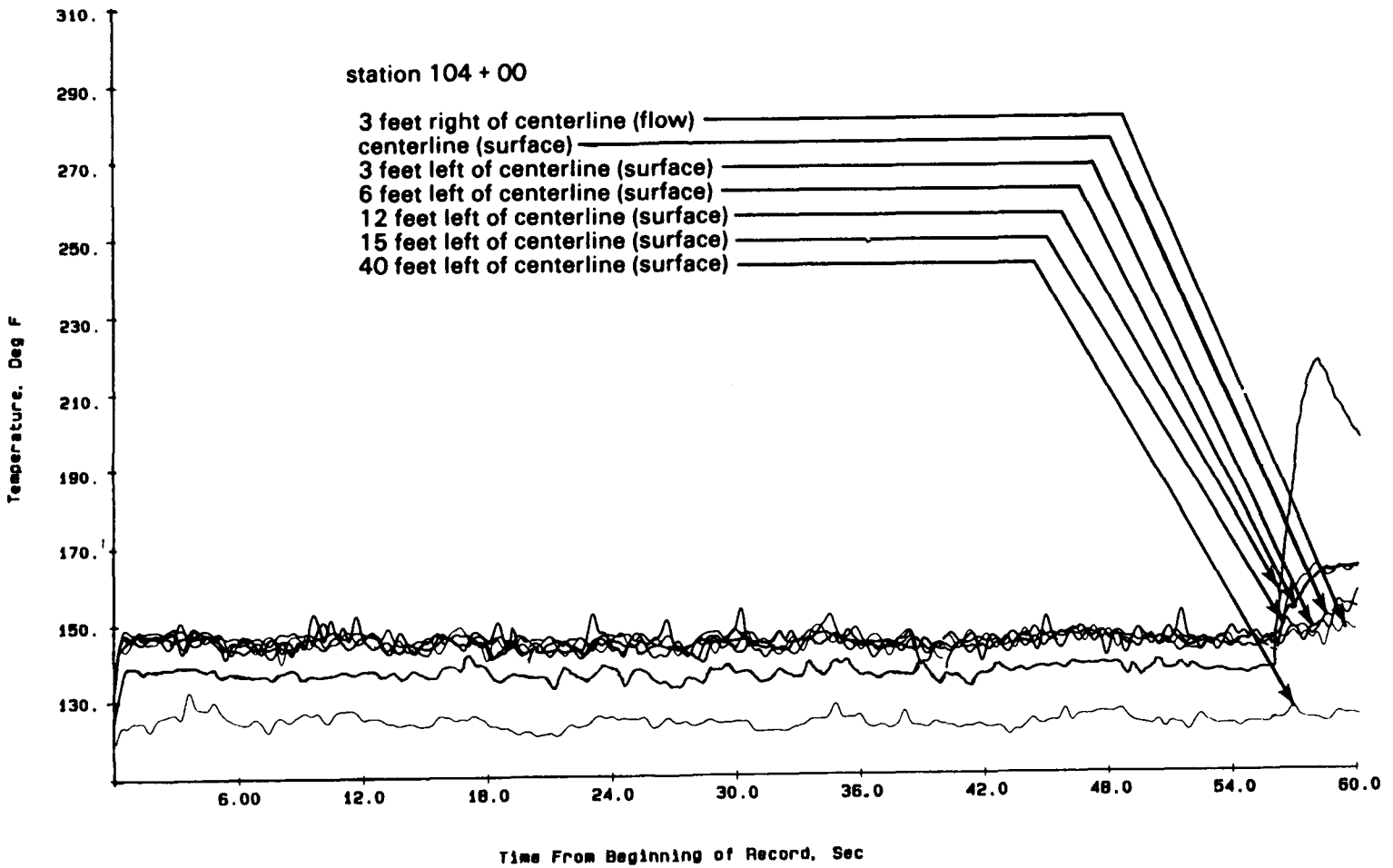

Figure 3-22. Temperatures at joint seal surface, and in flow 1/2 inch above surface of joint seal, during T-38 takeoff (takeoff at 1103, 6/16/88).

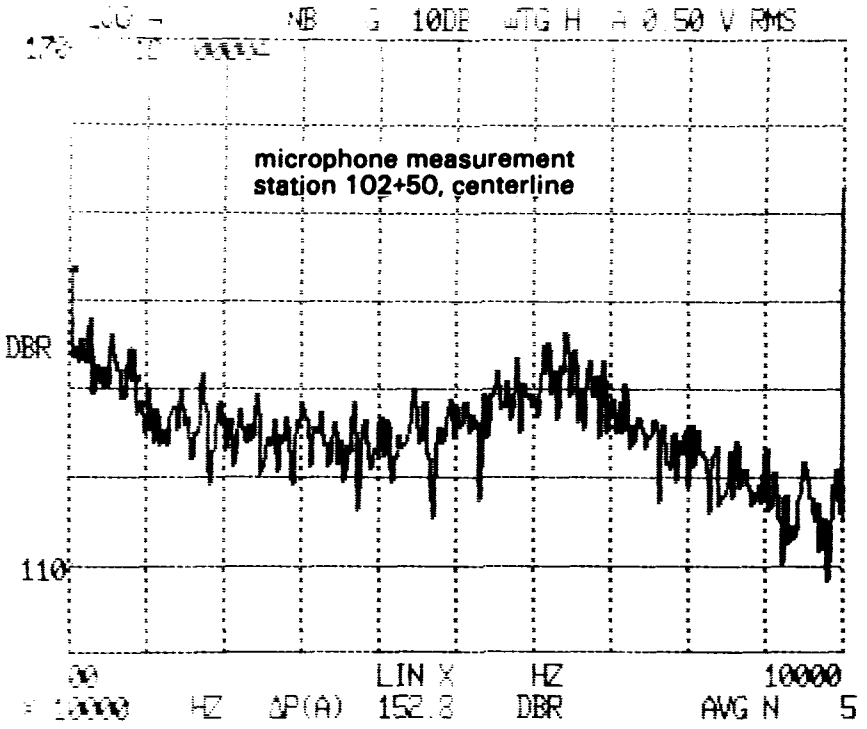

Figure 3-23. Narrow band spectrum of noise at joint seal surface during F-4 takeoff (takeoff at 1511, 6/15/88).

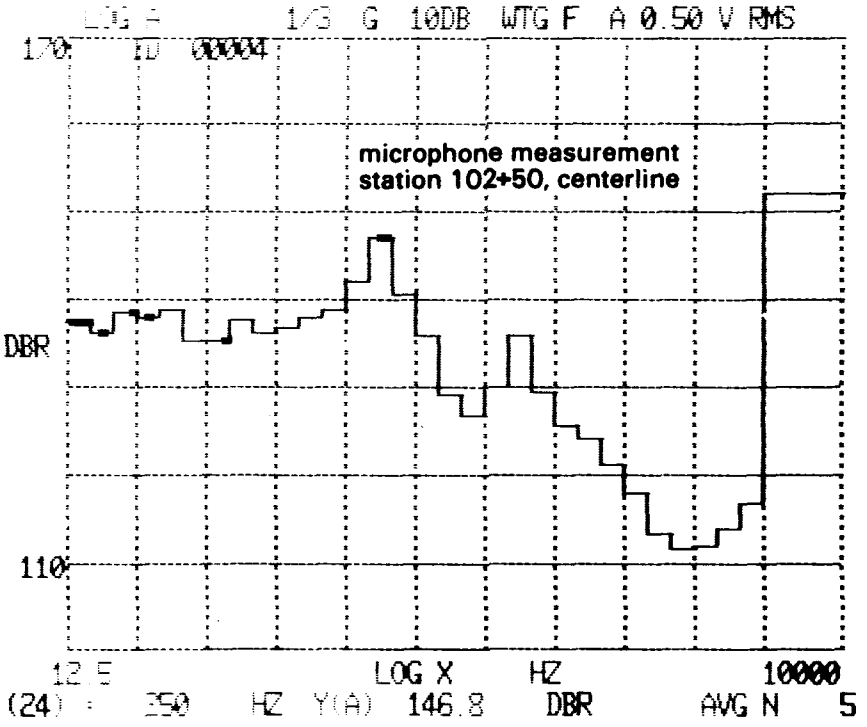

Figure 3-24. One-third octave band spectrum of noise at joint seal surface during F-4 takeoff (takeoff at 1511, 6/15/88).

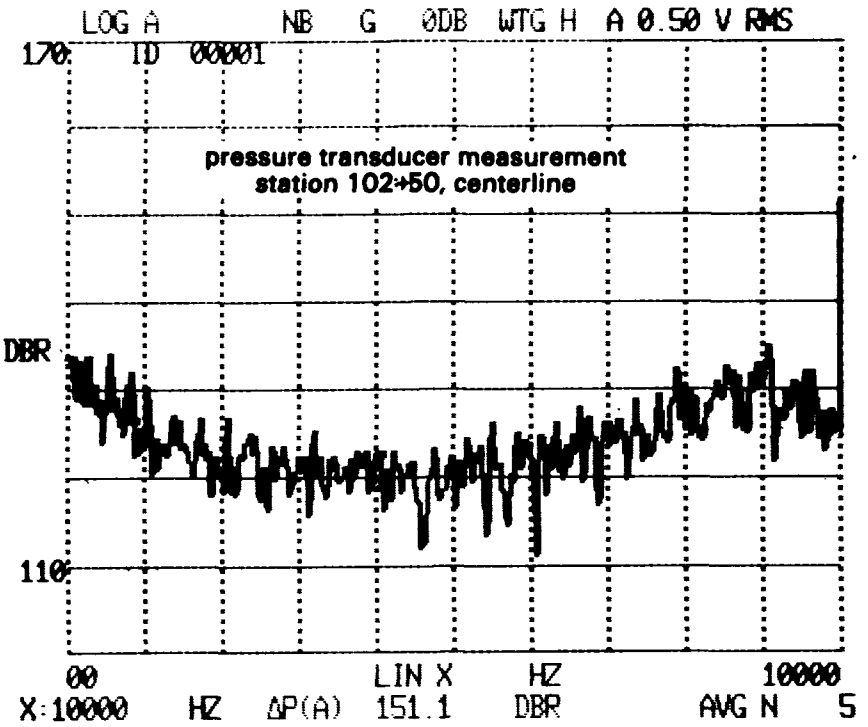

Figure 3-25. Narrow band spectrum of noise at joint seal surface during F-4 takeoff (takeoff at 1511, 6/15/88).

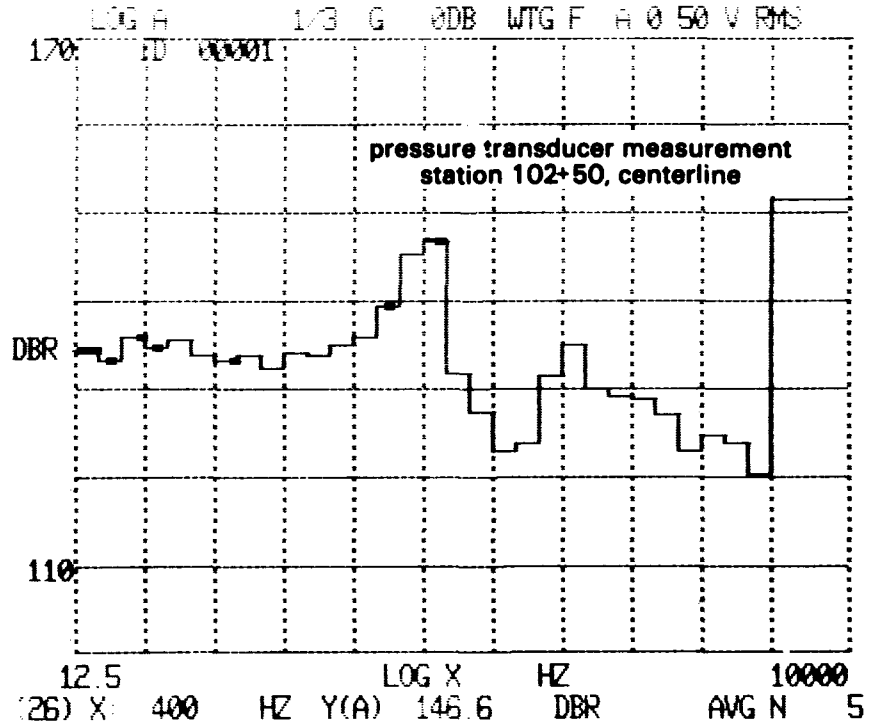

Figure 3-26. One-third octave band spectrum of noise at joint seal surface during F-4 takeoff (takeoff at 1511, 6/15/88).

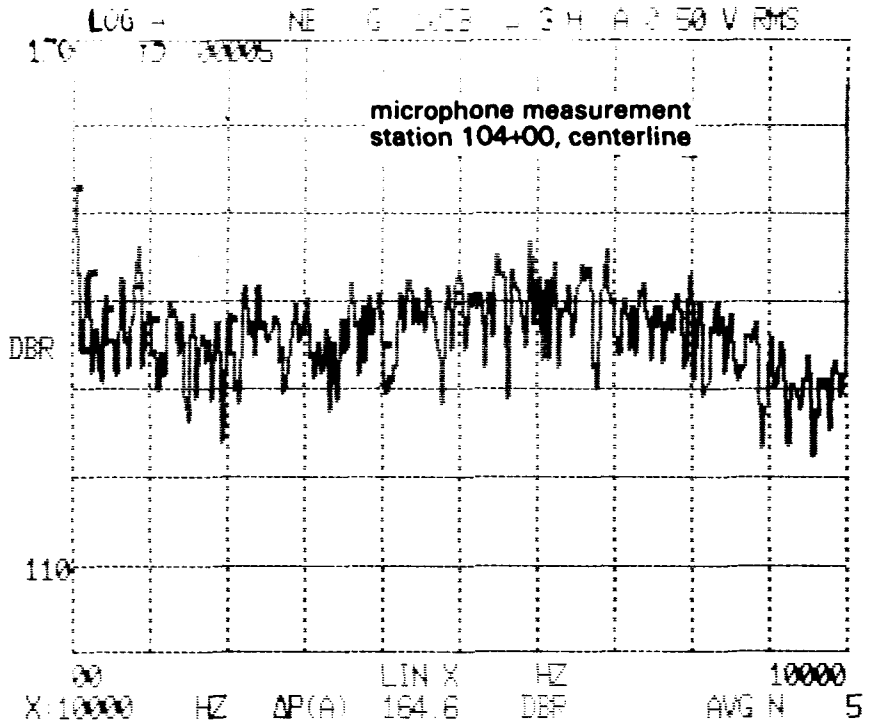

Figure 3-27. Narrow band spectrum of noise at joint seal surface during F-4 takeoff (takeoff at 1511, 6/15/88).

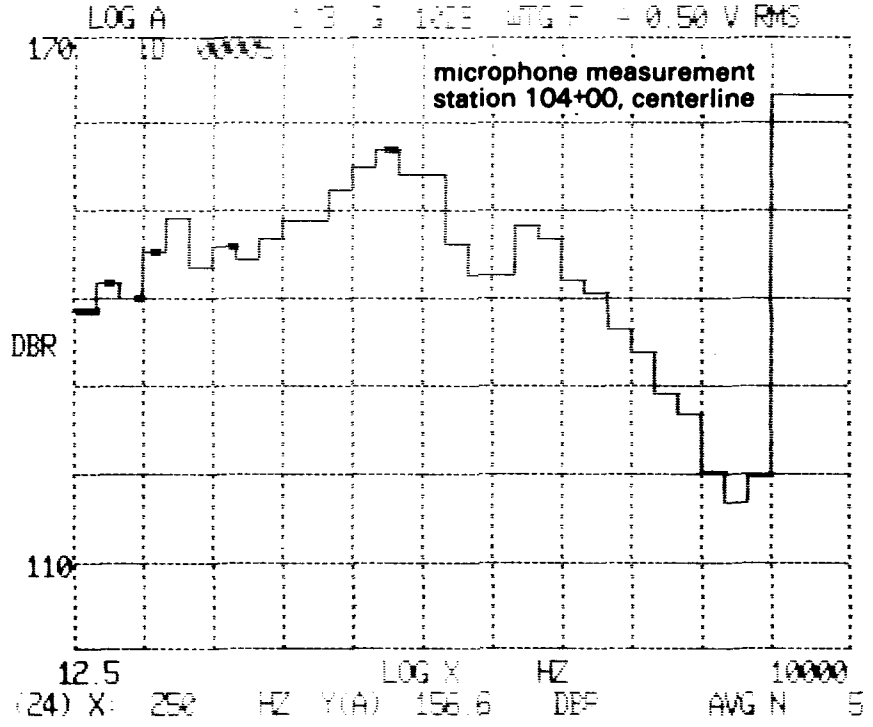

Figure 3-28. One-third octave band spectrum of noise at joint seal surface during F-4 takeoff (takeoff at 1511, 6/15/88).

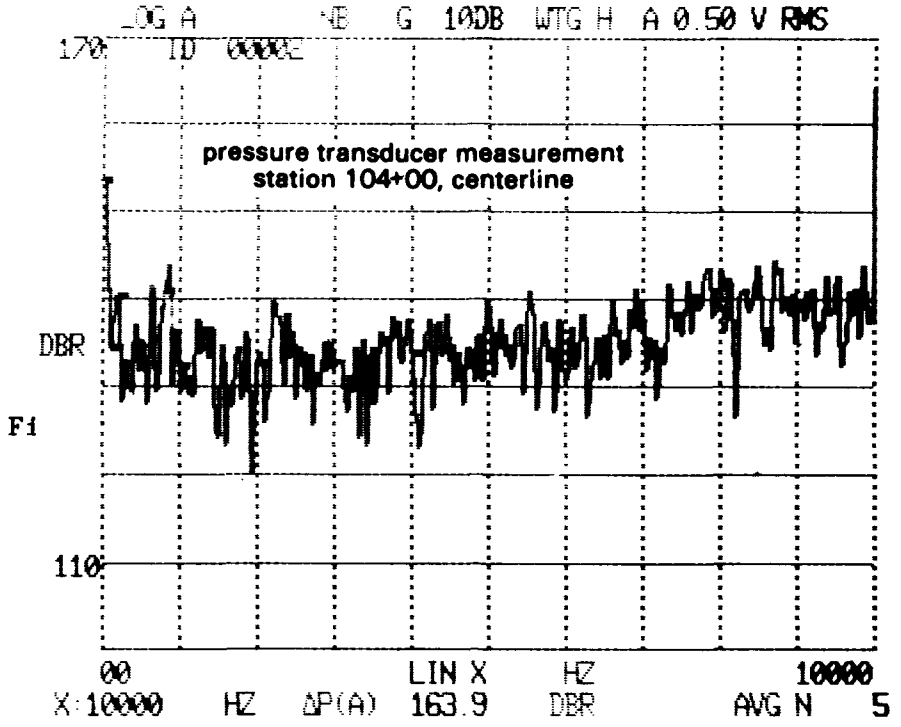

Figure 3-29. Narrow band spectrum of noise at joint seal surface during F-4 takeoff (takeoff at 1511, 6/15/88).

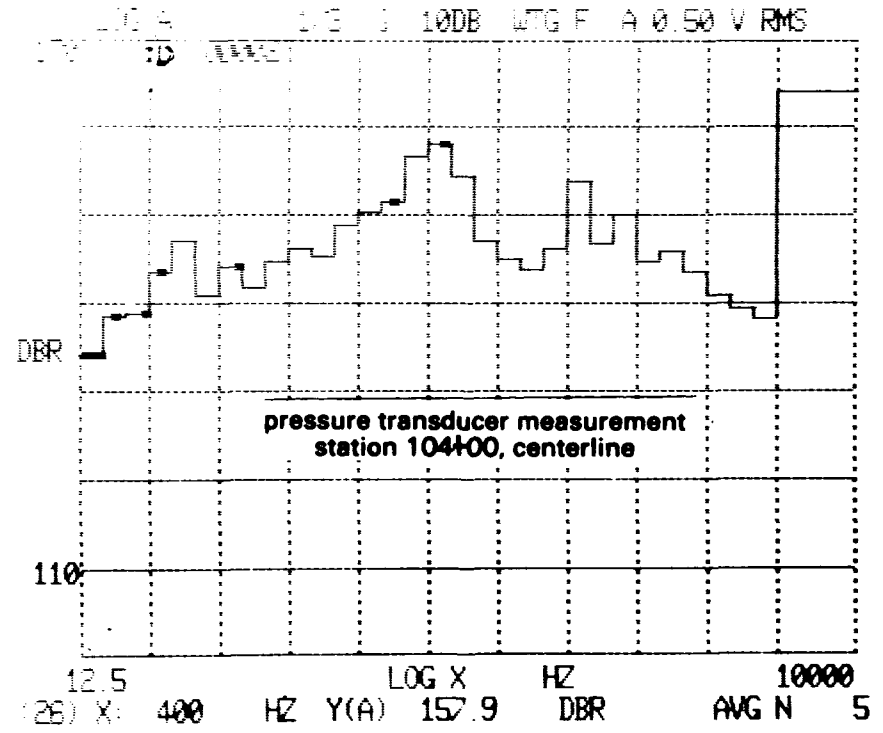

Figure 3-30. One-third octave band spectrum of noise at joint seal surface during F-4 takeoff (takeoff at 1511, 6/15/88).

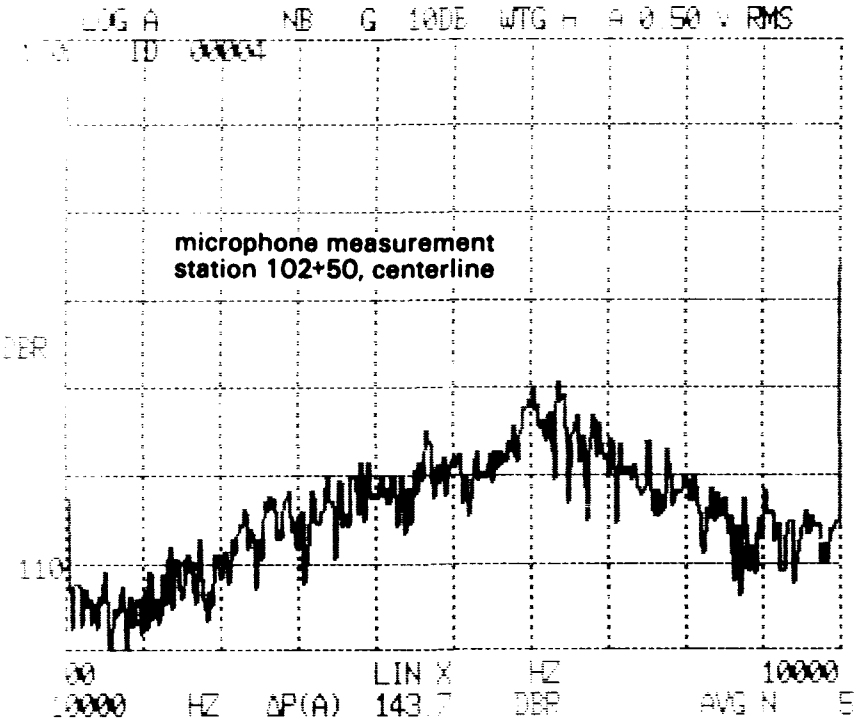

Figure 3-31. Narrow band spectrum of noise at joint seal surface during T-38 takeoff (takeoff at 1528, 6/15/88).

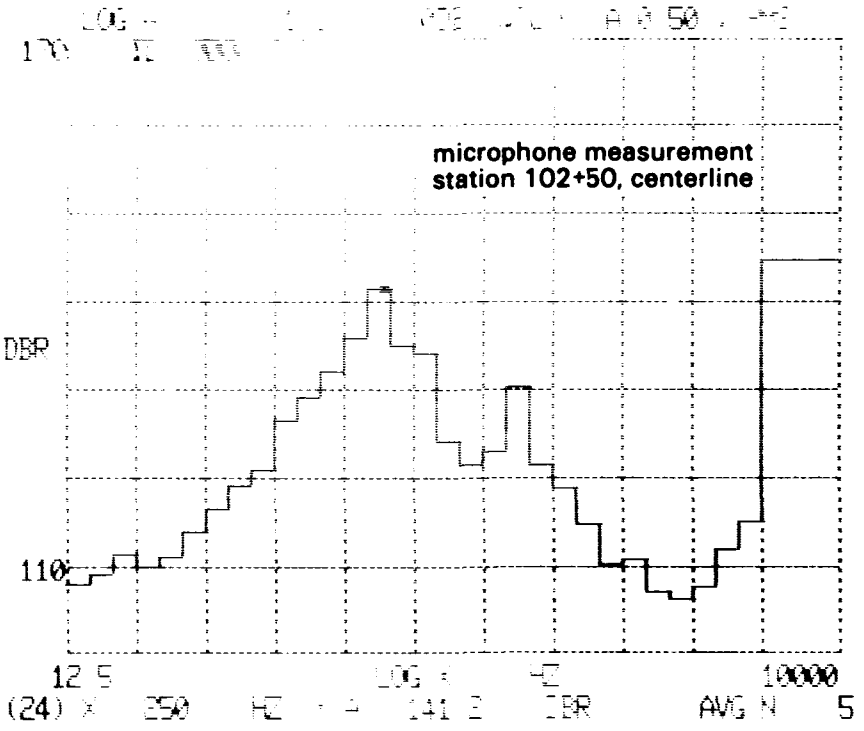

Figure 3-32. One-third octave band spectrum of noise at joint seal surface during T-38 takeoff (takeoff at 1528, 6/15/88).

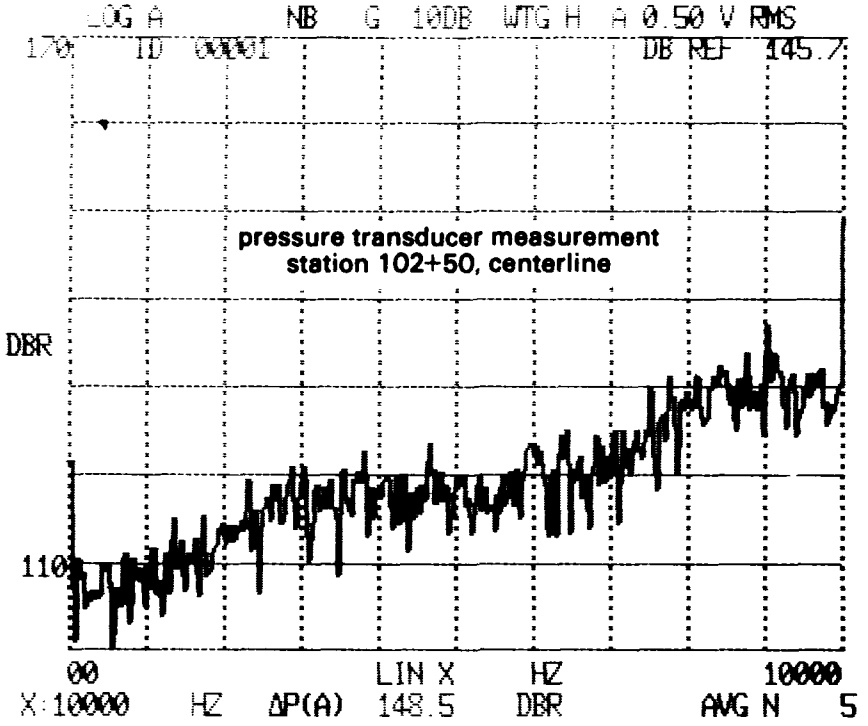

Figure 3-33. Narrow band spectrum of noise at joint seal surface during T-38 takeoff (takeoff at 1528, 6/15/88).

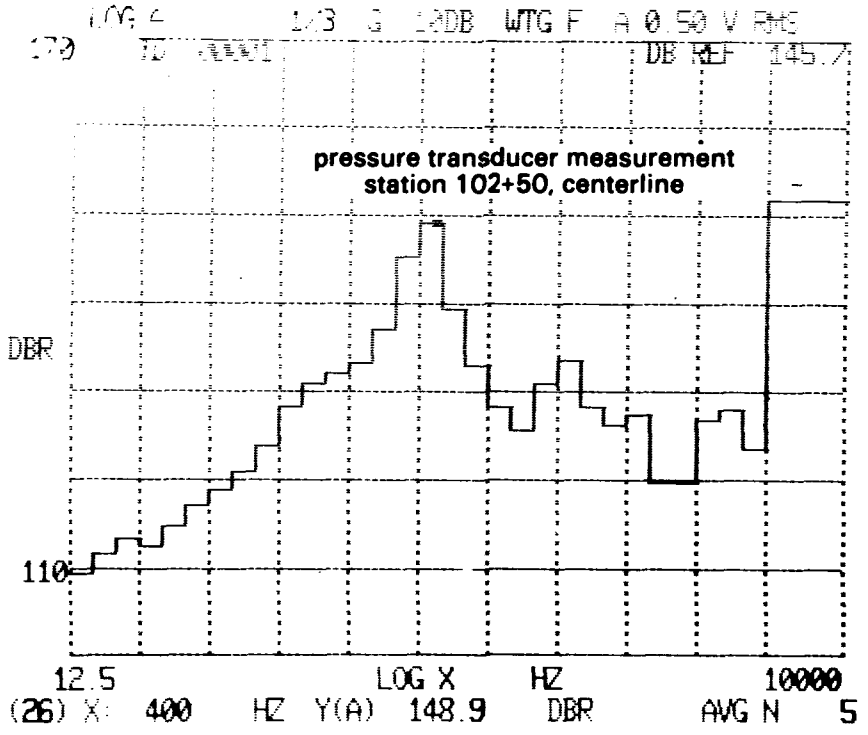

Figure 3-34. One-third octave band spectrum of noise at joint seal surface during T-38 takeoff (takeoff at 1528, 6/15/88).

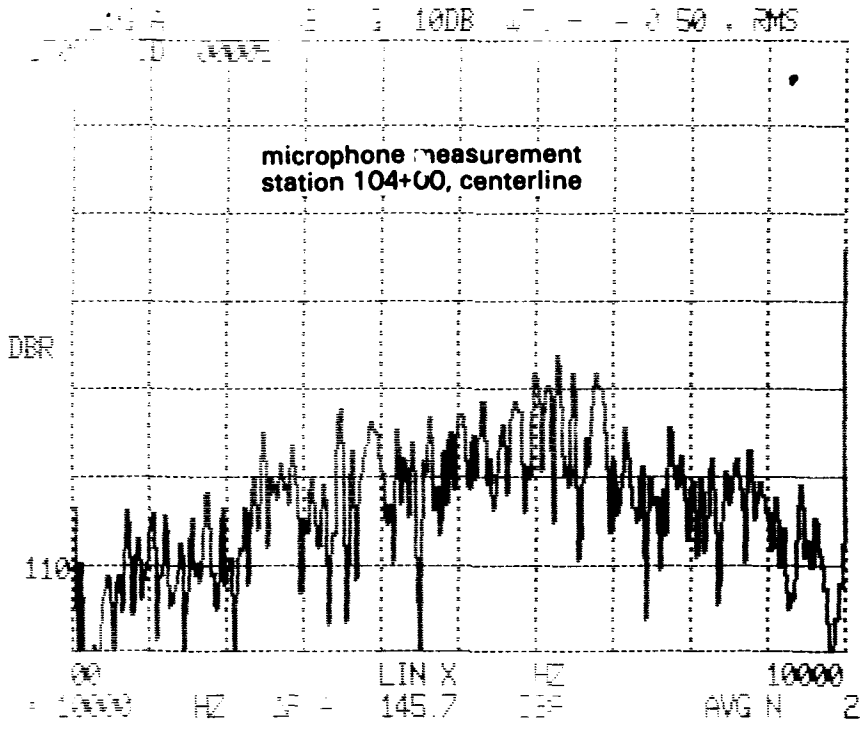

Figure 3-35. Narrow band spectrum of noise at joint seal surface during T-38 takeoff (takeoff at 1528, 6/15/88).

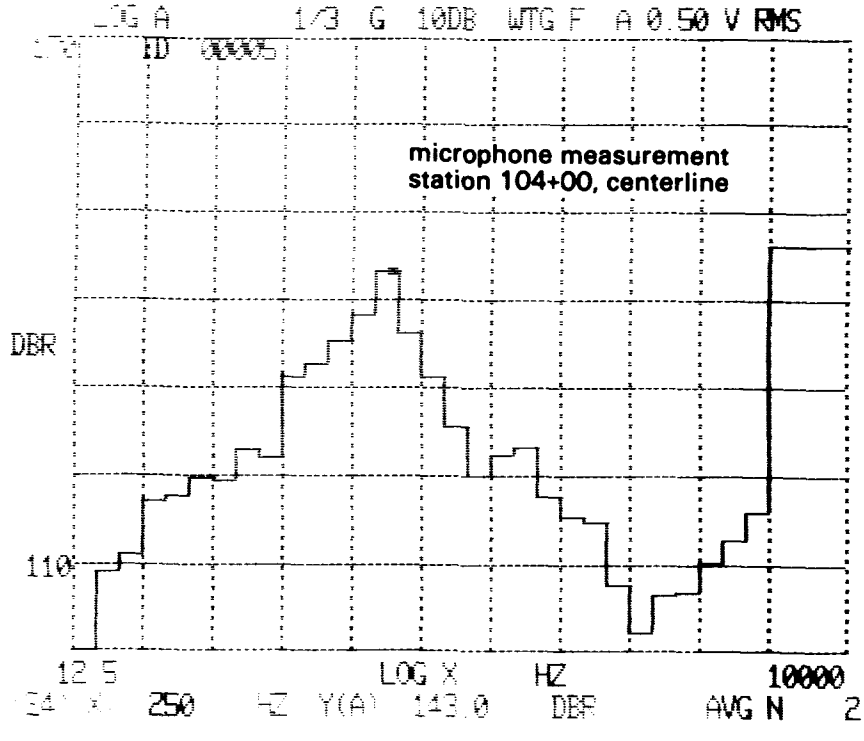

Figure 3-36. One-third octave band spectrum of noise at joint seal surface during T-38 takeoff (takeoff at 1528, 6/15/88).

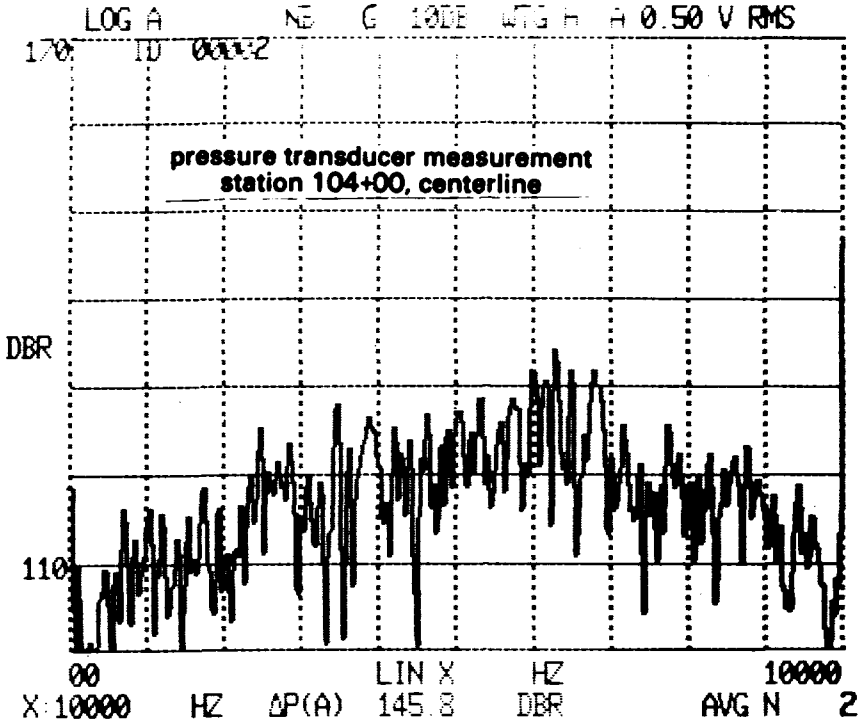

Figure 3-37. Narrow band spectrum of noise at joint seal surface during T-38 takeoff (takeoff at 1528, 6/15/88).

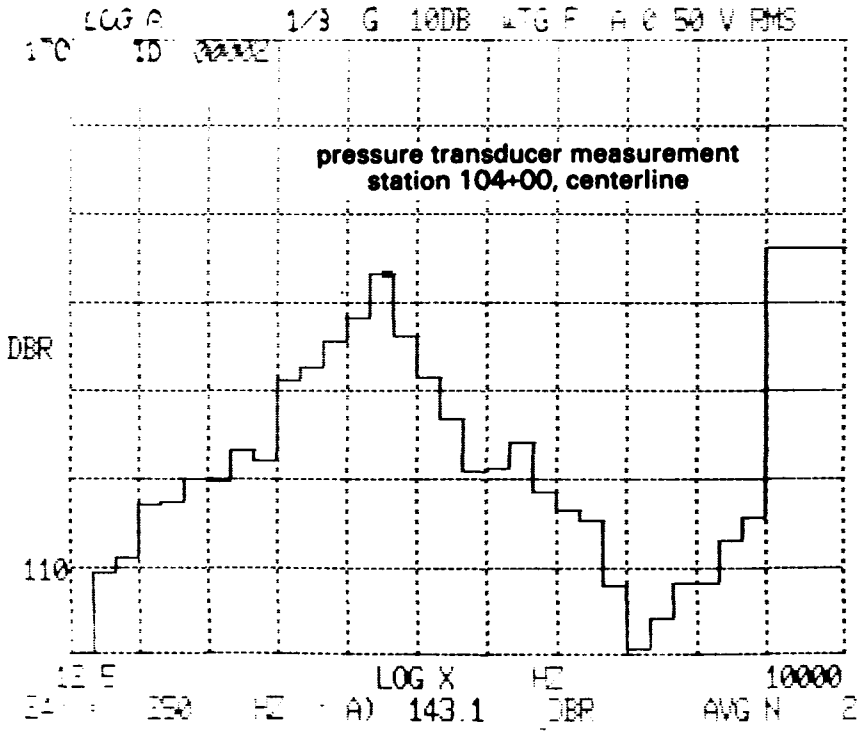

Figure 3-38. One-third octave band spectrum of noise at joint seal surface during T-38 takeoff (takeoff at 1528, 6/15/88).

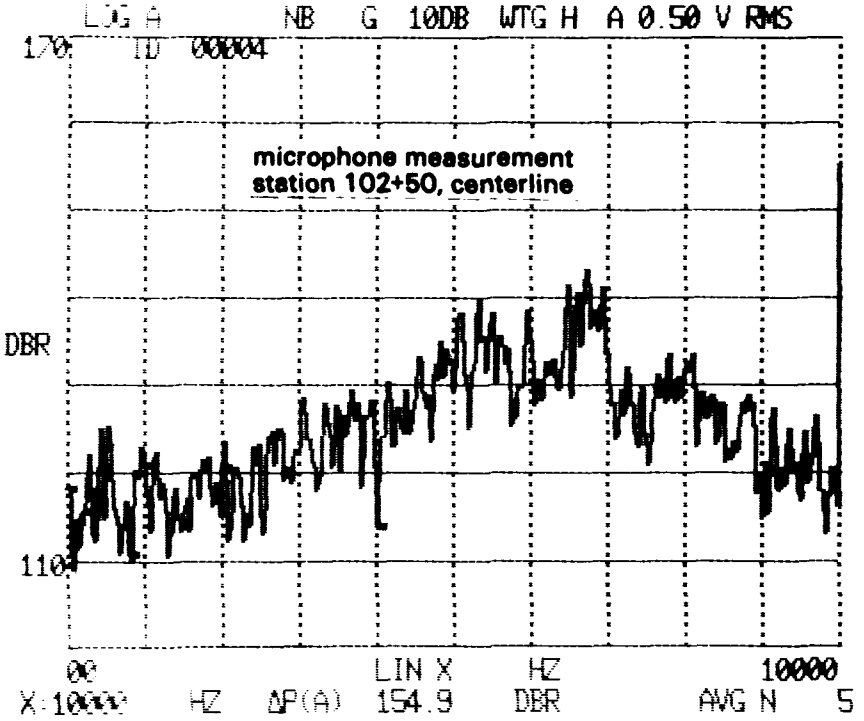

Figure 3-39. Narrow band spectrum of noise at joint seal surface during F-15 takeoff (takeoff at 1517, 6/15/88).

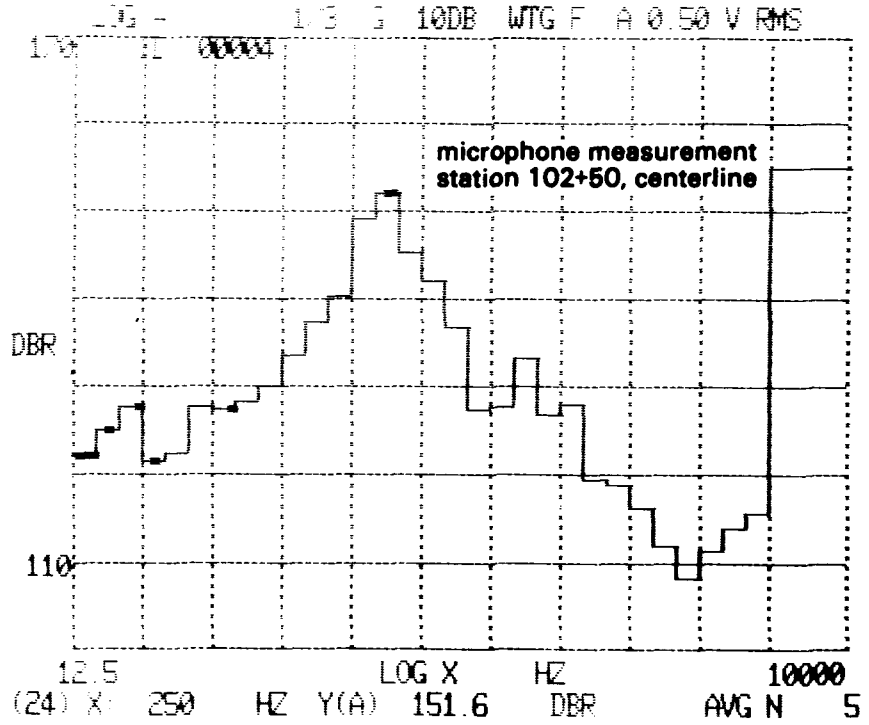

Figure 3-40. One-third octave band spectrum of noise at joint seal surface during F-15 takeoff (takeoff at 1517, 6/15/88).

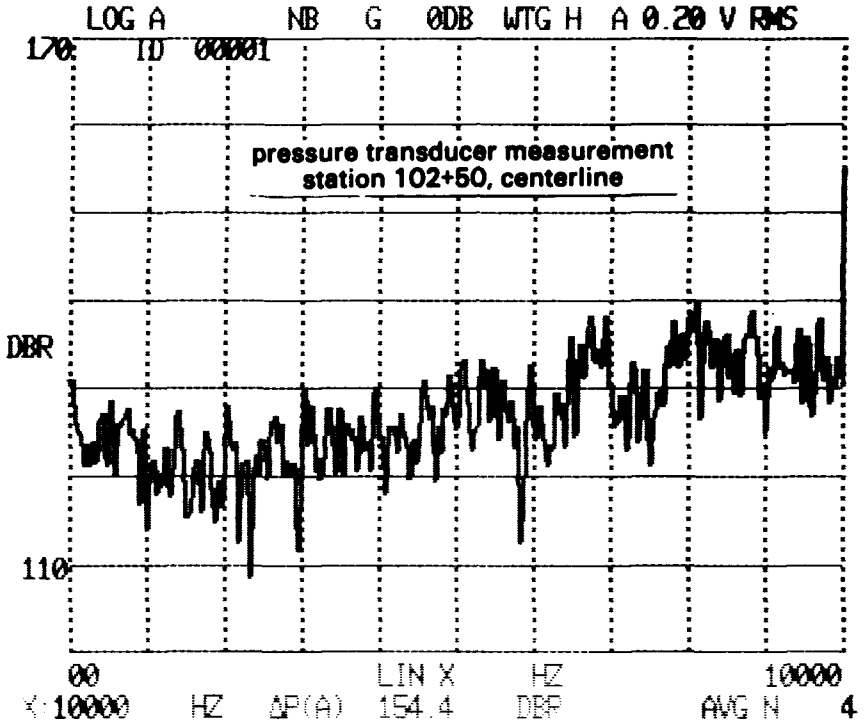

Figure 3-41. Narrow band spectrum of noise at joint seal surface during F-15 takeoff (takeoff at 1517, 6/15/88).

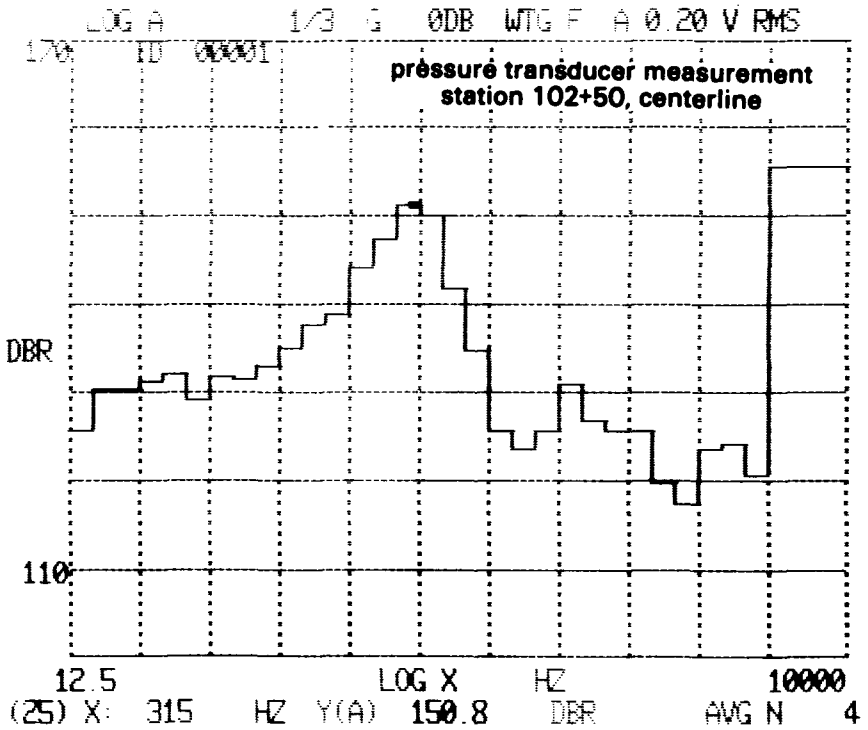

Figure 3-42. One-third octave band spectrum of noise at joint seal surface during F-15 takeoff (takeoff at 1517, 6/15/88).

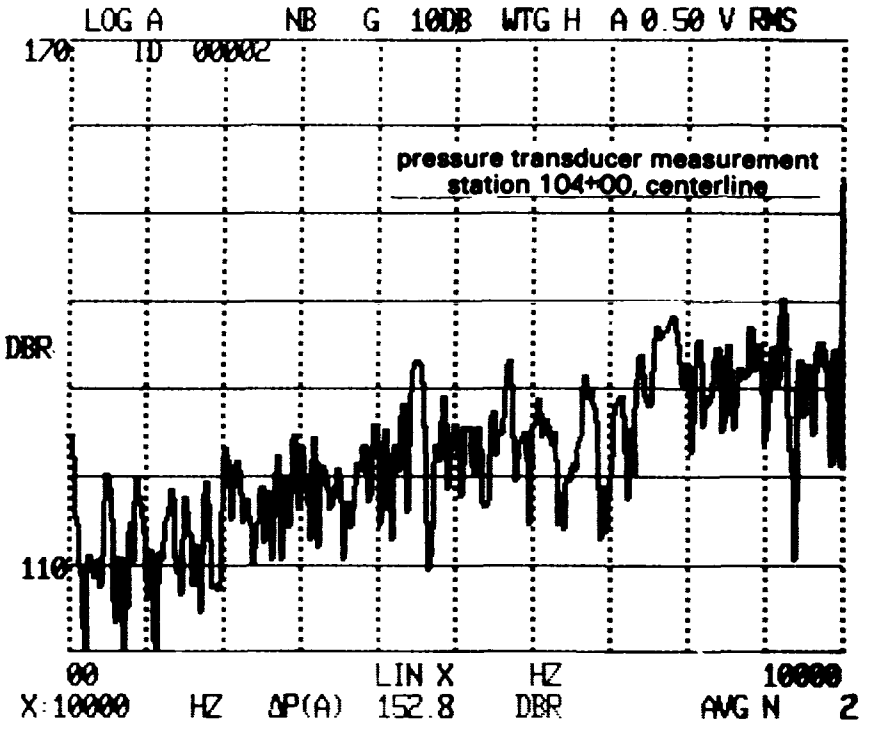

Figure 3-43. Narrow band spectrum of noise at joint seal surface during F-15 takeoff (takeoff at 1517, 6/15/88).

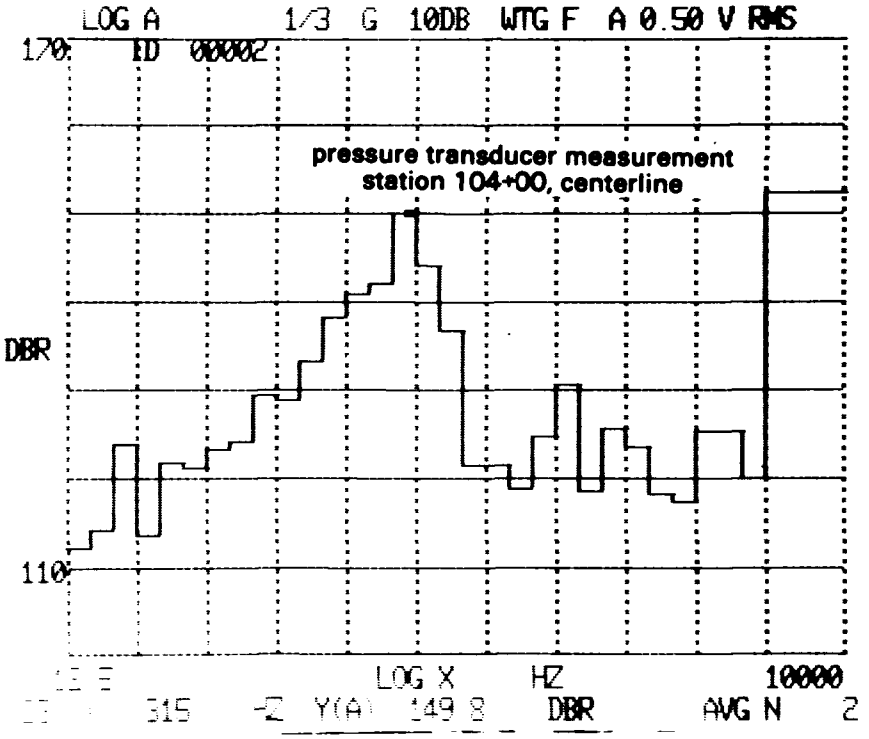

Figure 3-44. One-third octave band spectrum of noise at joint seal surface during F-15 takeoff (takeoff at 1517, 6/15/88).

4.0 ANALYSIS OF RESULTS

In addition to the temperatures and noise levels presented in Section 3.0 of this report, the potentials for thermal and acoustic energy input to the joint seal materials are of interest. Section 1.2 stated that the tests were conducted to determine the aerothermal environment; therefore the analyses below are presented to determine the potential for thermal and acoustic energy input.

Actually, the analyses for thermal and acoustic energy input are not independent. It is possible that energy absorbed by the joint seal material will cause an increase in the temperature of the material. It is also possible that acoustic energy absorbed by the material will result in changes in the chemical or physical structure of the sealant material. For example, long molecules may be broken into shorter molecules due to vibrations induced by the acoustic field. Regardless of the way in which the acoustic field affects the material, the possibility that acoustic energy may be absorbed must be included in the thermal energy analysis. This is done in Section 4.1.2.

4.1 Analysis of Thermal Energy Transfer

For analysis of thermal energy input, energy balances at two different conditions are considered. One energy balance is performed when the joint seal is exposed only to normal ambient conditions, but is not being heated by engine exhaust flow. This is called the "ambient equilibrium" condition. The other energy balance is performed when the joint seal material is being heated by engine exhaust flow.

4.1.1 Thermal Balance Without Engine Exhaust Flow Heat Input. First, an energy balance is performed on a section of the joint sealant assuming the sealant is not being heated by engine exhaust flow, but rather is exposed to solar insolation and has reached an equilibrium temperature distribution. The heat balance for this condition is illustrated in Figure 4-1. The thermal balance is:

(Rate of Energy Storage) = 0 = (Rate of Solar Energy Absorption)
-(Rate of Reradiation)
-(Rate of Convective Heat Transfer)
-(Rate of Heat Loss by Conduction)

The mathematical expression follows, assuming conductive heat loss from the joint seal material only occurs in the vertical direction, and assuming a straight line equilibrium temperature distribution has been established through the joint seal material. That is:

$$0 = \alpha S - \varepsilon\sigma T_{T,s}^4 - h_{NC}(T_{T,s} - T_{T,AMB}) - k(T_{T,s} - T_{T,Y}) \qquad (1)$$

Equation 1 can be solved for surface temperature, $T_{T,s}$, if the ambient conditions (S, $T_{T,AMB}$, $T_{T,Y}$, wind) are known, as well as material properties (α, ε, k). Ambient conditions vary with season, time of day, and the instantaneous weather conditions. Representative values for solar insolation at Edwards AFB during June were obtained

from Reference 5. Also, the ambient temperature, T_{AMB}, had been measured periodically on 15 and 16 June. Representative values for properties of the joint seal material were obtained from Reference 6. The equation for h_{NC} is from Reference 7. Values used for ambient conditions, material properties, and physical constants are listed below:

α = solar absorptivity = 0.9 (dimensionless)

ε = emissivity = 0.9 (dimensionless)

k = thermal conductivity = 2.69×10^{-5} Btu-ft/ft^2-sec-°R

$T_{T,AMB}$ = ambient temperature, absolute scale = $(T_{AMB} + 460)$°R

$T_{T,Y}$ = temperature of the joint seal material at the interface with the "backer rod," absolute scale $\simeq T_{T,s}$

S = rate of solar insolation (from Ref 5), Btu/ft^2-sec

σ = Stefan-Boltzmann's constant = 4.83×10^{-13} Btu/ft^2-sec-°R^4

h_{NC} = $(6.11 \times 10^{-5})(T_{T,s} - T_{T,AMB})^{1/3}$ Btu/ft^2-sec-°R

Figure 4-2 presents the diurnal variation of the joint seal surface temperature under equilibrium conditions. The calculated temperatures range from approximately 50 °F during evening and predawn conditions to 145 °F at 1200 hours when solar insolation is maximum, assuming no wind. Surface temperatures as high as 145 °F were recorded during the tests on 15-16 June. The surface temperatures were measured only after the sun was up and solar insolation was significant; therefore, it was not verified that the joint seal temperatures dropped to approximately 50 °F at night.

The effect of wind on surface temperature should be noted. Wind increases the convective heat transfer loss, and changes surface temperature. Figure 4-2 shows that a four-fold increase in convective heat transfer coefficient results in a reduction of peak surface temperature from about 145 °F to about 133 °F.

4.1.2 Thermal Balance with Engine Exhaust Flow Heat Input. For the second thermal energy balance, assume that the joint sealant is being heated by hot engine exhaust flow, and by solar insolation. For completeness, the heating by the hot engine exhaust flow is assumed to include the convective heat input (the thermal contribution) and the acoustic energy input (the acoustic contribution). Assume the joint sealant temperatures are transient, due to the transient nature of the heat input from the engine and the inability of joint sealant to conduct heat rapidly enough to reach equilibrium with the convective heat input. The heat balance for this condition is illustrated in Figure 4-3. The heat balance is:

(Rate of Energy Storage) = (Rate of Solar Energy Absorption)
-(Rate of Reradiation)
+(Rate of Convective Heat Transfer)
-(Rate of Heat Loss by Conduction)
+(Rate of Absorption of Acoustic Energy)

The energy balance is expressed mathematically below, with the (Rate of Convective Heat Transfer) + (Rate of Absorption of Acoustic Energy) transposed to the left-hand side where the sum becomes the unknown to be determined. The sum is the rate of energy input resulting from the aerothermal environment created by impingement of the engine exhaust flow on the joint sealant. In the remainder of the report, the sum will be called the rate of exhaust flow energy input. That is:

$$\text{(Rate of exhaust flow energy input)} = h_{Fc}\,(T_{T,r} - T_{T,s}) + \beta I$$

$$h_{FC}(T_{T,r} - T_{T,s}) + \beta I = \rho c \int_{y=0}^{y=Y} \frac{\partial T}{\partial t}\, dy - \alpha S + \varepsilon \delta T_{T,s}^4 + k \left[\frac{\partial T}{\partial y}\right]_{y=Y} \quad (2)$$

where ρ = density of the joint seal material = 65.5 lb_m/ft^3

c_p = specific heat of the joint seal material = 0.7 $Btu/lb_m\text{-}^\circ R$

β = fraction of incident acoustic energy absorbed by the joint sealant, dimensionless

I = acoustic intensity (see Section 4.2), $Btu/ft^2\text{-sec}$

The terms on the right-hand side can be evaluated using test data and knowing joint seal material properties and ambient conditions that applied at the time of the test. The ambient conditions and material properties are listed in the discussion of the steady-state thermal energy balance, Section 4.1.1. To illustrate computation of the terms on the right-hand side, use test data from the takeoff of the F-4 on 15 June 1988, and the ambient conditions that applied at the time of the takeoff (1517 hours). Use the temperature-time history from Station 104+00 at the centerline of the runway (see Figure 3-13). Terms on the right-hand side of Equation 2 are calculated in the following manner:

1. From Reference 5, the solar energy flux is typically 0.0738 $Btu/ft^2\text{-sec}$ at 1517 hours during June at Edwards AFB. Approximately 90 percent of energy falling on the joint sealant is absorbed. That is:

$$\text{(Rate of Solar Energy Absorption)} = \alpha S = 0.0664\ Btu/ft^2\text{-sec}$$

2. The reradiation loss term can be calculated using the temperature-time history measured by the thermocouple at the joint sealant surface. Figure 4-4 shows the reradiation loss term as a function of time corresponding to the temperature-time history during an F-4 takeoff. That is:

$$\text{(Rate of Reradiation)} \approx \varepsilon\sigma T_{T,s}^4 = \text{(see Figure 4-4)}$$

3. The heat conduction loss term is the same for a short-term transient case as for the steady-state case. Temperature-time traces of the subsurface thermocouples at Station 102+50 showed little or no temperature increases when the surface thermocouples were responding to hot exhaust flows. This means that the thermal conductivity of the joint sealant is so low that transient conduction effects are negligible even at 1/8 inch below the surface during the short duration of exposure to engine exhaust gases. The same is true, therefore, at the bottom of the joint seal:

$$\text{(Rate of Heat Loss by Conduction)} = k\left[\frac{\partial T}{\partial y}\right]_{y=Y} \approx k\,\frac{(T_{t,s} - T_{T,Y})_{t=0}}{Y}$$

$$= 0 \text{ Btu/ft}^2\text{-sec}$$

4. The net thermal energy gain of the sealant is evaluated from a transient finite-difference solution of the one-dimensional transient heat conduction equation. The solution is from Reference 7, and is described in Appendix C. The finite-difference solution was programmed on a LOTUS 123 spreadsheet. To run the program, the temperature-time history measured by the thermocouple at the joint seal surface was input as a boundary condition, and the temperature distribution through the joint seal just prior to impingement of the jet exhaust flow was input as the initial condition. Figure 4-4 shows the variation of the net thermal energy gain term as a function of time during an F-4 takeoff. The rate of energy storage equation is:

$$\text{(Rate of Energy Storage)} = \rho c_p \int_{y=0}^{y=Y} \frac{\partial T}{\partial t}\,dy \quad \text{(see Figure 4-4 and Appendix C)}$$

The rate of energy input by convective heat transfer plus absorption of acoustic energy is then calculated. There was no way to directly calculate the value of the convective heat transfer rate because it was not possible to measure the magnitudes and variations of all the aerodynamic conditions for computation of h_{FC} and $T_{T,r}$. Nor was it possible to directly calculate the absorption of acoustic energy because it was not possible to measure β, the fraction of incident energy actually absorbed by the sealant. In Section 4.2, the procedure is presented for computing acoustic intensity, I. However, knowledge of the magnitudes of all of the other terms in the transient thermal balance equations enables determination by simple algebra of the rate of exhaust flow energy input.

Figure 4-4 plots the rate of exhaust flow energy input and other terms in the energy balance at the point of most severe heating of the joint seal material during takeoff of an F-4 aircraft at afterburner power. The methodology outlined above can be applied to any point in the joint seal and to the operations of any aircraft for which a temperature-time history has been recorded by a thermocouple at the sealant surface.

Figures 4-5, 4-6, and 4-7 are plots of the rate of exhaust flow energy input and other terms in the joint sealant thermal energy balance during takeoff operations of F-16, F-15, and T-38 aircraft. Each figure is for a different location, as well as for a different airplane. For each aircraft, the location is at the position of the thermocouple where the greatest temperature increase occurred, and the positions depended on the aircraft and the alignment during takeoff. The exhaust flow energy input rates for different aircraft are compared in Table 4-1.

4.2 Analysis of Acoustical Energy Input

Reference 8 defines three different scales for measurement of noise levels. All use the designation "decibels" to represent the noise levels. The scales are:

1. Sound Pressure Level:

$$(db)_{SPrL} = 10 \log_{10} \frac{\overline{p^2}}{p^2_{ref}}$$

where $\overline{p^2}$ is the time-average of the square of fluctuating pressure resulting from the noise,

p_{ref} is a reference pressure, normally given the value 2×10^{-5} N/m^2 = 4.17×10^{-7} lb$_f$/ft^2 for measurements of sound pressure level in gases.

2. Sound Power Level:

$$(db)_{SPwL} = 10 \log_{10} \frac{\mathbb{P}}{\mathbb{P}_{ref}}$$

where $\mathbb{P}$ is the rate at which energy due to the noise passes an area,

$\mathbb{P}_{ref}$ is a reference power level, normally given the value 1×10^{-12} watts = 9.47×10^{-16} Btu/sec for measurements of sound power level in gases.

3. Sound Intensity Level:

$$(db)_{SIL} = 10 \log_{10} \frac{I}{I_{ref}}$$

where I is the rate per unit area at which energy due to the noise passes a point in the noise field,

I_{ref} is a reference level of intensity, normally given the value 1×10^{-12} watts/m^2 = 8.80×10^{-17} Btu/ft^2-sec for measurements of sound intensity in gases.

The data presented in Figures 3-23 through 3-44 are from measurements of sound pressure level. For comparison of noise energy with thermal energy, the noise data are needed in terms of sound intensity level. With the noise data expressed in intensity units of Btu/ft^2-sec, direct comparison can be made with convective heat transfer, also expressed in Btu/ft^2-sec.

Reference 8 gives the conversion from $(db)_{SPrL}$ to intensity, I. That is:

$$I = \frac{\overline{P^2}\, g_c}{\rho_o\, c_o\, J} = \frac{P_{ref}^2\, g_c}{\rho_o\, c_o\, J} \times 10^{[(db)_{SPrL}/10]} \qquad (3)$$

Calculations of intensities were made using measurements of (db) SPrL, and

ρ_o = density of air just above surface = $P_{AMB}/(R \times T_{T,AMB})$

($P_{AMB} \simeq 14.6$ lbf/in^2 = 2102 lbf/ft^2)

(R = 53.3 ft-lbf/lbm-^oR)

($T_{T,AMB} \simeq 760^oR$)

c_o = speed of sound in air just above surface
= $(\gamma \times g_c \times R \times T_{T,AMB})^{1/2}$

(γ = ratio of specific heats
= 1.4 (dimensionless))

J = Joules' constant for conversion of mechanical work units to thermal energy units = 778 ft-lbf/Btu

g_c = constant for conversion of mass-length-time units to Force units = 32.2 lbm-ft/lbf-sec^2

Table 4-1 presents peak acoustical intensities measured during takeoffs of F-4, F-15, and T-38 aircraft. The intensities are from 2.50 Btu/ft^2-sec for the F-4 to 0.08 Btu/ft^2-sec for the T-38. It was noted in Section 3.3 of this report that the noise readings for the T-38 are probably low because the T-38 exhaust flow was displaced several feet to the left of the acoustic instrumentation at the centerline of the runway.

Table 4-1 also directly compares the overall rate of exhaust flow energy input with the potential acoustic energy input to the joint seal material. The overall rate of exhaust flow energy input is approximately 1-1/2 to 2 times that of acoustic energy input for each airplane. The conclusion drawn from this comparison is that the acoustic energy input is certainly significant with respect to the thermal energy levels. Since the instrumentation for the tests at Edwards Air Force Base was not designed to separate the convective heat transfer rate from the acoustic energy absorption rate, the only thing that can be concluded is that:

I is of the order of $h_{Fc} (T_{T,r} - T_{T,s}) + \beta I$

It was not possible for this report to determine the magnitude of β or the relative magnitudes of βI and $h_{Fc} (T_{T,r} - T_{T,s})$, although the intuituve historical assumption has been that β is small and $\beta I << h_{Fc} (T_{T,r} - T_{T,s})$.

Table 4-1. Comparison of Total (Thermal + Acoustic) Energy Input Rates and Acoustic Intensities from Engine Exhaust Flow to Joint Seal Materials

Aircraft	Peak Rate of Total Energy Input (Btu/ft^2-sec)	Peak Acoustic Intensity (Btu/ft^2-sec)
F-4	3.50	2.50
F-15	0.55	0.32
F-16	3.47	----
T-38	1.73	0.08

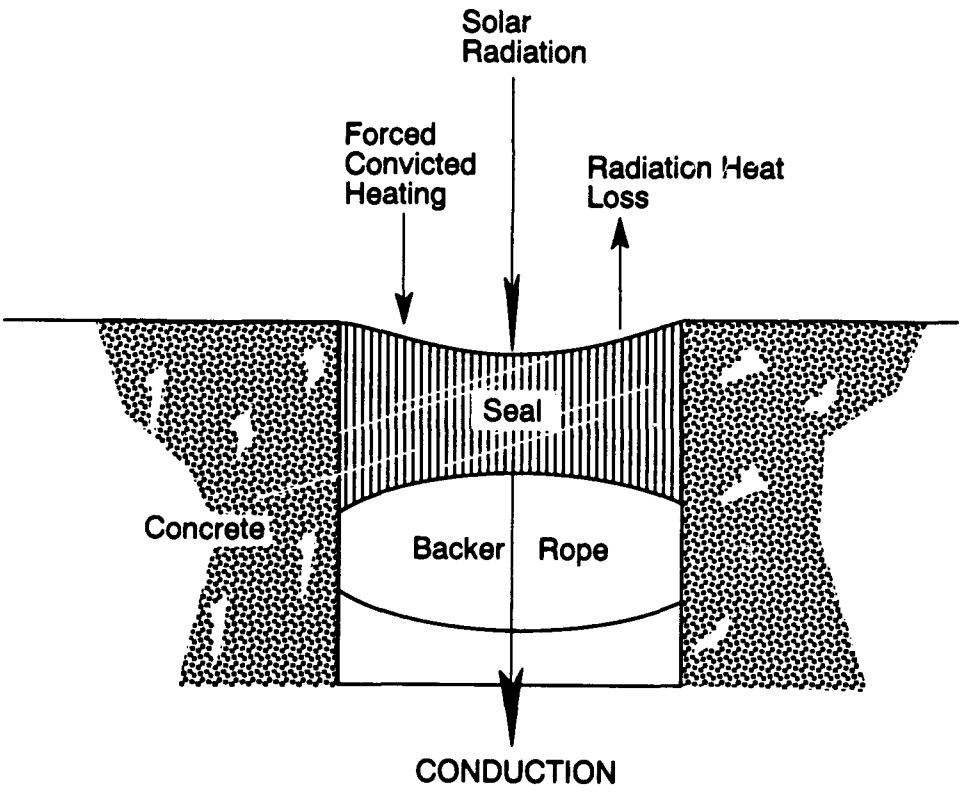

Figure 4-1. Thermal energy balance on joint seal material without impingement of engine exhaust flow.

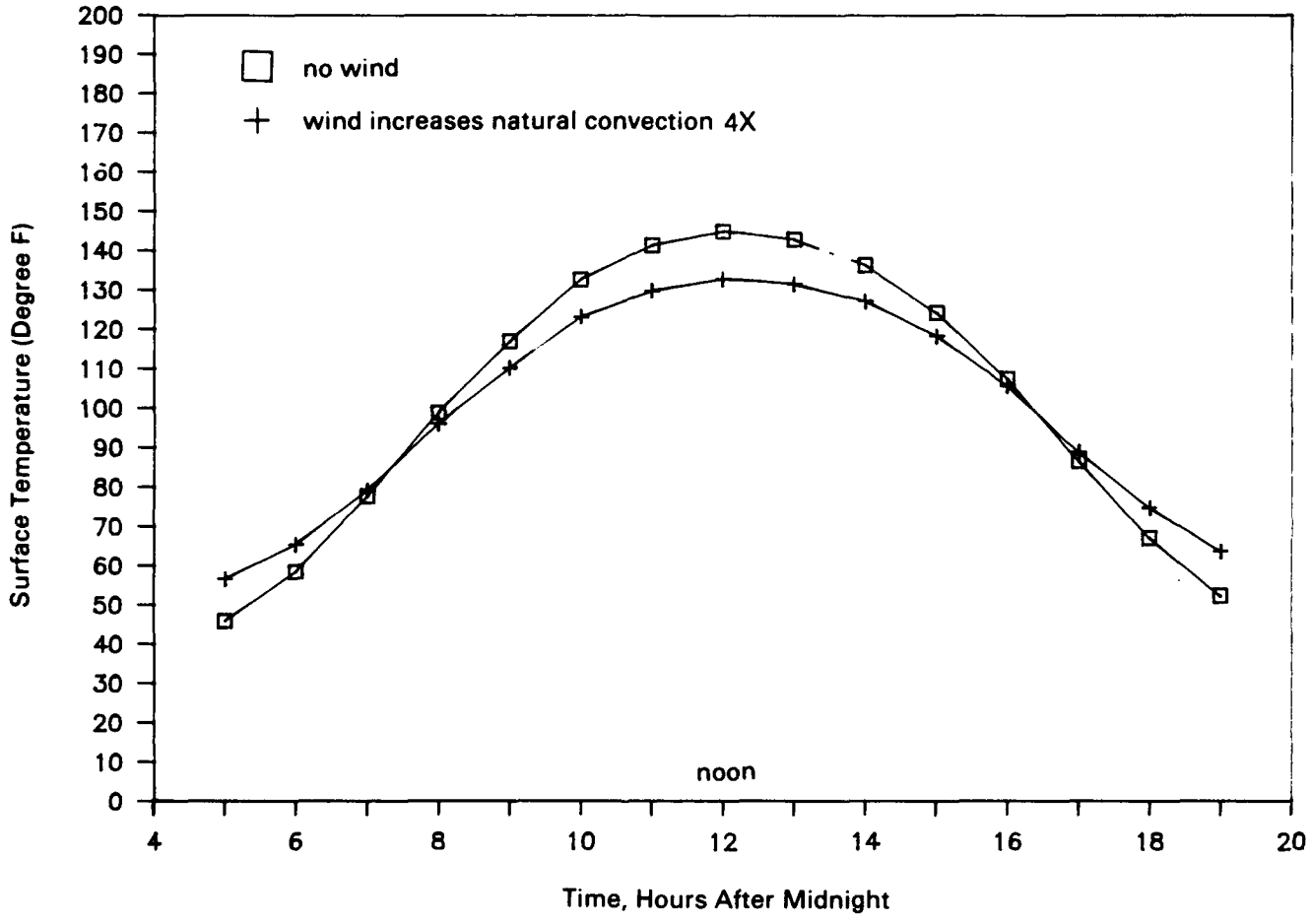

Figure 4-2. Variation of equilibrium temperatures of joint seal surface throughout the day.

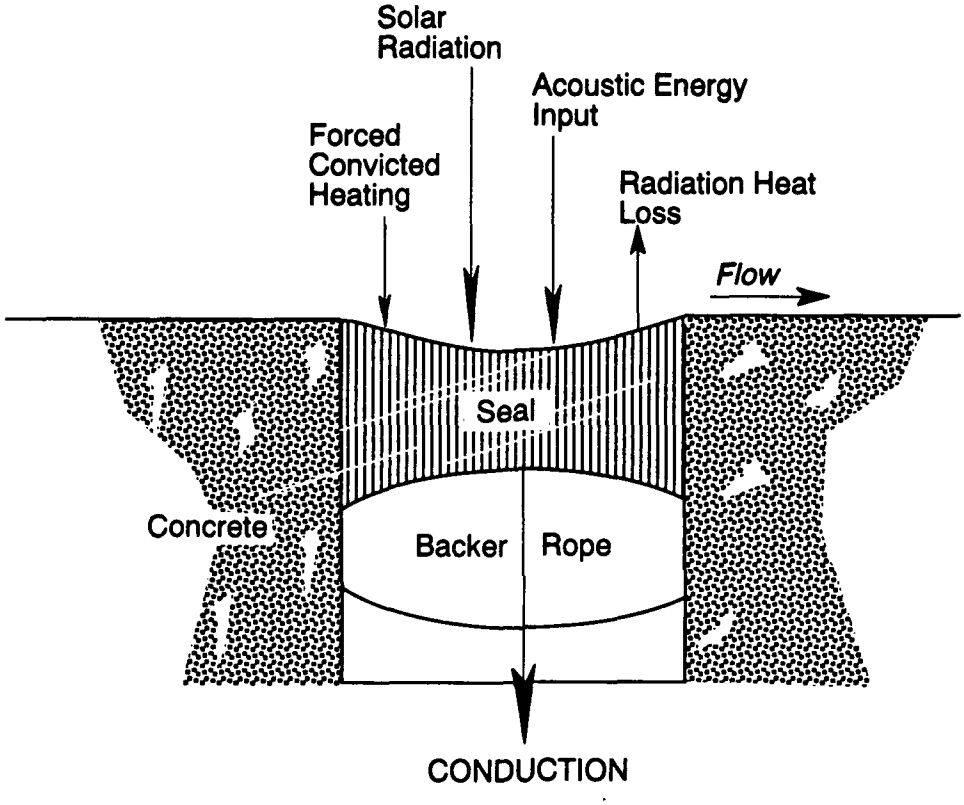

Figure 4-3. Energy balance on joint seal material with impingement of engine exhaust flow.

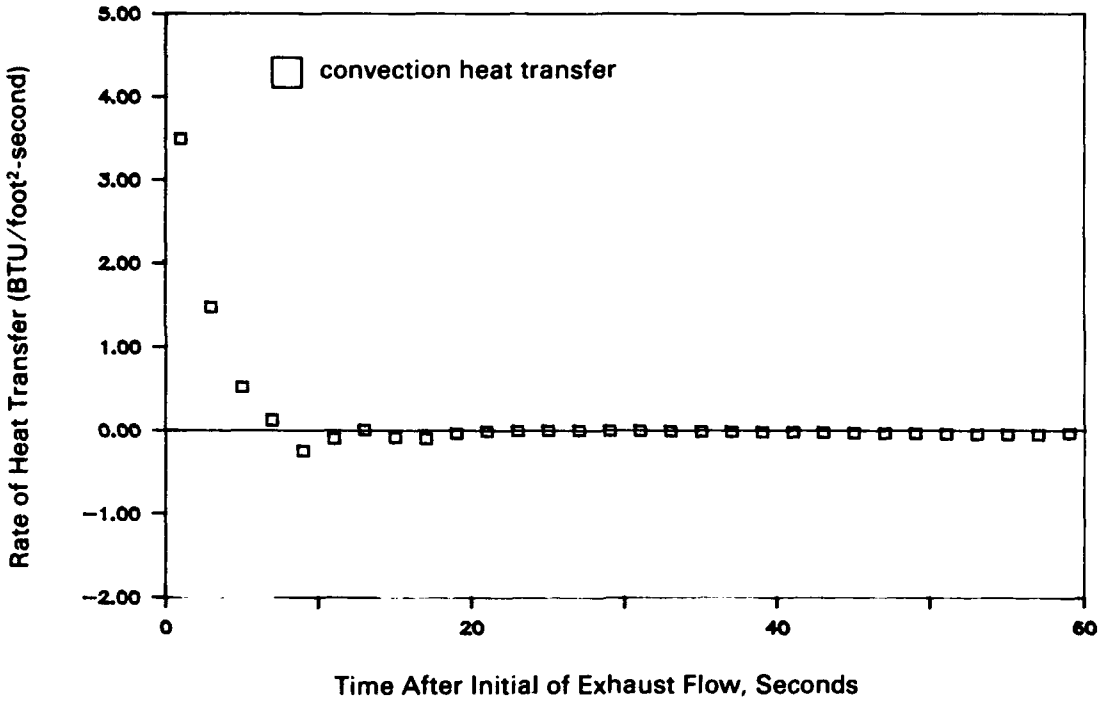

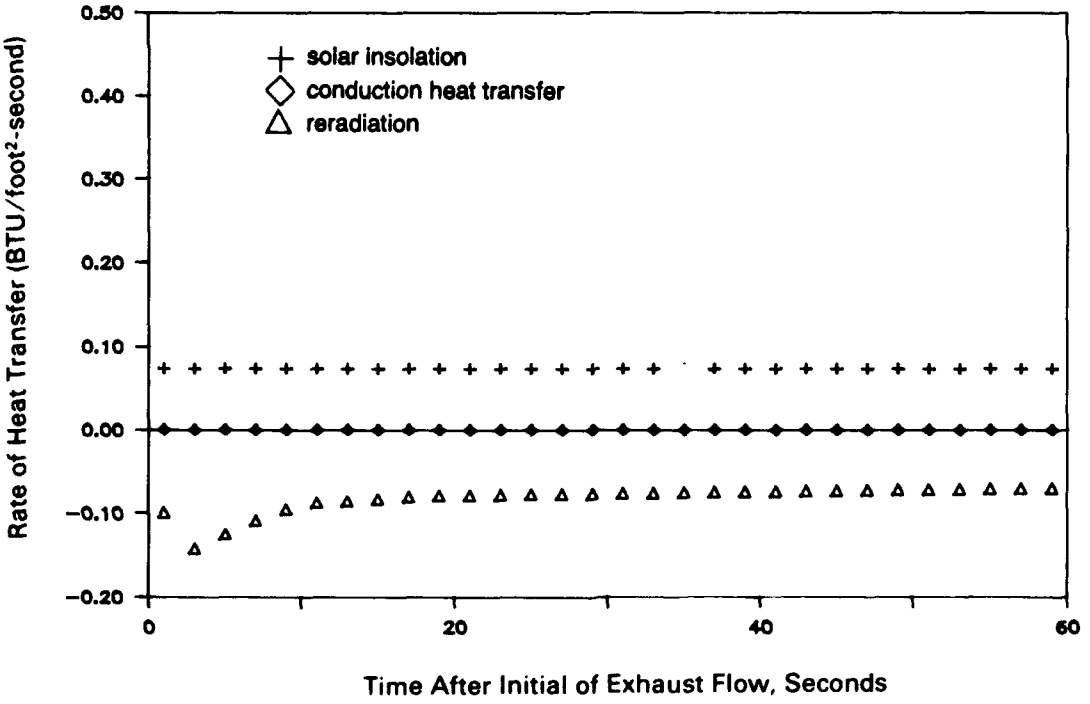

Figure 4-4. Rates of heat transfer for joint seal material exposed to F-4 engine exhaust flow (F-4 takeoff at 1511, 6/15/88).

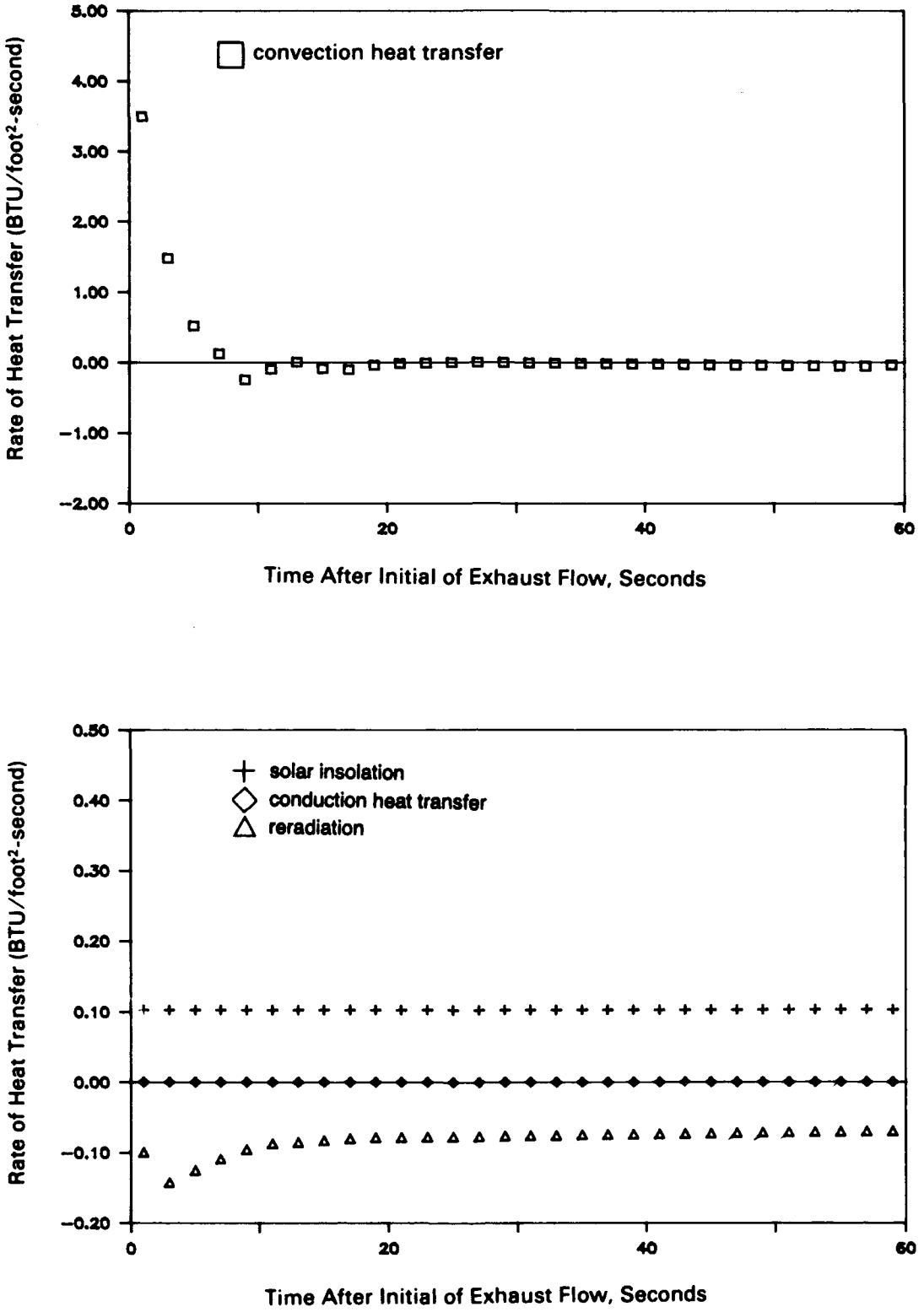

Figure 4-5. Rates of heat transfer for joint seal material exposed to F-16 engine exhaust flow (F-16 takeoff at 1134, 6/16/88).

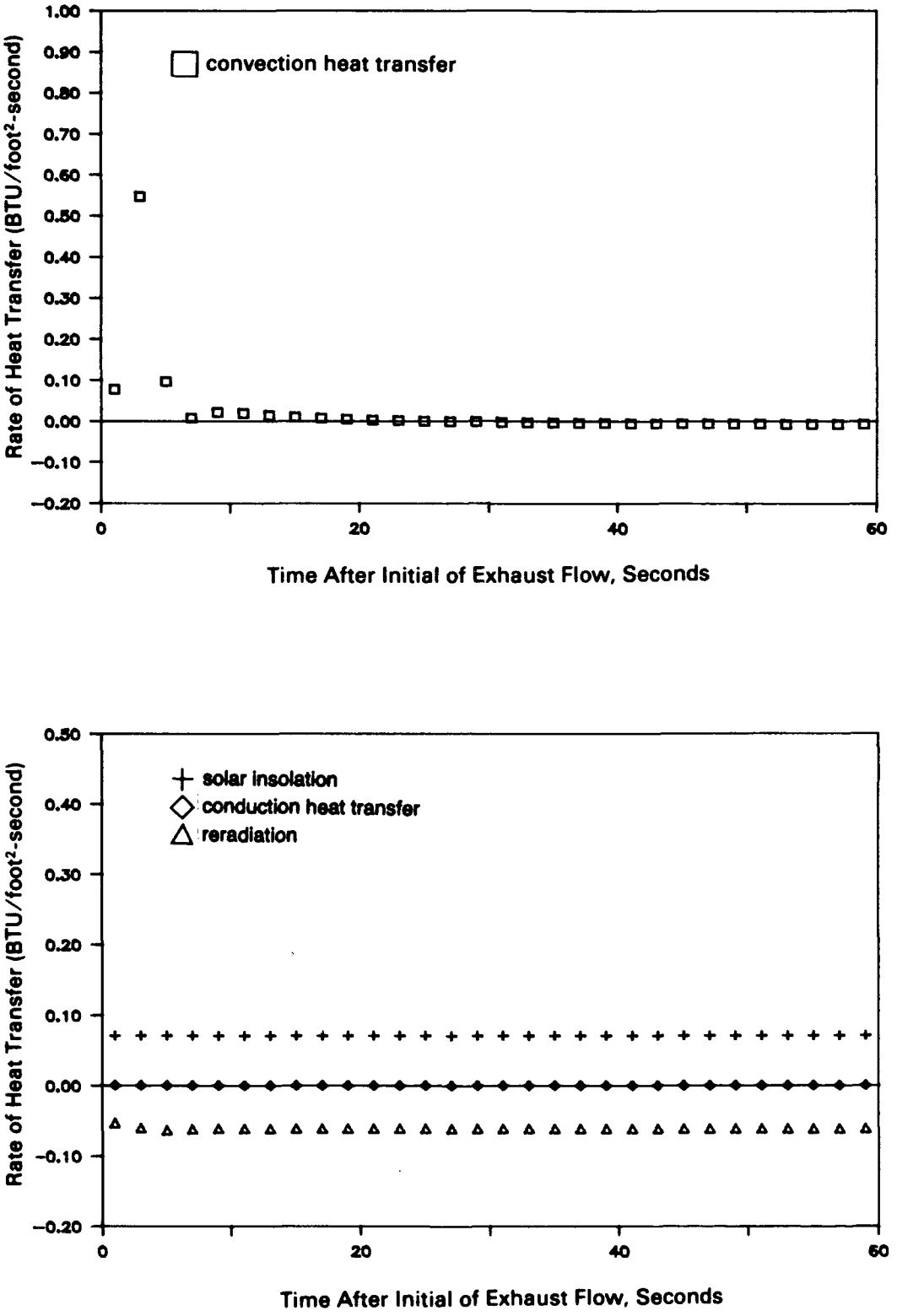

Figure 4-6. Rates of heat transfer for joint seal material exposed to F-15 engine exhaust flow (F-15 takeoff at 1517, 6/15/88).

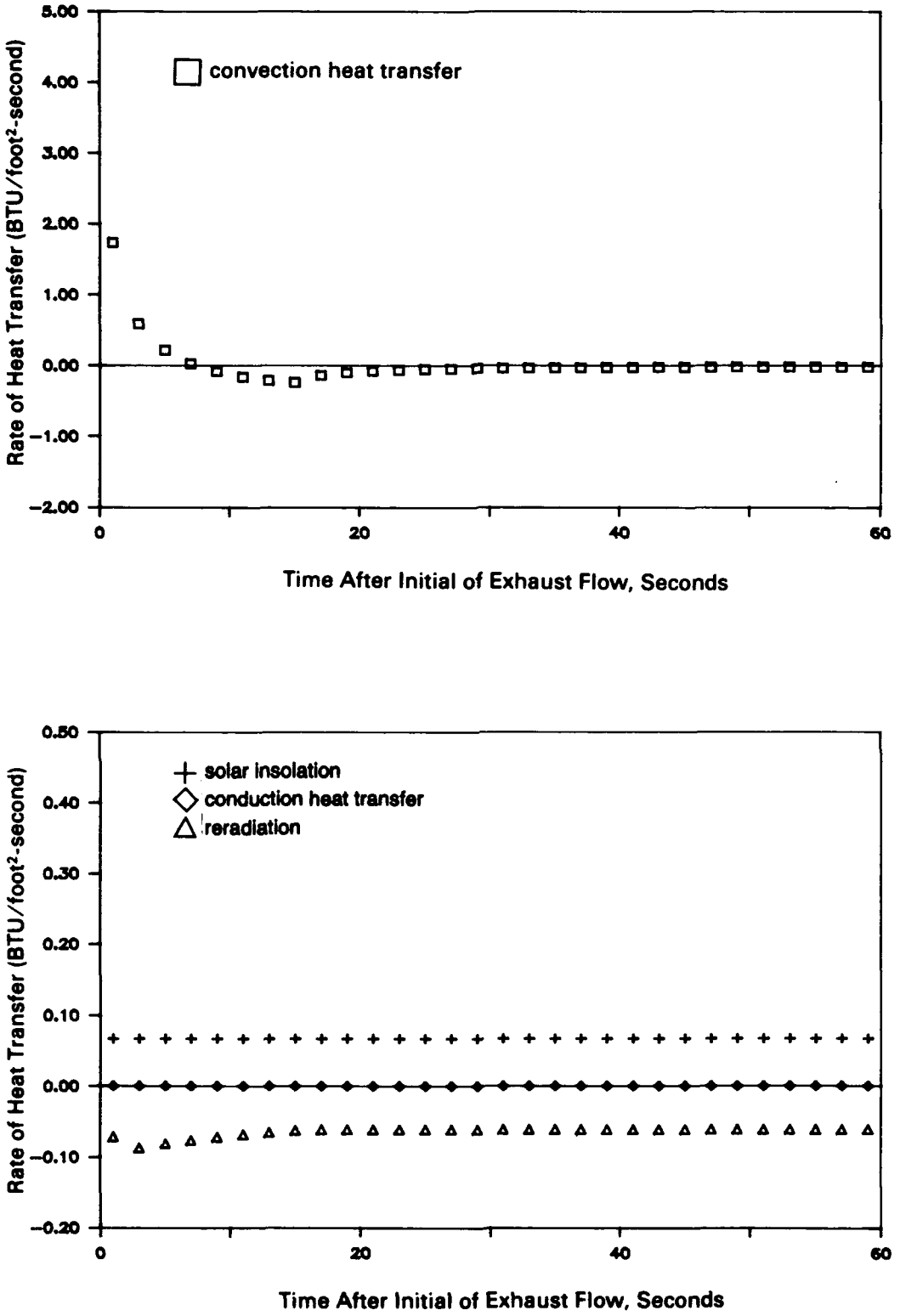

Figure 4-7. Rates of heat transfer for joint seal material exposed to T-38 engine exhaust flow (T-38 takeoff at 1528, 6/16/88).

5.0 CONCLUSIONS

1. Takeoffs of the F-4 aircraft at afterburner power created the most severe noise and temperature environments for the joint seal material. Measured noise levels reached 164 db and temperature of the flow just above the surface of the joint seal reached 600 °F. The temperature of the joint seal material itself reached 310 °F, which was 165 °F above the equilibrium ambient temperature of the sealant, when exposed to the F-4 exhaust flow at afterburner power.

2. Takeoffs of the F-16, F-15, F14, and T-38 aircraft at afterburner power all created severe aerothermal environments as well, but less severe than the F-4. Temperatures approximately 1/2 inch above the surface of the joint seal reached 275 to 325 °F. Temperatures on the surface of the joint sealant increased 40 to 80 °F above the ambient equilibrium temperatures. Noise levels of 148 to 155 decibels were measured.

3. The potential for transfer of acoustical energy from the exhaust flow to the joint seal material is nearly as great as for transfer of thermal energy. For the F-4, F-15, and T-38, the peak acoustical intensity expressed in Btu/ft^2-sec was approximately two-thirds the peak rate of exhaust flow energy energy input, also expressed in Btu/ft^2-sec. The temperature rise of the joint seal material during impingement of the jet exhaust flow is evidence that energy is transferred from the exhaust flow to the sealant material. The analysis in this report is based on the assumption that the temperature rise was due to the transfer of thermal energy. However, if acoustical energy is absorbed by the joint seal material, the absorption could manifest itself as a temperature rise, or in other ways such as breaking of long molecules in the material or as breaking of the adhesion to the concrete. There is a need to determine the effects of high-intensity noise on joint seal materials.

4. Aircraft without afterburners, particularly multiengine cargo and bomber aircraft such as the KC-135 and B-52, created the least severe noise and thermal environmental conditions at the joint seal surface. Based on examination of the strip chart recordings of the noise readings, noise levels were much lower than during takeoffs of the fighter-type aircraft with afterburner power. The recorded noise data were not calibrated, however, to quantify the decibel levels. Temperatures changed less than 5 °F from those at ambient conditions.

5. The F-4 created the most severe aerothermal environment because its engines are beneath the fuselage, resulting in the exhaust gases being only a few inches above the runway surface when they leave the engines, and being directed slightly downward from the horizontal. Very little mixing occurs between the exhaust gases and ambient air before the exhaust gases impinge on the runway and the joint sealant. Therefore, at impingement, the exhaust gases are relatively hot and moving at a relatively high velocity. The engines of other aircraft equipped with and using afterburner power during takeoffs (F-16, F-15, F-14, and T-38)

all have engines with exhausts higher above the runway surface and directed more horizontally. Greater mixing between the exhaust gases and ambient air takes place before the exhaust gases impinge on the runway, so the temperatures and flow velocities are not so high.

6. During landing operations, noise and temperature environmental conditions on the joint seal material were much less severe than during takeoff operations. Again, a quick examination of the noise levels plotted on the strip chart recorder revealed much lower noise levels than during takeoffs. The noise data were not calibrated to get decibel readings. Also, during landings no measurable changes occurred at the surface of the joint sealant, or even in the air temperature just above the joint seal.

7. Thermocouples mounted approximately 1/8 inch below the surface of the joint seal material showed no perceptible change in temperature at that depth, even during takeoff operations of the aircraft equipped with afterburners. The low thermal conductivity and relatively high thermal capacity (density times specific heat) of the joint seal material apparently limits the temperature fluctuations due to aircraft operations to a thin layer near the surface.

8. Spectral analysis of the noise data shows that all the aircraft at afterburner power have a broad-band spectrum with peak power in the frequency range 250 to 400 Hz. However, significant power occurs at all frequencies at least up to 10,000 Hz.

9. Ambient conditions in the desert can raise the temperature of the joint seal material to about 145 °F at about 2 p.m. in June at Edwards AFB. This is the time of day at which solar insolation is maximum. The ambient equilibrium temperature (i.e., the temperature at which the joint seal material is in thermal equilibrium with ambient conditions) varies with time of day. Wind and nonhorizontal orientation of the surface receiving solar insolation can reduce the ambient equilibrium temperature. Nonhorizontal orientation of some of the thermocouples at the joint seal surface, and/or wind, may be the cause of variations of as much as 20 °F in the temperatures of joint seal material even when not affected by engine exhaust flows.

10. Temperature data recorded on 15-16 June had significant electronic noise-to-electronic signal ratio. The electronic noise was possibly due to the nonsinusoidal output of the 15-kW mobile generator which was the power source for the temperature instrumentation and recorders, or to the inability to establish a common electronic ground level, or possibly due to the software used. The cause was not isolated and corrected during the tests. Electronic noise was not significant in the acoustic instrumentation and recorders. Power for the acoustic instrumentation and recorders was from the 2-kW portable generator.

6.0 RECOMMENDATIONS

1. Expand the data base showing the equivalence of potential for energy input to joint seals from exhaust flow noise and from exhaust flow temperature, performing the tests where conditions can be more closely controlled. Any subsequent testing should be done on a run-up pad or taxiway rather than on an active runway. Preferably the testing can be conducted where the following factors can be controlled:

   (a) 110-volt power is available from the utility grid.

   (b) There is ready access to the sensors installed in the joint seal (access on an active runway is extremely limited).

   (c) The aircraft can be positioned to align with the sensors and to establish the desired distance between the engine exhaust and the sensors.

   (d) Duration of exposure of the joint seal material to the exhaust conditions can be specified.

2. Conduct analyses and basic tests of the influence of intense noise fields on joint seal materials (i.e., the actual rate of energy absorption by the materials and the resulting changes in joint seal material properties).

3. If the recommended tests show noise criteria should be included, revise the joint seal material specifications.

REFERENCES

1. Naval Civil Engineering Laboratory. Memorandum to files on the effects of chemical, environmental, and aircraft exhaust on portland cement concrete airfield pavement joint seals, by Charles C. Dahl and Melvin C. Hironaka. Port Hueneme, CA (in preparation).

2. Federal Specification SS-S-200E: Sealants, joint, two-component, jet blast resistant, cold-applied, for portland cement concrete pavement, 15 Aug 1984.

3. Federal Specification SS-S-1401C: Sealant, joint, non-jet-fuel-resistant, hot-applied, for portland cement and asphalt concrete pavements, 15 Aug 1984.

4. Federal Specification SS-S-1614A: Sealants, joint, jet-fuel-resistant, hot applied, for portland cement and tar concrete pavements, 15 Aug 1984.

5. National Bureau of Standards. "Hourly solar radiation data for vertical and horizontal surfaces on average days in the United States and Canada," National Bureau of Standards Building Science Series 96, Apr 1977, pp 202-203.

6. Handbook of Chemistry and Physics, 36th Edition. Cleveland, OH, Chemical Rubber Publishing Company, 1954-1955.

7. Max Jakob and George A. Hawkins. Elements of heat transfer, 3rd Edition, New York, NY, John Wiley & Sons, 1950, pp 71-72 and 127-131.

8. William K. Blake. Mechanics of flow-induced sound and vibration; Volume I, General concepts and elementary sources. San Diego, CA, Academic Press, Inc., 1986, pp 31-32.

Appendix A

PROCEDURES FOR CALIBRATING INSTRUMENTATION AND FOR REDUCING AND DISPLAYING DATA

TEMPERATURE MEASUREMENTS

All temperature measurements were made with chromel-alumel (K-type) thermocouples. The thermocouples were "Ribbon Contact Thermocouples," NANMAC Corporation Model RCF/Part No. B4-1, with junctions already made and attached to thin arrow-shaped sensing elements for rapid response.

Temperature Measurements Made 15-16 June 1988

For the temperature measurements made 15-16 June, the thermocouples were connected to a reference temperature junction (Kaye Instrument Uniform Temperature Reference) placed at the edge of the runway, from which the wires were run 300^{+} feet to the data recorder. The reference temperature junction eliminates the need for calibrating individual thermocouples, and eliminates the need for ice bath reference junctions. An explanation of the principle of operation of reference temperature junctions is given in the publication by Omega Engineering, Inc., "Complete Temperature Measurement Handbook and Encyclopedia," pages T6-T11. Figure A-1 shows circuitry associated with the reference temperature junction. Confidence in the thermocouple temperature measurements using the reference temperature junction was established by comparison within 1 °F with readings from a calibrated Fluke 8024A multimeter probe at ambient conditions.

During the tests of 15-16 June, temperature data were recorded on a Zenith Model Z248 microcomputer with an 80287 math coprocessor using the ASYST program to digitize the analog temperature signals, set up files for the data, convert the voltage readings to temperature, and store the temperature readings on 5-1/4-inch floppy disks along with corresponding times. For display of the data for the report, the ASYST graphing routine was used.

The ASYST program was only able to handle 15 temperature readings simultaneously. Therefore, temperature readings were taken only from Stations 102+50 and 104+00. No temperature readings were taken from Station 105+50. However, temperatures of the joint seal at 105+50 were less than those at 102+50 and 104+00 because the aircraft were moving rapidly and the times of exposure of the joint seal to the hot exhaust flows were less at the downstream station.

Measurements of temperatures during the first test series were plagued by electronic noise in the signals. The Zenith Z248 computer, its monitor and printer, and the power supply for the external reference

temperature junction were all powered by the 15-kW mobile generator. The generator output was not a clean sine wave. Also, establishing a common ground for all the equipment was difficult in the dry desert conditions. Small ripples, due to electronic noise, were always evident in the digitized temperature data. Randomly, large errors also occurred, showing up as "spikes" in the temperature traces. Before plotting the data from the ASYST files, a digital filtering option available in the ASYST program was used to eliminate the temperature "spikes."

Temperature Measurements Made 4 August 1988

During the tests on 4 August, temperature data were taken with different equipment. Figure A-2 shows the schematic of the instrumentation. Data at Station 104+00 were recorded on a Campbell Scientific Model 21X Micrologger datalogger. Instrumentation was not available to record data from Stations 102+50 and 105+50.

The microphones and pressure transducers installed for the earlier tests had been removed before the second tests, so no noise or pressure data were taken. An advantage to using the Campbell dataloggers was that they are battery-powered, so electronic noise, which was a nuisance during the first tests, was eliminated.

Figure A-2 shows that a reference temperature junction (Kaye Instrument Uniform Temperature Reference) was used in the second test series as it was in the first. The external reference temperature junction was used, even though each Campbell datalogger has an internal temperature reference, because it was again necessary to extend thermocouple wires approximately 300 feet from the edge of the runway to the edge of the "clear zone" where the dataloggers were located, and consequently it was necessary to know the temperature at the junction where wires from the thermocouples were connected to wires to the dataloggers.

In the field, the Campbell dataloggers converted the analog millivolt signal from each of the connected thermocouples to digital signals, and stored the results in appropriate files for later retrieval. Storage capacity of the Campbells was sufficient to record data from approximately 20 takeoffs, with each set of data being for a period of 15 to 30 seconds. The dataloggers were started just as the aircraft increased engine power and started to roll for takeoff, and were stopped when the aircraft were well downstream of Station 104+00.

The digital data in the Campbell 21X dataloggers were stored on Campbell data storage modules (SM192 or SM716) at the site. The storage module data were transferred to an IBM PC. At NCEL, a program called SPLIT was used to convert the recorded millivolt readings to temperature and corresponding time files on 5-1/4-inch floppy disks. From the floppy disks, the temperature and time files were imported to LOTUS 123 files, and the LOTUS 123 graphing routine was used to plot temperatures versus time.

PRESSURE TRANSDUCER MEASUREMENTS

Three Kulite Miniature IS^{R} Pressure Transducers, Model XST-190, were installed at Stations 102+50, 104+00, and 105+50 along the runway centerline. Figure A-3 illustrates the Kulite XST-190 transducer and lists its performance characteristics.

A "positive shunt calibration" was performed for the pressure transducers. This is basically a calibration in which the instrument voltage outputs are determined in the laboratory at various pressures imposed on the transducer, and the instrument outputs can be simulated in the field for calibration of the signal processing and recording equipment. The steps of the calibration are:

In The Laboratory

1. Measure output (millivolts) of the pressure transducer as a function of applied pressure (lbf/in^2). Pressure was applied with a King Nutronics Corporation Pneumatic Calibrator, Model 3540.

2. Connect the pressure transducer leads to the signal conditioning circuit depicted in Figure A-4. The signal conditioning circuit is part of the calibrator/amplifier unit, a Validyne Signal Conditioner Model SG71. Determine the shunt resistance which results in output voltage with the shunt switch closed equal to that when a preselected calibration pressure (in this case, 2.5 lbf/in^2 above atmospheric) is applied to the transducer with the shunt switch open. The preselected calibration pressure is designated P_{CAL}.

In The Field

3. Connect the pressure transducers to the calibrator, amplifier (Validyne Signal Conditioner Model SG71), and recorders (Honeywell Model 101 14 Track Tape Recorder, Honeywell Visicorder Model 1858 Strip Chart Recorder) as shown in Figure A-1.

4. Start with pressure transducer P1 for calibration of the installation in the field. With the shunt switch open, and with the pressure transducer exposed to the local atmospheric pressure, make a 3- to 5-second record on the Honeywell tape recorder of the output dc voltage from the Validyne Signal Conditioner. This is the "zero" voltage, V(0), for the selected pressure transducer.

5. For the same pressure transducer, close the shunt switch of the calibrator. Make another 3- to 5-second record on the Honeywell tape recorder of the output dc voltage from the Validyne Signal Conditioner. This is the voltage corresponding to the preselected calibration pressure, $V(P_{CAL})$, for the selected pressure transducer.

6. Repeat steps 4 and 5 for each pressure transducer.

7. Record data with the shunt switches of the calibrators open. Start the tape recorder at 15 inches/second tape speed just before the start of a takeoff or landing, and stop it when the plane is clear of Station 105+50. For each transducer, this records the time-dependent analog voltage signal, which is proportional to the instantaneous pressure incident on the transducer. On the voice channel (channel A), record the time, type(s) of aircraft, whether the plane is taking off or

landing, and any other significant information. For further reference, also record time from the Systron-Donner Model 5154 Time Code Generator on channel 14.

During Data Reduction

8. Connect the Honeywell Model 101 14 Channel Tape Recorder to the data processing equipment as shown in Figure A-5. Playback of channels 14 and A through the Time Code Generator and a speaker, respectively, enables one to locate and identify the records on the tape.

9. Locate the records for V(0) and $V(P_{CAL})$ for the first pressure transducer. Play them back through a dc voltmeter (Hewlett-Packard Model 3456A Digital Voltmeter), and read $V_1(0)$ and $V_1(P_{CAL})$. Calculate the calibration constant:

$$k_1 = \frac{P_{CAL} - P_{ATM}}{V_1(P_{CAL}) - V_1(0)}$$

10. Repeat step 9 for each pressure transducer.

11. Locate the analog record to be analyzed for noise during a takeoff or landing. Displaying the record on an oscilloscope (Techtronix Model 5441 Storage Oscilloscope with Model 5A48 Dual Trace Amplifier) helps determine the duration of the signal and the peak values of voltage, which in turn helps in the selection of settings for the spectrum analyzer (Scientific Atlanta Spectral Dynamics Model SD375 Dynamic Analyzer II). Play the selected transducer record into the spectrum analyzer. Display the spectrum initially as volts versus Hertz, narrow band, both linear scales. Change the y-scale to "engineering units," and input the k_n which is the calibration factor for the selected transducer. This changes the y-scale to units of lbf/in^2. Next, display the results in pressure versus Hertz, x-scale 1/3 octave, y-scale linear. Move the cursor to the peak pressure, and read it. Calculate db as follows:

$$db_{PEAK} = 20 \text{ Log } \frac{P_{PEAK} - P_{ATM}}{P_{REF} - P_{ATM}} = 20 \text{ Log } \frac{P_{PEAK} - P_{ATM}}{2.89 \times 10^{-9} \text{ lbf/ft}^2}$$

Input the calculated value of db_{PEAK}. This completes calibration of the results.

12. Display the results on the CRT of the spectrum analyzer as desired. Obtain "hard copies" of the results from the Techtronix Model 4632 Video Hard Copy Unit.

MICROPHONE MEASUREMENTS OF NOISE

Three quartz microphones, Model 106B from PCB Piezotronics Inc., were installed at stations 102+50, 104+00, and 105+50 along the runway centerline, as near as possible to the Kulite pressure transducers.

Figure A-6 illustrates the Model 106B microphone and lists its performance characteristics.

A calibration curve is provided by the manufacturer for each microphone purchased. The calibration is for the microphone itself, however, and not for the field installation. The procedures for determining any change from the manufacturer-supplied calibration and for calibration the field installation are explained below.

In The Laboratory

1. Measure output (millivolts) of the microphone as a function of applied sound pressure (lbf/in^2). This was done using the microphone adapter of a Bruel & Kjaer Hydrophone Calibrator Kit, Type 4223. For the microphones used in the tests at Edwards AFB, the laboratory calibration verified the calibration curves furnished by the manufacturer of the microphones.

2. Connect the microphone leads to the signal conditioning circuit depicted in Figure A-7. The signal conditioning circuit is built into the microphone amplifier unit (PCB Piezotronics, Inc., Model 483M92). Set up the signal conditioning circuit so that closure of the "calibration switch" inputs a voltage to the amplifier equal to that when a preselected calibration sound pressure level, P_{CAL}, (in this case, 2.5 lbf/in^2) is applied to the microphone.

In The Field

3. Connect the microphones to the calibrator/amplifier (PCB Piezotronics, Inc., Model 483M92) and recorders (Honeywell Model 101 14 Track Tape Recorder, Honeywell Visicorder Model 1858 Strip Chart Recorder) as shown in Figure A-1.

4. Start with microphone M1 for calibration of the installation in the field. With the calibration switch open, and with the microphone exposed to the local atmospheric pressure, make a 3- to 5-second record on the Honeywell tape recorder of the output dc voltage from the PCB Calibrator/Amplifier. This is the "zero" voltage, V(0), for the selected microphone.

5. For the same microphone, close the calibration switch of the calibrator/amplifier. Make another 3- to 5-second record on the Honeywell tape recorder of the output dc voltage from the PCB Calibrator/Amplifier. This is the voltage corresponding to the preselected calibration pressure, $V(P_{CAL})$, for the selected microphone.

6. Repeat steps 4 and 5 for each microphone.

7. Record data with the calibration switch of the calibrator/amplifier open. Start the tape recorder at 15 inches/second tape speed just before start of a takeoff or landing, and stop it when the plane is well clear of Station 105+50. For each microphone, this records the time-dependent analog voltage signal, which is proportional to the instantaneous pressure

incident on the microphone. On the voice channel (channel A), record the time, type(s) of aircraft, whether the plane is taking off or landing, and any other significant information. For further reference, also record time from the Systron-Donner Model 5154 Time Code Generator on channel 14.

During Data Reduction

8. Connect the Honeywell Model 101 14 Channel Tape Recorder to the data processing equipment as shown in Figure A-5. Playback of channels 13 and 14 through the Time Code Generator and a speaker, respectively, enables one to locate and identify the records on the tape.

9. Locate the records for V(0) and $V(P_{CAL})$ for the first pressure transducer. Play them back through a dc voltmeter (Hewlett-Packard Model 3456A Digital Voltmeter), and read $V_1(0)$ and $V_1(P_{CAL})$. Calculate the calibration constant:

$$k_1 = \frac{P_{CAL} - P_{ATM}}{V_1(P_{CAL}) - V_1(0)}$$

10. Repeat step 9 for each microphone.

11. Locate the analog record to be analyzed for noise during a takeoff or landing. Displaying the record on an oscilloscope (Techtronix Model 5441 Storage Oscilloscope with Model 5A48 Dual Trace Amplifier) helps determine the duration of the signal and the peak values of voltage, which in turn helps in the selection of settings for the spectrum analyzer (Scientific Atlanta Spectral Dynamics Model SD375 Dynamic Analyzer II). Play the selected microphone record into the spectrum analyzer. Display the spectrum initially as volts versus Hertz, narrow band, both linear scales. Change the y-scale to "engineering units," and input the k_n which is the calibration factor for the selected microphone. This changes the y-scale to units of lbf/in^2. Next, display the results in pressure versus Hertz, x-scale 1/3 octave, y-scale linear. Move the cursor to the peak pressure, and read it. Calculate db as follows:

$$db_{PEAK} = 20 \text{ Log } \frac{P_{PEAK} - P_{ATM}}{P_{REF} - P_{ATM}} = 20 \text{ Log } \frac{P_{PEAK} - P_{ATM}}{2.89 \times 10^{-9} \text{ lbf/ft}^2}$$

Input the calculated value of db_{PEAK}. This completes calibration of the results.

12. Display the results on the CRT of the spectrum analyzer as desired. Obtain "hard copies" of the results from the Techtronix Model 4632 Video Hard Copy Unit.

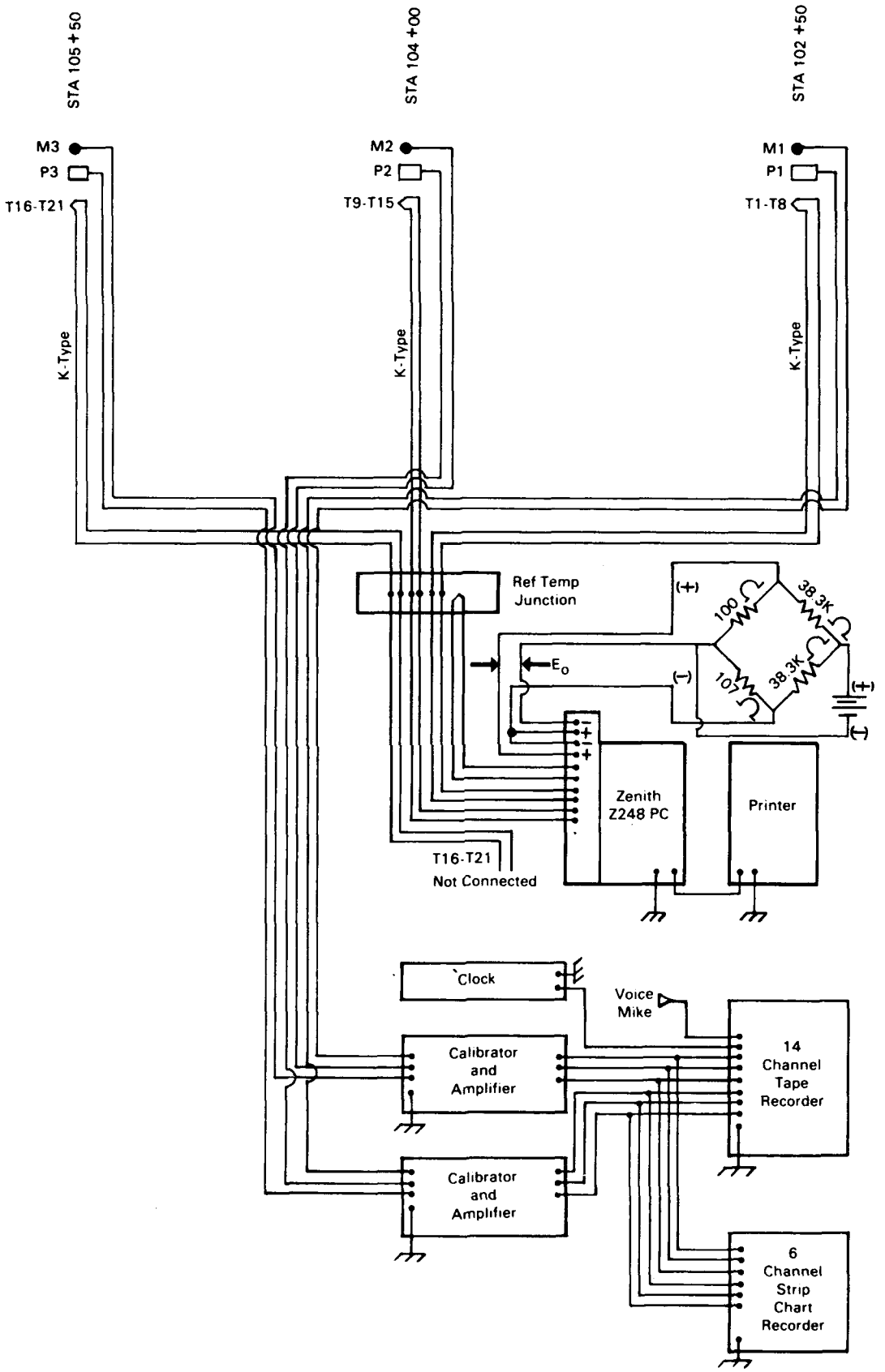

Figure A-1. Schematic of instrumentation for acquisition of data, 15-16 June 1988.

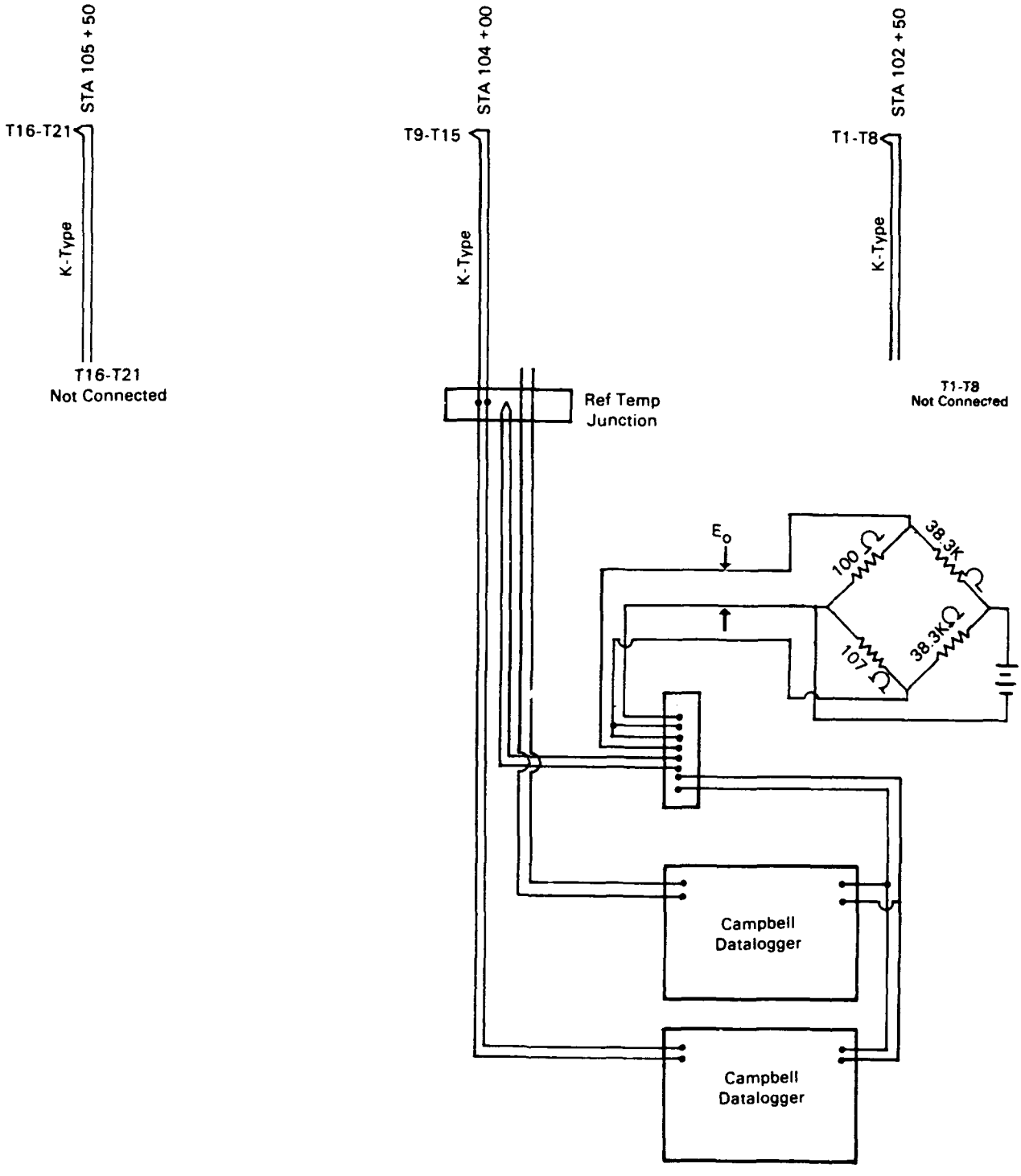

Figure A-2. Schematic of instrumentation for acquisition of data, 4 August 1988.

MINIATURE IS® PRESSURE TRANSDUCER

XST-190 SERIES
LOW PRESSURE HIGH OVERLOAD

- **25 To 200 Times Overpressure Without Damage**
- **Integrated Sensor (IS)®**
- **Easy Installation**
- **Operational Mode**
  Sealed Gage (SG)
  Absolute (A)

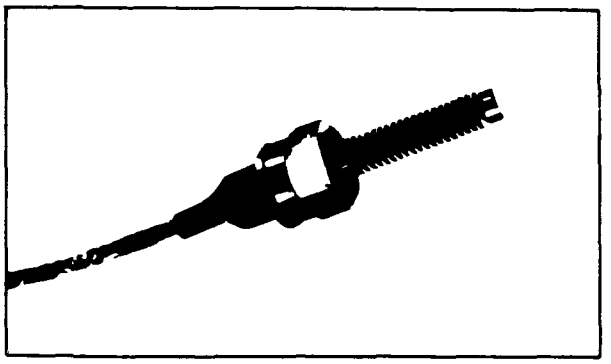

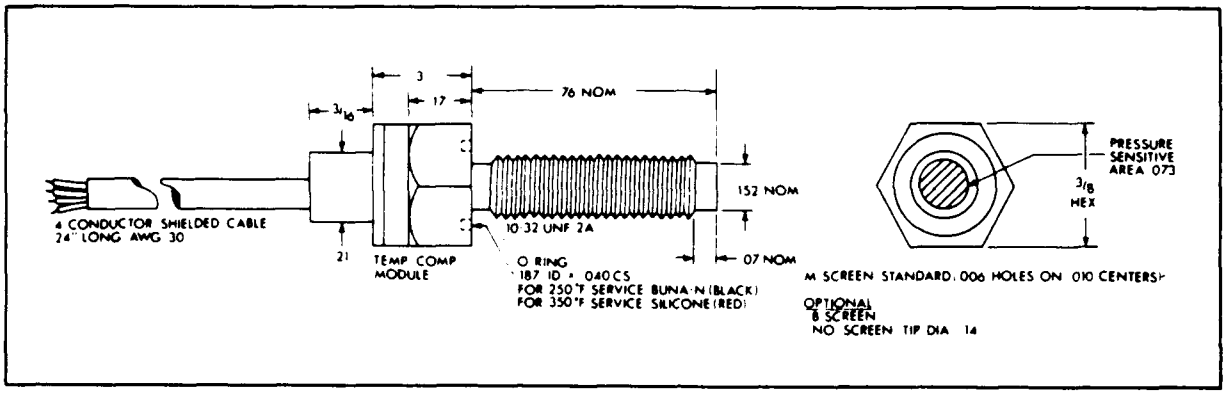

Rated Pressure psi	5	200
Maximum Pressure psi	1000	5000
Output (nom)	75mV	
Input Impedance (min) Output Impedance (nom)	500Ω 350Ω	
Acceleration Sensitivity % FS/g Perpendicular Transverse	 .005 .0005	 .00013 .000026
Natural Frequency	100kHz	200kHz
Excitation	10V DC or AC (20V max)	
Bridge Type	Fully active four arm Wheatstone Bridge	
Zero Balance	± 3% FS (max)	
Combined Nonlinearity and Hysteresis	± 0.3% FS BFSL	
Repeatability	0.1% FS	
Compensated Temperature Range	80°F to 180°F (25°C to 80°C) Any 200°F range within the operating range on request	
Operating Temperature Range	– 65°F to 250°F (– 55°C to 120°C) Temperatures to 350°F (175°C) available on special order	
Change of Sensitivity With Temperature	± 2.0%/100°F (max)	
Change of No-Load Output With Temperature	± 2.0%FS/100°F (max)	
Resolution	Infinite	

Figure A-3. Kulite model XST-190 pressure transducer and performance characteristics.

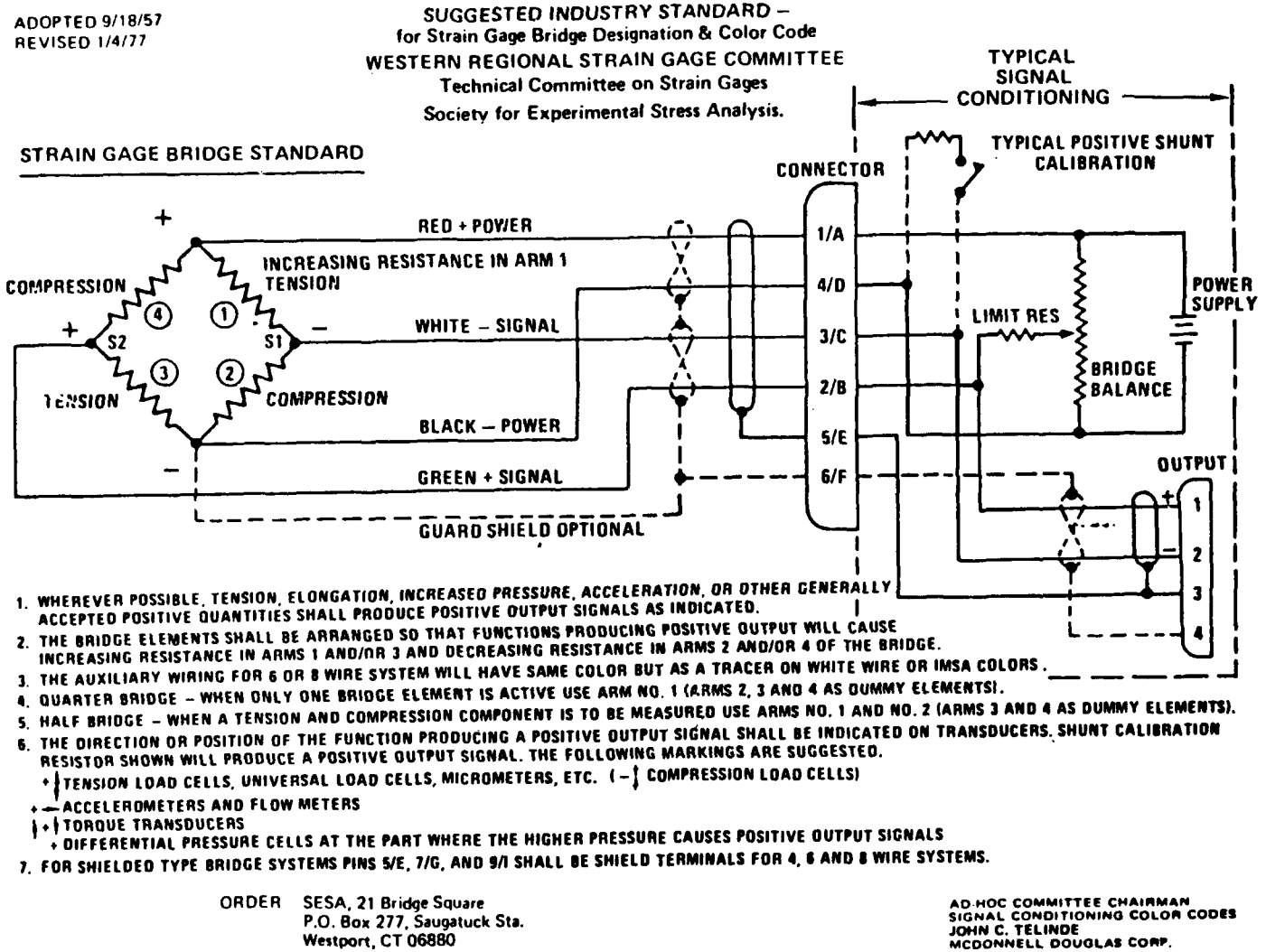

Figure A-4. Signal conditioning circuit for calibration of pressure transducers.

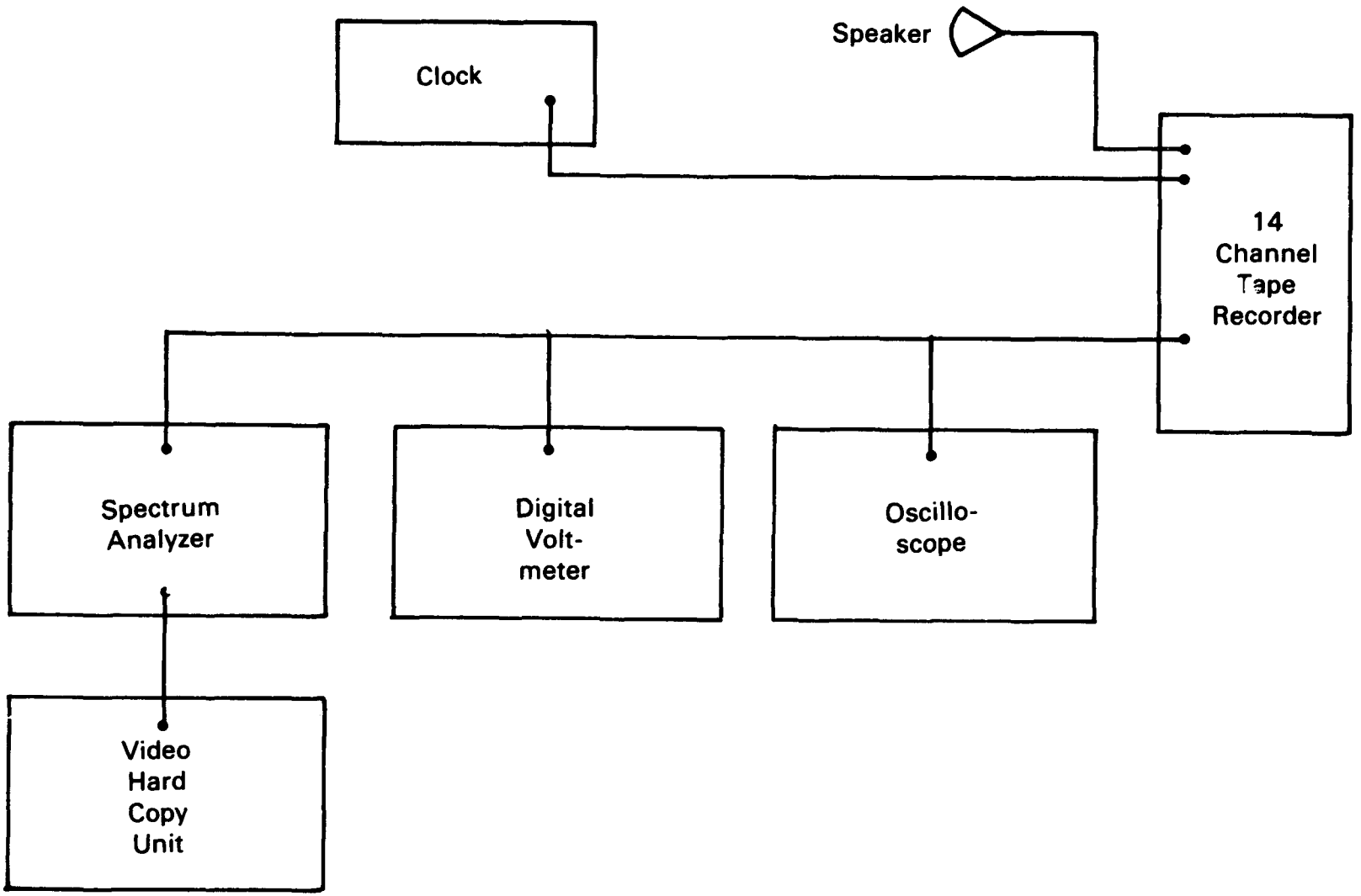

Figure A-5. Block diagram of instrumentation for reduction of microphone and pressure transducer data.

QUARTZ SOUND PRESSURE
MICROPHONE
w / built-in amplifier
Models 106B & 106B50

PCB PIEZOTRONICS

sound PRESSURE

Models 106B & 106B50 voltage-mode vibration compensated sound pressure microphones with built-in amplifier measure acoustic phenomena.

Model 106B is a voltage-mode ICP version of the high-temperature Model 116B with a built-in low-noise isolation (line-driver) amplifier, which improves resolution and simplifies system operation. It functions to transfer acoustic phenomena in gases or liquids into electrical signals compatible with readout and analyzing instruments. The Model 106B50 is a larger, more sensitive version with a resolution of 80 dB. These instruments usually install in a stepped hole, seal at a shoulder and are retained by a hollow clamp nut. Optional ground-isolated installations are available with nylon-type plastic or emralon coating. Battery type power units offer the lowest electrical system noise.

SPECIFICATIONS: Model No.		106B	106B50
Range (2.5 volt output)	psi	8.3	5.0
Maximum Pressure (slow)	psi	1000	500
Resolution (rms)	psi (dB)	0.0001 (91)	0.00003 (80)
Sensitivity mV/psi	(mV/Pa)	300 (0.04)	500 (0.07)
Resonant Frequency	kHz	60	40
Low Frequency (-5%)	Hz	0.5	0.5
Rise Time	μsec	5	8
Discharge Time Constant	sec	1.0	1.0
Linearity (best straight line)	%	1.0	1.0
Output Impedance	ohms	100	100
Output Bias (nominal)	volts	4	4
Acceleration Sensitivity	psi/g	0.002	0.002
Temperature Coefficient	%/°F	0.03	0.03
Temperature Range	°F	-65 to +250	-65 to +250
Flash Temperature	°F	3000	3000
Vibration, Shock	g's peak	1000, 2000	500, 1000
Seal	Welded	Hermetic	Hermetic
Case, Diaphragm		S.S.	S.S.
Weight	gm	15	32
Connector	micro	10-32	10-32
Dimensions	in	0.5 x 1.5	0.7 x 1.6
Excitation Voltage	VDC	+18 to 24	+18 to 24
Excitation Current (constant)	mA	2 to 20	2 to 20

A typical laboratory or field system (Model GK106B) consists of 106B sensor, 480D06 battery power unit with gain, 002A10 coaxial sensor cable and 002C03 scope cable (with BNC connector).

MODEL 106B

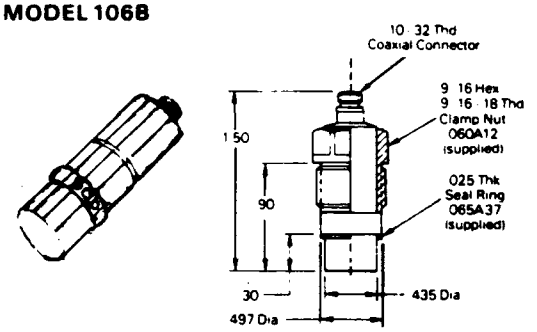

DIMENSIONS Model 106B

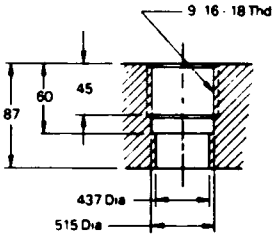

INSTALLATION PORT for Model 106B

MODEL 106B50

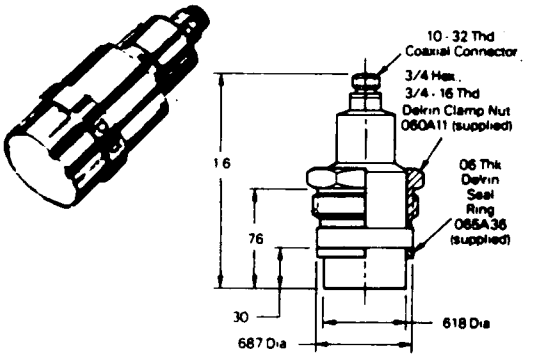

DIMENSIONS Model 106B50

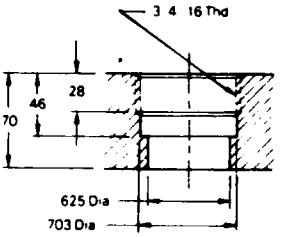

INSTALLATION PORT for Model 106B50

Figure A-6. PCB model 106B microphone and performance characteristics.

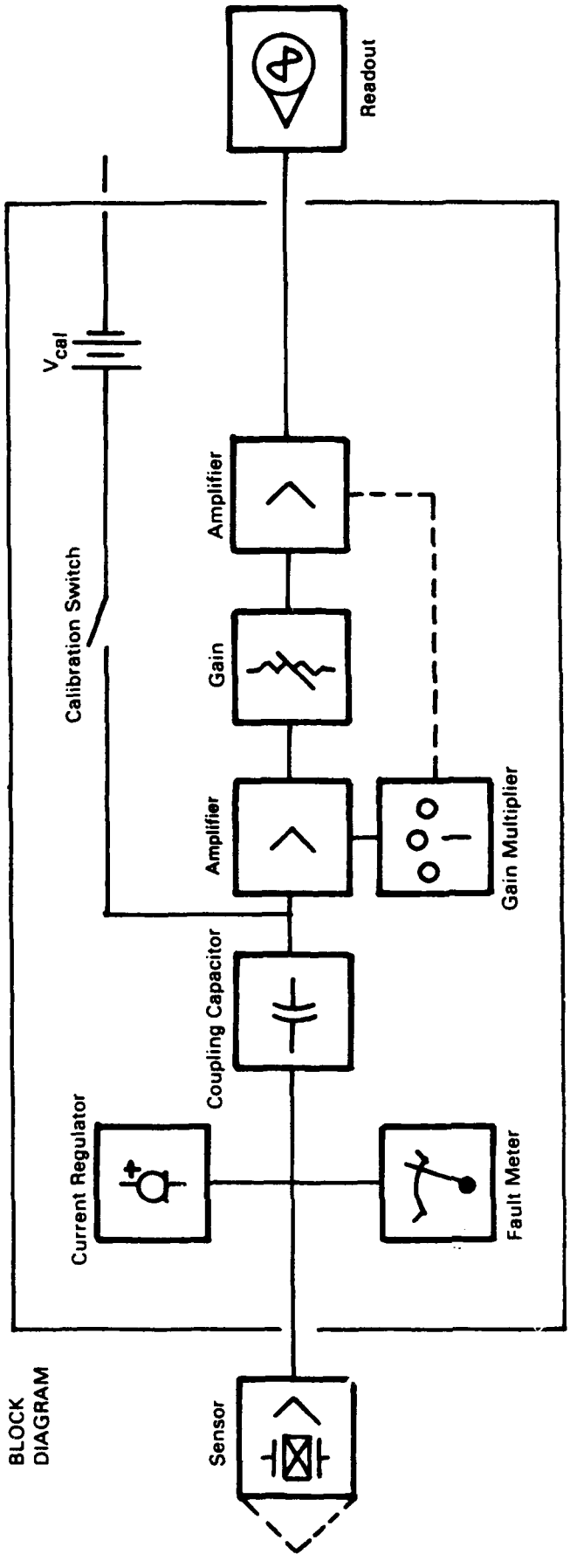

Figure A-7. Signal conditioning circuit for calibration of microphones.

Appendix B

SPECTRUM ANALYZER NOTATIONS

This appendix presents the typical notations found on noise plots from the spectrum analyzer. Figures B-1 and B-2 display the location of the data. The following explanations correlate with the note locations on Figures B-1 and B-2:

Note 1. Horizontal scale is linear, going from 0 Hz at the leftmost vertical line to 10,000 Hz at the rightmost vertical line. Each vertical line represents 1,000 Hz.

Note 2. Horizontal scale is logarithmic, going from 12.5 Hz at the leftmost vertical line to 10,000 Hz at the next-to-rightmost vertical line. Each vertical line represents doubling of frequency.

Note 3. The vertical scale range is 100 to 170 decibels, and a reference sound pressure level (in this case, 20 microPascals) represents 0 decibels.

Note 4. The vertical scale is $\log_{10}$ of "A", where "A" is the signal representing sound pressure level.

Note 5. A narrow band spectrum is plotted.

Note 6. A 1/3 octave band spectrum is plotted.

Note 7. A gain of 0 decibels has been applied to the vertical scale in order to show the range as 100 to 170 decibels.

Note 8. "Hanning" weighting was selected and applied to the input signal by the spectrum analyzer.

Note 9. "Full" weighting was selected and applied to the input signal by the spectrum analyzer.

Note 10. The approximate RMS voltage of signal "A" from the tape recorder to the spectrum analyzer was 0.50 Volts. The 0.50-volt scale on the spectrum analyzer was the lowest scale which did not "chop off" peaks of the input signal.

Note 11. Five samples of signal "A" were averaged.

Note 12. The total sound pressure level, integrated over the entire frequency spectrum, is 164.6 decibels.

Note 13. At 250 Hz, maximum sound pressure level of 156.6 decibels occurs.

Note 14. The spectrum was analyzed up to 10,000 Hz.

Note 15. 250 Hz represents the 24th third octave band from $\log_{10}(\text{freqency})=0$.

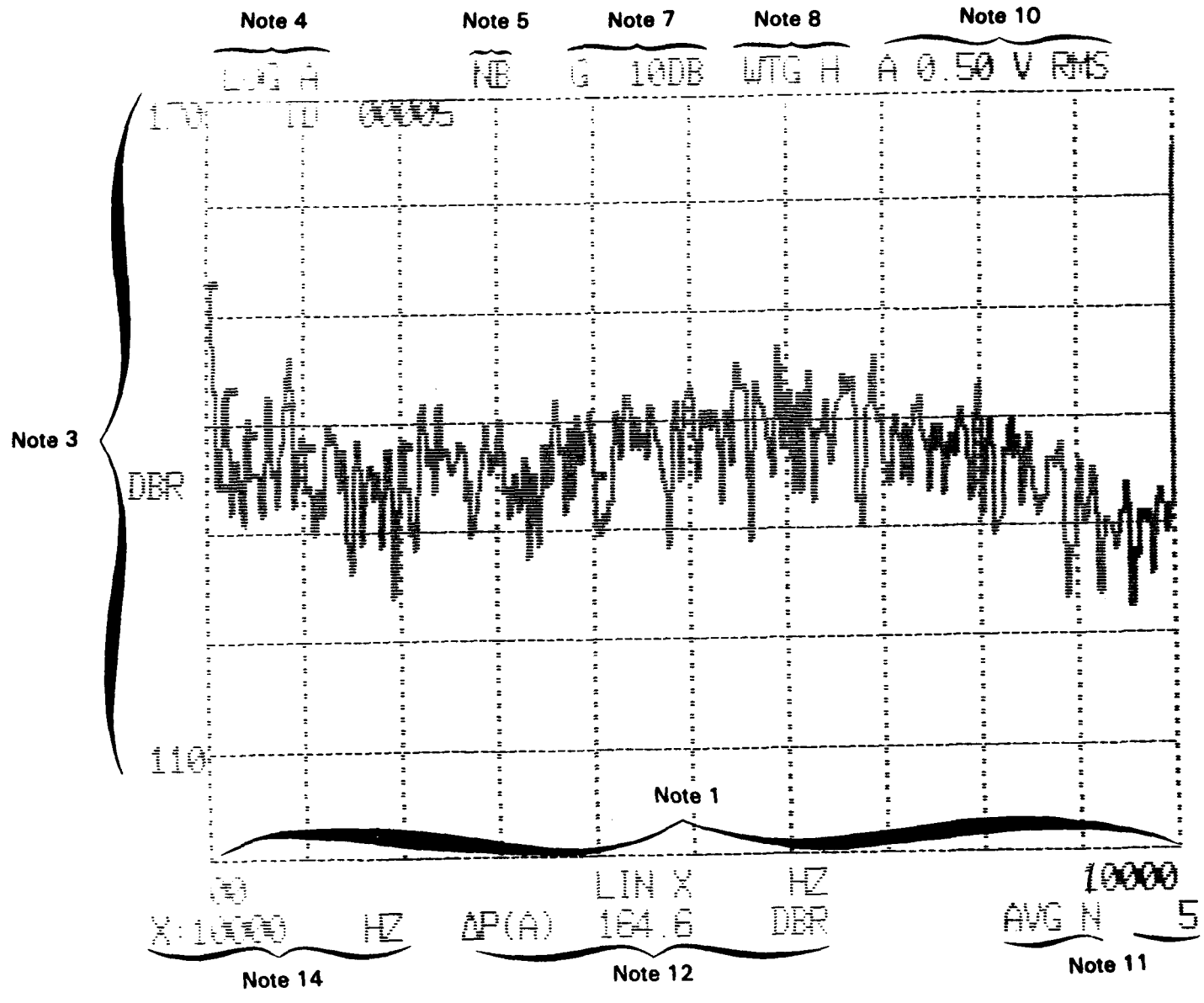

Figure B-1. Explanation of terms on plots of narrow band spectra of noise.

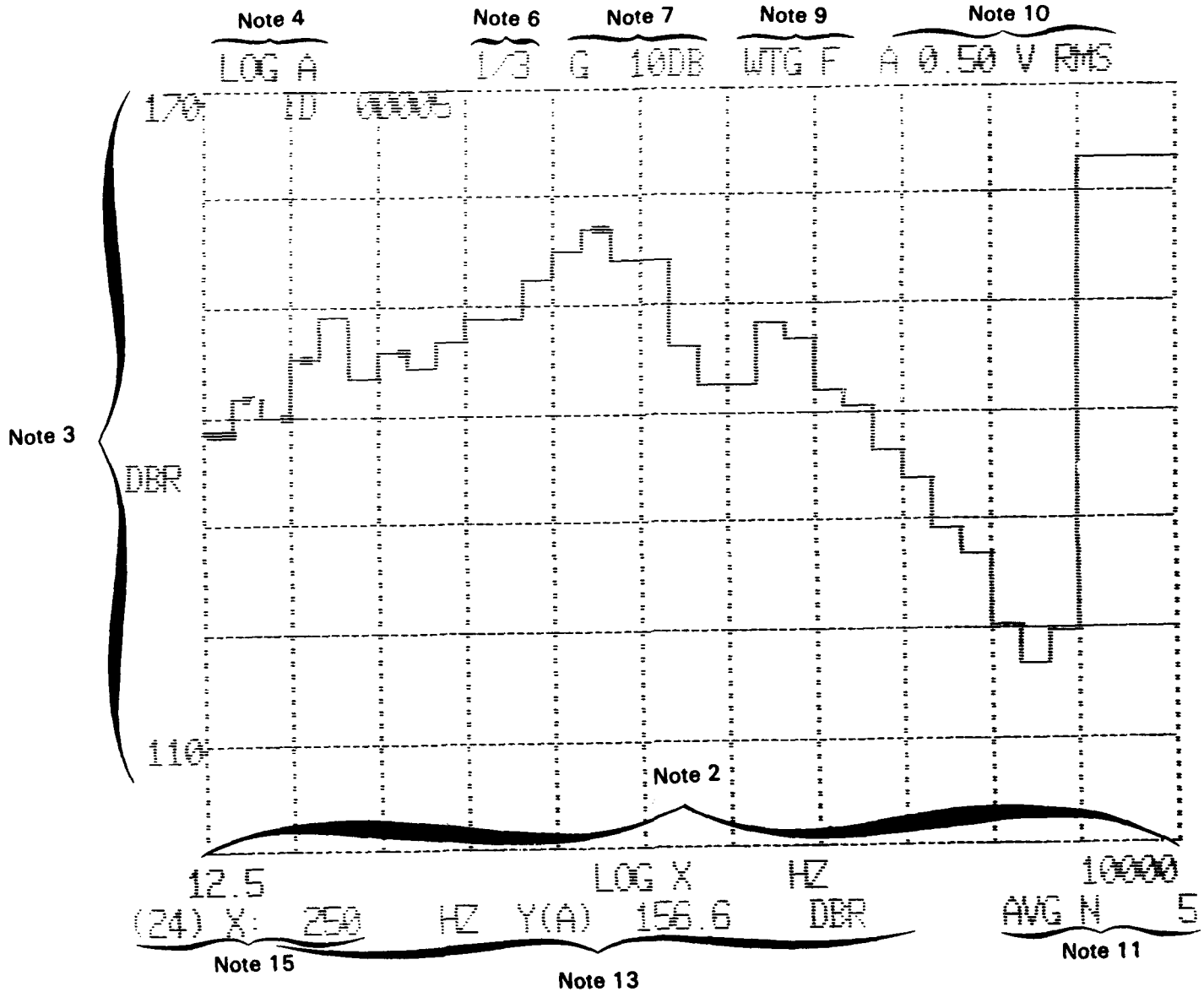

Figure B-2. Explanation of terms on plots of one-third octave band spectra of noise.

Appendix C

METHOD OF COMPUTATION OF RATE OF THERMAL ENERGY STORAGE IN JOINT SEAL MATERIALS

One-dimensional, transient conduction of heat through a material with constant thermal conductivity is described by the following partial differential equation:

$$\rho c_p \frac{\partial T}{\partial t} = k \frac{\partial^2 T}{\partial y^2}$$

One approach to solve for $T = T(t,y)$ is to use finite difference analysis. Make the following approximations.

$$\frac{\partial T}{\partial t} \simeq \frac{T(t + \Delta t, y) - T(t,y)}{\Delta t}$$

$$\frac{\partial T}{\partial y} \simeq \frac{T(t,y) - T(t, y - \Delta y)}{\Delta y}$$

$$\frac{\partial^2 T}{\partial y^2} \simeq \frac{\dfrac{T(t,y + \Delta y) - T(t,y)}{\Delta y} - \dfrac{T(t,y) - T(t,y - \Delta y)}{\Delta y}}{\Delta y}$$

$$= \frac{T(t,y + \Delta y) - 2T(t,y) + T(t,y - \Delta y)}{\Delta y^2}$$

Substitute the finite difference approximations for the partial derivatives, and solve for $T(t + \Delta t, y)$.

$$T(t + \Delta t, y) = \frac{T(t,y + \Delta y) + \left[\dfrac{\rho c_p \Delta y^2}{k \Delta t} - 2 \right] T(t,y) + T(t, y - \Delta y)}{\dfrac{\rho c_p \Delta y^2}{k \Delta t}}$$

The nondimensional grouping $(\rho c_p \Delta y^2 / k \Delta t)$ is called the "modulus," M. The value of the modulus is restricted. If $M < 2$, the finite difference solution is unstable (i.e., a large value of $T(t,y)$ results in a small value of $T(t + \Delta t, y)$). If $M >> 2$, the number of computational steps is far greater than necessary. Preferably, $3 < M < 4$.

For a specific material, the properties of the material (ρ c_p, k) are given. The value of modulus M can be controlled by selecting Δy and Δt. In the solutions for the thermal energy stored in joint sealant, the following values were used:

Δt = 2 seconds

Δy = Y/20 = 0.025 inches = 0.002083 feet

Y = 0.5 inches (typical thickness of joint seal)

ρ = 65.5 lbm/ft^3 (density)

c_p = 0.7 Btu/lbm-°R (specific heat)

k = 2.69 x 10^{-5} Btu-ft/ft^2-sec-°R (thermal conductivity)

M = 3.6977

To carry out the finite difference solution, an initial condition and two boundary conditions were applied:

Initial Condition: At t = 0, the temperature distribution through the joint seal, T(0,y), was input for each node, spaced at intervals of Δy = 0.025 inches.

Boundary Condition 1: At y = 0, the temperature-time history from a surface thermocouple, T(t,0), was input for each time interval of 2 seconds.

Boundary Condition 2: At the bottom of the joint seal, y = 0.5 inches, the rate of heat was assumed to be constant at the value occurring during ambient conditions. The governing equation at the bottom node is:

$$T(t + \Delta t, Y) = \frac{2T(t, Y - \Delta y) + (M - 2)T(t, Y)}{M} - \frac{2T(0, Y - \Delta y) - 2T(0, Y)}{M}$$

After solving for the temperature distribution, the rate of energy storage was calculated at each time step:

$$\text{(Rate of Energy Storage)} = \rho \, c_{p_y} \sum_{y=2\Delta y}^{y=20\Delta y} \left[\frac{T(t,y) - T(t - \Delta t, y)}{\Delta t} + \frac{T(t, y - \Delta y) - T(t - \Delta t, y - \Delta y)}{\Delta t} \right] \frac{\Delta y}{2}$$

DISTRIBUTION LIST

AFESC / TECH LIB, TYNDALL AFB, FL
ARMY CERL / LIB, CHAMPAIGN, IL
ARMY CEWES / CODE GP-Q (LYNCH), VICKSBURG, MS
ARMY CRREL / LIBRARY, HANOVER, NH
ARMY EWES / LIBRARY, VICKSBURG, MS
DAHL / VENTURA, CA
DTIC / ALEXANDRIA, VA
FAA / ARD 200, MCLAUGHLIN, WASHINGTON, DC
FAA / ARD 200, TOMITA, WASHINGTON, DC
NAVFACENGCOM / CODE 03, ALEXANDRIA, VA
NAVFACENGCOM / CODE 04, ALEXANDRIA, VA
NAVFACENGCOM / CODE 04B1 (M.P. JONES), ALEXANDRIA, VA
NAVFACENGCOM / CODE 163, ALEXANDRIA, VA
NAVFACENGCOM / CODE 1632B, ALEXANDRIA, VA
NAVFACENGCOM LANTDIV / CODE 411, NORFOLK, VA
NAVFACENGCOM NORTHDIV / CODE 408AF, PHILADELPHIA, PA
NAVFACENGCOM PACDIV / CODE 102, PEARL HARBOR, HI
NAVFACENGCOM PACDIV / CODE 405, PEARL HARBOR, HI
NAVFACENGCOM PACDIV / LIBRARY, PEARL HARBOR, HA
NAVFACENGCOM SOUTHDIV / CODE 4023, CHARLESTON, SC
NAVFACENGCOM SOUTHDIV / LIBRARY, CHARLESTON, SC
NAVFACENGCOM WESTDIV / CODE 04A2.2 LIB, SAN BRUNO, CA
NAVFACENGCOM WESTDIV / CODE 102, SAN BRUNO, CA
NAVFACENGCOM WESTDIV / CODE 411, SAN BRUNO, CA
SPRINGBORN LABORATORIES / W. HOLLEY, ENFIELD, CT
UNIVERSITY OF IDAHO / LANCEY, IDAHO FALLS, ID

DISTRIBUTION QUESTIONNAIRE

The Naval Civil Engineering Laboratory is revising its primary distribution lists.

SUBJECT CATEGORIES

1 **SHORE FACILITIES**
1A Construction methods and materials (including corrosion control, coatings)
1B Waterfront structures (maintenance/deterioration control)
1C Utilities (including power conditioning)
1D Explosives safety
1E Aviation Engineering Test Facilities
1F Fire prevention and control
1G Antenna technology
1H Structural analysis and design (including numerical and computer techniques)
1J Protective construction (including hardened shelters, shock and vibration studies)
1K Soil/rock mechanics
1L Airfields and pavements
1M Physical security
2 **ADVANCED BASE AND AMPHIBIOUS FACILITIES**
2A Base facilities (including shelters, power generation, water supplies)
2B Expedient roads/airfields/bridges
2C Over-the-beach operations (including breakwaters, wave forces)
2D POL storage, transfer, and distribution
2E Polar engineering
3 **ENERGY/POWER GENERATION**
3A Thermal conservation (thermal engineering of buildings, HVAC systems, energy loss measurement, power generation)
3B Controls and electrical conservation (electrical systems, energy monitoring and control systems)
3C Fuel flexibility (liquid fuels, coal utilization, energy from solid waste)
3D Alternate energy source (geothermal power, photovoltaic power systems, solar systems, wind systems, energy storage systems)
3E Site data and systems integration (energy resource data, integrating energy systems)
3F EMCS design
4 **ENVIRONMENTAL PROTECTION**
4A Solid waste management
4B Hazardous/toxic materials management
4C Waterwaste management and sanitary engineering
4D Oil pollution removal and recovery
4E Air pollution
4F Noise abatement
5 **OCEAN ENGINEERING**
5A Seafloor soils and foundations
5B Seafloor construction systems and operations (including diver and manipulator tools)
5C Undersea structures and materials
5D Anchors and moorings
5E Undersea power systems, electromechanical cables, and connectors
5F Pressure vessel facilities
5G Physical environment (including site surveying)
5H Ocean-based concrete structures
5J Hyperbaric chambers
5K Undersea cable dynamics
ARMY FEAP
BDG Shore Facilities
NRG Energy
ENV Environmental/Natural Responses
MGT Management
PRR Pavements/Railroads

TYPES OF DOCUMENTS

D = Techdata Sheets; **R** = Technical Reports and Technical Notes; **G** = NCEL Guides and Abstracts; **I** = Index to TDS; **U** = User Guides; ☐ None - remove my name

Old Address:

_____

_____

_____

_____

Telephone No.: _____

New Address:

_____

_____

_____

_____

Telephone No.: _____

INSTRUCTIONS

The Naval Civil Engineering Laboratory has revised its primary distribution lists. To help us verify our records and update our data base, please do the following:

- Add - circle number on list
- Remove my name from all your lists - check box on list.
- Change my address - line out incorrect line and write in correction **(DO NOT REMOVE LABEL).**
- Number of copies should be entered after the title of the subject categories you select.
- Are we sending you the correct type of document? If not, circle the type(s) of document(s) you want to receive listed on the back of this card.

Fold on line, staple, and drop in mail.

DEPARTMENT OF THE NAVY
Naval Civil Engineering Laboratory
560 Laboratory Drive
Port Hueneme CA 93043-4328

Official Business
Penalty for Private Use, $300

BUSINESS REPLY CARD
FIRST CLASS PERMIT NO. 12503 WASH D.C.

POSTAGE WILL BE PAID BY ADDRESSEE

NO POSTAGE NECESSARY IF MAILED IN THE UNITED STATES

COMMANDING OFFICER
CODE L34
560 LABORATORY DRIVE
NAVAL CIVIL ENGINEERING LABORATORY
PORT HUENEME CA 93043-4328

NCEL DOCUMENT EVALUATION

You are number one with us; how do we rate with you?

We at NCEL want to provide you our customer the best possible reports but we need your help. Therefore, I ask you to please take the time from your busy schedule to fill out this questionnaire. Your response will assist us in providing the best reports possible for our users. I wish to thank you in advance for your assistance. I assure you that the information you provide will help us to be more responsive to your future needs.

R. N. STORER, Ph.D, P.E.
Technical Director

DOCUMENT NO. _____ TITLE OF DOCUMENT: _____

_____

Date: _____ Respondent Organization : _____

Name: _____ Activity Code: _____
Phone: _____ Grade/Rank: _____

Category (*please check*):

Sponsor ____ User ____ Proponent ____ Other (*Specify*) _____

Please answer on your behalf only; not on your organization's. Please check (*use an X*) only the block that most closely describes your attitude or feeling toward that statement:

SA Strongly Agree **A** Agree **O** Neutral **D** Disagree **SD** Strongly Disagree

---

		SA	A	N	D	SD
1.	The technical quality of the report is comparable to most of my other sources of technical information.	( )	( )	( )	( )	( )
2.	The report will make significant improvements in the cost and or performance of my operation.	( )	( )	( )	( )	( )
3.	The report acknowledges related work accomplished by others.	( )	( )	( )	( )	( )
4.	The report is well formatted.	( )	( )	( )	( )	( )
5.	The report is clearly written.	( )	( )	( )	( )	( )
6.	The conclusions and recommendations are clear and directly supported by the contents of the report.	( )	( )	( )	( )	( )
7.	The graphics, tables, and photographs are well done.	( )	( )	( )	( )	( )

Do you wish to continue getting NCEL reports? ☐ YES ☐ NO

Please add any comments (e.g., in what ways can we improve the quality of our reports?) on the back of this form.

Comments:

Fold on line, staple, and drop in mail.

DEPARTMENT OF THE NAVY
Naval Civil Engineering Laboratory
560 Laboratory Drive
Port Hueneme CA 93043-4328

Official Business
Penalty for Private Use, $300

NO POSTAGE NECESSARY IF MAILED IN THE UNITED STATES

BUSINESS REPLY CARD

FIRST CLASS PERMIT NO. 12503 WASH D.C.

POSTAGE WILL BE PAID BY ADDRESSEE

COMMANDING OFFICER
CODE L03
560 LABORATORY DRIVE
NAVAL CIVIL ENGINEERING LABORATORY
PORT HUENEME CA 93043-4328